LIBRARY
FISH & WILDLIFE SERVICE
PACIFIC OCEANIC FISHERY
INVESTIGATIONS

SEARS FOUNDATION FOR MARINE RESEARCH
BINGHAM OCEANOGRAPHIC LABORATORY, YALE UNIVERSITY

JOURNAL OF MARINE RESEARCH

VOLUME XI, 1952

NUMBER 1

ISSUED JULY 15, 1952, NEW HAVEN, CONN., U. S. A.

JOURNAL OF MARINE RESEARCH

PUBLISHED BY

SEARS FOUNDATION FOR MARINE RESEARCH

BINGHAM OCEANOGRAPHIC LABORATORY, YALE UNIVERSITY

BOARD OF EDITORS

Chairman: A. E. PARR
American Museum of Natural History
New York

C. O'D. ISELIN
Woods Hole Oceanographic Institution

H. U. SVERDRUP
Norsk Polarinstitutt
Oslo, Norway

DANIEL MERRIMAN
Bingham Oceanographic Laboratory

C.-G. ROSSBY
Institut für Meteorologi
Stockholm, Sweden

THOMAS G. THOMPSON
Oceanographic Laboratories
University of Washington

MANAGING EDITOR

YNGVE H. OLSEN
Bingham Oceanographic Laboratory
Yale University
New Haven, Conn.

The Journal is normally issued in three numbers per year constituting one volume, except for volume V, published in 1942–1944, and volume VI, published in 1946 and 1947. All the income derived from subscriptions is used solely to increase the volume and improve the quality of the Journal for the benefit of its subscribers and contributors.

Subscription price three dollars per volume, or one dollar per number. Sverdrup Anniversary Number (Vol. VII, No. 3) available only by purchase of complete Vol. VII at $3.00. Address all communications to the Managing Editor. See inside rear cover for Note to Authors.

ALPHABETICAL INDEX BY AUTHORS' NAMES

Page

M. BAKER: See Goldberg, Baker and Fox.

R. E. BANKS: See Ford, Longard and Banks.

K. BENDSCHNEIDER and R. J. ROBINSON: A new spectrophotometric method for the determination of nitrite in sea water. (No. 1, July 15, 1952). 87

T. J. CHOW and T. G. THOMPSON: The determination and distribution of copper in sea water. Part I. The spectrophotometric determination of copper in sea water. (No. 2, November 15, 1952) 124

E. F. CORCORAN: See Fox, Isaacs and Corcoran.

L. C. DAVIS: See Hershey, Johnson and Davis.

G. A. EDWARDS: See Wyman, Scholander, Edwards and Irving.

D. B. ERICSON: See Kulp, Volchok, Holland and Ericson.

ERRATA 293

H. G. FARMER: See Stommel and Farmer.

M. P. FISH, A. S. KELSEY, Jr., and W. H. MOWRAY: Studies on the production of underwater sound by North Atlantic coastal fishes. (No. 2, November 15, 1952) 180

W. L. FORD, J. R. LONGARD and R. E. BANKS: On the nature, occurrence and origin of cold low salinity water along the edge of the Gulf Stream. (No. 3, December 31, 1952) 281

W. L. FORD and A. R. MILLER: The surface layer of the Gulf Stream and adjacent waters. (No. 3, December 31, 1952) 267

D. L. FOX, J. D. ISAACS and E. F. CORCORAN: Marine leptopel, its recovery, measurement and distribution. (No. 1, July 15, 1952) 29

E. D. GOLDBERG, M. BAKER and D. L. FOX: Microfiltration in oceanographic research. I. Marine sampling with the molecular filter. (No. 2, November 15, 1952) 194

J. V. GRIEL and R. J. ROBINSON: Titanium in sea water. (No. 2, November 15, 1952) 173

W. H. HASTINGS and C. F. SPENCER: Determinations of free and bound ascorbic acid in fishery products. (No. 2, November 15, 1952) 241

J. B. HERSHEY, H. R. JOHNSON and L. C. DAVIS: Recent findings about the deep scattering layer. (No. 1, July 15, 1952) 1

H. D. HOLLAND: See Kulp, Volchok, Holland and Ericson.

L. IRVING: See Wyman, Scholander, Edwards and Irving. .....

J. D. ISAACS and A. E. MAXWELL: The ball-breaker, a deep water bottom signalling device. (No. 1, July 15, 1952) 63

See also Fox, Isaacs and Corcoran.

H. R. JOHNSON: See Hersey, Johnson and Davis.

G. H. JUNG: Note on the meridional transport of energy by the oceans. (No. 2, November 15, 1952) 139

Page

A. S. KELSEY: See Fish, Kelsey and Mowbray.

J. L. KULP, H. L. VOLCHOK, H. D. HOLLAND and D. B. ERICSON: Thick source alpha activity of some North Atlantic cores. (No. 1, July 15, 1952) 19

E. C. LAFOND and D. W. PRITCHARD: Physical oceanographic investigations in the eastern Bering and Chukchi seas during the summer of 1947. (No. 1, July 15, 1952) 69

J. R. LONGARD: See Ford, Longard and Banks.

M. S. LONGUET-HIGGINS: On the statistical distribution of the heights of sea waves. (No. 3, December 31, 1952) 245

W. V. R. MALKUS and M. E. STERN: Determination of ocean transports and velocities by electromagnetic effects. (No. 2, November 15, 1952) 97

A. E. MAXWELL: See Isaacs and Maxwell.

A. R. MILLER: See Ford and Miller.

W. H. MOWBRAY: See Fish, Kelsey and Mowbray.

W. H. MUNK and G. A. RILEY: Absorption of nutrients by aquatic plants. (No. 2, November 15, 1952) 215

C. H. OPPENHEIMER and C. E. ZoBELL: The growth and viability of sixty-three species of marine bacteria as influenced by hydrostatic pressure. (No. 1, July 15, 1952) 10

D. W. PRITCHARD: Salinity distribution and circulation in the Chesapeake Bay estuarine system. (No. 2, November 15, 1952) 106

See also LAFOND and Pritchard.

F. A. RICHARDS: The estimation and characterization of plankton populations by pigment analyses. I. The absorption spectra of some pigments occurring in diatoms, dinoflagellates, and brown algae. (No. 2, November 15, 1952) 147

F. A. RICHARDS with T. G. THOMPSON: The estimation and characterization of plankton populations by pigment analyses. II. A spectrophotometric method for the estimation of plankton pigments. (No. 2, November 15, 1952) 156

G. A. RILEY: See Munk and Riley.

R. J. ROBINSON: See Bendschneider and Robinson; Griel and Robinson.

P. F. SCHOLANDER: See Wyman, Scholander, Edwards and Irving.

C. F. SPENCER: See Hastings and Spencer.

M. E. STERN: See Malkus and Stern.

H. STOMMEL and H. G. FARMER: Abrupt change in width in two-layer open channel flow. (No. 2, November 15, 1952) 205

T. G. THOMPSON: See Chow and Thompson; Richards with Thompson.

H. L. VOLCHOK: See Kulp, Volchok, Holland and Ericson.

J. WYMAN, JR., P. F. SCHOLANDER, G. A. EDWARDS and L. IRVING: On the stability of gas bubbles in sea water. (No. 1, July 15, 1952) 47

C. E. ZoBELL: See Oppenheimer and ZoBell.

SEARS FOUNDATION FOR MARINE RESEARCH
BINGHAM OCEANOGRAPHIC LABORATORY, YALE UNIVERSITY

JOURNAL OF
MARINE RESEARCH

VOLUME XI 1952 NUMBER 1

RECENT FINDINGS ABOUT THE DEEP SCATTERING LAYER[1]

By

J. B. HERSEY, H. R. JOHNSON AND L. C. DAVIS

Woods Hole Oceanographic Institution

ABSTRACT

Sound scattering observations in deep water are reported for the frequency range from 2 to 20 kc. An explosive sound source was employed to give a sound having high acoustic pressures throughout the frequency range. The receiver was directed vertically downward in the water; the recorder allowed simultaneous recording over several frequency bands. Scattering showed marked peaking as a function of both depth and frequency down to 5 kc, but not below, so far as the observations extend. Peaked scattering at all frequencies exhibits diurnal migration; thus there is continued indication that marine animals are the principal scatterers throughout the frequency range studied. The peaking as a function of frequency above 5 kc suggests that common and abundant animals in deep water do not greatly exceed linear dimensions of the order of 30 cm. The marked differences observed in the frequency and depth dependence of scattering from place to place, compared with their reproducibility over a limited area and time, suggest that the frequency dependence of scattering may eventually be employed for limited identification of the animals.

INTRODUCTION

The occurrence of stratification of sound scattering, first discovered in the Pacific Ocean [(2), (3), (4), (5) and (6)], has been found to be nearly world-wide, and such characteristics as the correlation between layer depth and altitude of the sun have been studied [(8), (9) and (10)]. The hypothesis by Johnson (4) that the scatterers are marine

[1] Contribution No. 562 from the Woods Hole Oceanographic Institution.

animals is widely accepted, but there is no general agreement about their identity. Several animal groups have been proposed: Hersey and Moore (9) suggested euphausid shrimp, Lyman (10) proposed squid, and Chapman (7) suggested that fish are responsible. A recent discussion by Marshall (11) reviews previous analyses and suggests that certain bathypelagic fishes with swim bladders have appropriate distribution and habits to account for some of the scattering. Definite identification will depend on some direct means such as net towing or underwater photography. However, acoustic observations are of value in approximating the size and distribution of the scatterers. The present paper describes an approach to this end by investigating their frequency dependent characteristics.

The acoustic record, plotted as a function of time, presents the combined echo level from all scatterers in a volume of water determined by the time after the emission of the sound signal and its own duration. Standard methods (2) for analyzing the scattering record give, as a function of distance from the sound source, the average fraction of sound energy scattered per cubic meter of water. This may be regarded as the total scattering cross section that "intercepts" the sound beam per cubic meter; it is dependent on the population density of scatterers, their size distribution, their acoustical properties, and the frequency of the sound signal.

The scattering cross section of an individual, in general not equal to the physical cross section it presents to the sound beam, depends on its physical size in relation to the wave length of the sound beam and on its own acoustical properties. Hence no acoustical measurement of cross section will yield the physical size distribution directly. Raitt (15) has observed the distribution of the acoustical cross section of individual scatterers by measuring the amplitude of many individual echoes from very short pulses of sound.

The detailed scattering properties of marine animals are expected to be complicated, and it is unlikely that theoretical expressions for their scattering can be derived by any practical effort. However, it is reasonable to expect that the effects of shape and size will turn out to be sufficiently similar to those of simpler forms of scatterers to permit some conclusions to be drawn about the size distribution from frequency dependence. In the usual treatment of the scattering problem, three regions of approximation, in which rather different types of frequency dependence hold, are useful from a practical standpoint:

I. The scatterer is much smaller than the wave length of sound,
II. The scatterer is comparable to the wave length, and
III. The scatterer is much larger than the wave length.

In I, Rayleigh [(16) vol. II, paragraph 296] has shown that the acoustic pressure of the scattered wave is proportional to the square of the frequency and to the volume of the scatterer regardless of its shape. Hence for wave lengths long compared with the scatterer, scattering should increase rapidly with frequency. In II, the scattering in any given direction may fluctuate considerably with frequency, depending on the acoustical properties of the scatterer compared with the medium. The general nature of results to be anticipated in marine scattering was outlined by Anderson (1), who computed in detail the back scattering from fluid spheres; he considered this to be a reasonable starting point for the study of marine animal scattering. In III, scattering is independent of frequency and depends only on the acoustical properties of the scatterer and the cross section it presents to the sound beam.

Since marine animals vary in size from a fraction of a centimeter to a few meters, it is apparent that they may occupy in turn any of the three regions of approximation discussed above for the ordinary sonic and lower ultrasonic frequencies. A study (3) has been made in which scattering at 10, 20, 40 and 80 kc was observed in rapid succession to investigate frequency dependence in the deep scattering layer. The results indicated that the scattering does not follow the Rayleigh law. By extending sonic observations to lower frequencies it should be possible to find the region where the wave length is much larger than the largest abundant scatterers and hence determine where scattering falls off sharply as the frequency is decreased. The present paper describes an investigation in which scattering was recorded down to 2 kc in an attempt to do this by means of a technique which allowed simultaneous recording of several frequency bands.

OBSERVATIONS

The first observations were made in the vicinity of Lat. 38° 30′ N Long. 71° W on cruises of the R/V CARYN from 2 to 11 August 1949 and of the R/V ATLANTIS from 22 to 30 September 1949. A third cruise, on the R/V ATLANTIS between January and April 1950, covered a considerable area between Cape Cod and the Antilles.

The sound source employed was a ½ lb. block of TNT which was detonated at a depth of about ½ m and 30 to 50 m from the receiver. The receiver was a somewhat directional rochelle salt transducer towed at shallow depth astern of the observing ship on the first cruise; subsequently it was mounted in the keel. In both cases the transducer was directed vertically downward. Sounds received by the transducer were filtered by band-pass filters in the separate channels of a multi-

channel amplifier, rectified, and then fed to galvanometers to be recorded photographically. Fig. 1 shows representative records. Here four channels were employed and three were recorded at two dynamic levels, roughly 20 db apart, thereby allowing both loud and faint sounds to be recorded on the same record. Timing markers, vertical lines 1/100 seconds apart, were recorded by a suitably controlled interrupter with every tenth line accentuated to facilitate scaling. Depth in meters and the corresponding travel times are indicated below the record. The explosion provides an intense source of sound at all frequencies, and the filtered amplifiers provide a means of recording scattering from the explosion in various frequency bands. The receiver, directed vertically downward, discriminates against sound scattered from surface waves or from scatterers in the water at wide angles from the vertical.

Fig. 2 is a series of records from the CARYN cruise in which various frequency bands from 19.6 to 2 kc were employed. The 19.6 kc filter was used throughout the series for comparison. The change in character from one band to another is apparent from an inspection of the records. Observe that there is a peak of scattering at about 140 m on the 15 and 19.6 kc traces which does not appear at any of the low frequencies. Similarly, the very prominent scattering at 400 to 500 m at 15 and 19.6 kc is reproduced at 10 kc but at no lower frequency. At 8 kc a peak of different shape and of slightly different depth is recorded. At 5 kc a much broader and deeper peak is recorded, while at 2 kc there is no evidence of peaking. The very sharp character of the peak at 400 to 500 m on the 19.6 kc trace is found consistently only in certain localities in the Atlantic; it is best known just north of the Gulf Stream where this series was recorded. Fig. 1 shows a more usual recording in which the deep scattering layer (i. e., on the 15 kc trace) is broader and more diffuse; this record was also made north of the Gulf Stream but at a different location.

A General Radio Sound Analyzer (Type 760A) was used to examine in detail the peak at 5 kc. Fig. 1 shows three records in which the Analyzer was employed as a filter at 3, 5.5, and 7.5 kc. In the first (3 kc) the scattered return is relatively low in amplitude compared with the second (5.5 kc), while the third (7.5 kc) is of lower amplitude and is somewhat different in character, since the shallower peak begins to appear here. We had no means of examining in such detail the transition from one frequency band to another above 7.5 kc.

Several sequences of records taken at 5 and 10 minute intervals were made through both sunrise and sunset. Although there are striking individual differences in the various sets of observations, all

show marked evidence of vertical migration of some of the scatterers at all frequencies. This is illustrated by Fig. 3, showing selected records taken from a series from 1410 to 1850 on March 4, 1950 at Lat. 29° 00′ N, Long. 62° 05′ W. (The time of local sunset was 1815.) All four records were taken at the same gain settings of the analyzer, and relative amplitudes on the same frequency trace from record to record at a given depth may be compared as a rough measure of the concentration of scatterers there. The record at 1410 is a typical mid-day record for this region. The scattering from 0 to about 75 m on the 20 and 15 kc traces and from 0 to about 150 m at the lower frequencies is probably a combination of scattering from surface waves and scatterers in the water. In many instances, peaks of scattering are reproducible at shallower depths, but generally the record is not usable for about 0.1 sec. after the shock wave (i. e., 75 m). On the 20 kc trace a somewhat complicated layer extends from about 250 to 290 m. At greater depths no scattered return is above the general background level on the sensitive trace. On the 1627 record this layer is not evident, the scattering being diffuse and of low amplitude at depths greater than about 110 m. On the 1805 and 1850 records, however, marked stratification is found from about 75 to 180 m where none was previously evident. On the 15 kc traces a somewhat more striking migration is seen where a mid-day layer extending from 380 to 650 m apparently split by 1627, the shallower portion migrating to a very shallow depth by 1805 (55 to 220 m); meanwhile the deeper portion, though still identifiable as a layer at about its mid-day depth throughout the series, apparently weakens in concentration between 1805 and 1850 to a small fraction of its mid-day amplitude. At 10, 8, and 5 kc the scattering is diffusely distributed in depth to slightly deeper than 1000 m. Hence the migration is not evident progressively through these records. However, an increase in the scattering amplitude at the shallower depths is evident at all three frequencies between 1805 and 1850, which coincides with a general decrease in the scattering amplitude at depth. These records were selected from a more detailed sequence which demonstrates that the changes described took place in a gradual manner throughout the period covered.

DISCUSSION

The examples of scattering records in Figs. 1, 2 and 3 are not representative of all of the variations that have been observed amongst the 200-odd records which have now been taken in the western North Atlantic, but they may be taken as typical. The records of each figure, taken within a few miles of one another, are reproducible, in

general character at least. However, the locations for the three figures differ, and there is correspondingly considerable variation from one figure to another, not only in the character of the depth dependence at any one frequency but also in even the most general aspects of the frequency dependence. For example, in the case of Fig. 2, the 10 kc record is very similar to those at 15 and 19.6 kc but different from those at 8 and 5 kc, whereas in Fig. 1 the 10 kc trace is strikingly different from all frequencies but 7.5 kc. Again in Fig. 3 the 10, 8, and 5 kc traces are all rather similar. Other individual features, such as the peak in Fig. 2 at 70 m depth on the 15 and 19.6 kc traces, which do not appear at the lower frequencies, have proven to be reproducible in local areas that may be miles in extent. Diurnal migration, which is observed at all frequencies for which there are scattering peaks, is strong evidence that marine animals are the principal scatterers. Hence, observations of this type provide a means of following the migration and of determining the extent and concentration of different groups of marine animals, discriminated from one another by means of frequency dependence.

All records obtained thus far show some evidence of variation of scattering with both depth and frequency. No pronounced peaking as a function of frequency has been observed below 5 kc. This suggests that no heavy concentrations of animals larger than 30 cm, the wave length at 5 kc, have been encountered during the observations and hence are not commonly found in the western North Atlantic. However, since the frequency region below 2 kc has not been investigated extensively, and since we know little in detail of the exact manner in which marine animals scatter sound, it is premature to conclude that this is necessarily so. Further, for the latter reason we cannot now predict the detail with which it may be possible to interpret the sound scattering through the region of peaking. However, it seems possible that the scattering variation with frequency may tell enough about the physical size of the scatterers to allow some limited identification of kinds of animals, particularly if the mode of taking the scattering observations allows the determination of other characteristics such as schooling habits, movement of groups or individuals, or other features that would aid identification.

Much of the justification for such a prediction must rest on a satisfactory demonstration that the supposed scatterers are present and are capable of scattering sound as observed. In the series of observations discussed here, net tows at different depths were made only on the August 1949 cruise of the R/V CARYN. These were made with a pair of ¾ m stramen nets towed at speeds from 1.5 to 2 knots.

The biologist making the collections aptly remarked that such an operation would catch only "the maimed, the halt and the blind." However, daytime hauls below 250 m did catch appreciable numbers of animals whose lengths were comparable with the wave length over much of the frequency range observed. The question whether planktonic forms have adequate scattering cross sections to account for observed scattering coefficients is not completely answered. Nevertheless, a good indication that they do comes from unpublished measurements of scattering from small inshore shrimp made by Mr. P. F. Smith at Woods Hole. At frequencies between 20 and 30 kc he found that shrimp [*Palaemonetes vulgaris* (Say)], roughly 2.5 to 3.5 cm long, had quite adequate scattering power to account for the scattering coefficients observed for the peak of the scattering layer given in the University of California work (2), assuming concentrations of the order of 20 shrimp per cubic meter. Thus it seems reasonable to suppose that planktonic crustaceans of various sizes may be capable of scattering sound over a considerable frequency range with sufficient power to account for much of the observed scattering. Of course, this does not preclude the possibility that other types of animals, not necessarily all planktonic, can scatter sound sufficiently to be observed in the scattering layers of the deep ocean.

CONCLUDING REMARKS

1. Peaks of sound scattering as a function of frequency occur in the deep ocean for frequencies at and above 5 kc, suggesting, by analogy to the scattering properties of simple geometrical forms, that the physical size of the common abundant scatterers is comparable to the wave length above that frequency, i. e., wave lengths less than 30 cm.

2. Observations of diurnal migration at all frequencies where peaking occurs is a strong indication that the scatterers are zooplankton. Other measurements indicate that planktonic crustaceans or other associated organisms such as fish probably have adequate scattering power to account for the observed scattering.

3. Sound scattering as a function of both depth and frequency is reproducible, in general outline at least, over limited areas, but it varies considerably over the part of the ocean studied. This suggests that concentrations of different animals characteristic of a given general locality control the observed scattering, thus providing a limited means of identifying them.

ACKNOWLEDGMENTS

The considerable assistance of various members of the underwater acoustics group at the Woods Hole Oceanographic Institution, working under Contract NObsr-43270 with the Bureau of Ships, Navy Depart-

ment, has contributed greatly to the completion of this study and is much appreciated. Mr. Willard Dow designed the five channel analyzer and several other components of the electronic gear. Mr. Sydney Knott designed and constructed both the oscillograph camera, with which the records were taken, and the handling gear for towing the receiver from the R/V CARYN. Mr. P. F. Smith assisted in taking the first observations and Mr. Frank Mather made the net tows on the CARYN. Dr. Hilary B. Moore and Mr. W. E. Schevill have assisted the work considerably by discussing the findings with the authors and by giving most helpful criticism of the manuscript.

REFERENCES

(1) ANDERSON, V. C.
1950. Sound scattering from a fluid sphere. J. acous. Soc. Amer., *22:* 426–431.

(2) CALIFORNIA, UNIVERSITY OF, DIVISION OF WAR RESEARCH
1942. Reverberation studies at 24 kc. UCDWR No. U7.

(3) 1943. Volume reverberation; scattering and attenuation versus frequency. UCDWR No. U50.

(4) 1946. Stratification of sound scatterers in the ocean. UCDWR File Rept. No. M397, 13 pp. (ozalid) + 18 figs. (photostat), Feb. 16, 1946. (Copies available as PB 60290 from United States Department of Commerce, Office of Technical Service, Washington 25, D. C.).

(5) 1946. Forward scattering from the deep scattering layer. UCDWR No. M398.

(6) 1946. Studies of the deep scattering layer. UCDWR No. M445.

(7) CHAPMAN, W. McL.
1947. The wealth of the ocean. Sci. Mon., *64:* 192–197.

(8) DIETZ, R. S.
1948. Deep scattering layer in the Pacific and Antarctic Oceans. J. Mar. Res., *7* (3): 430–442.

(9) HERSEY, J. B. AND H. B. MOORE
1948. Progress report on scattering layer observations in the Atlantic Ocean. Trans. Amer. geophys. Un., *29:* 341–354.

(10) LYMAN, JOHN
1948. The sea's phantom bottom. Sci. Mon., N. Y., *66* (1): 87–88.

(11) MARSHALL, N. B.
1951. Bathypelagic fishes as sound scatterers in the ocean. J. Mar. Res., *10:* 1–17.

(12) MOORE, H. B.
1948. Report on the biological interpretation of the deep scattering layer in the North Atlantic. W.H.O.I. Rep. under contract NObsr-2083 with the Bureau of Ships.

(13) 1950. The relation between the scattering layer and the Euphausiacea. Biol. Bull. Woods Hole, *99* (2): 181–212.

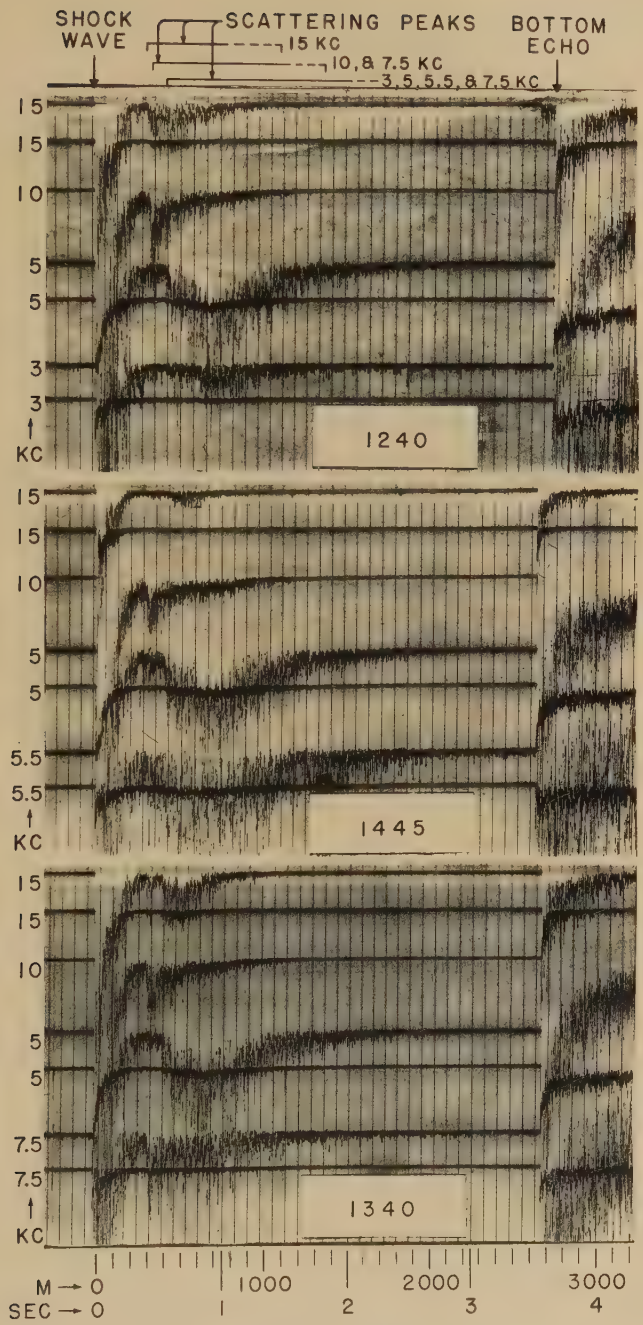

Figure 1. Representative scattering records.

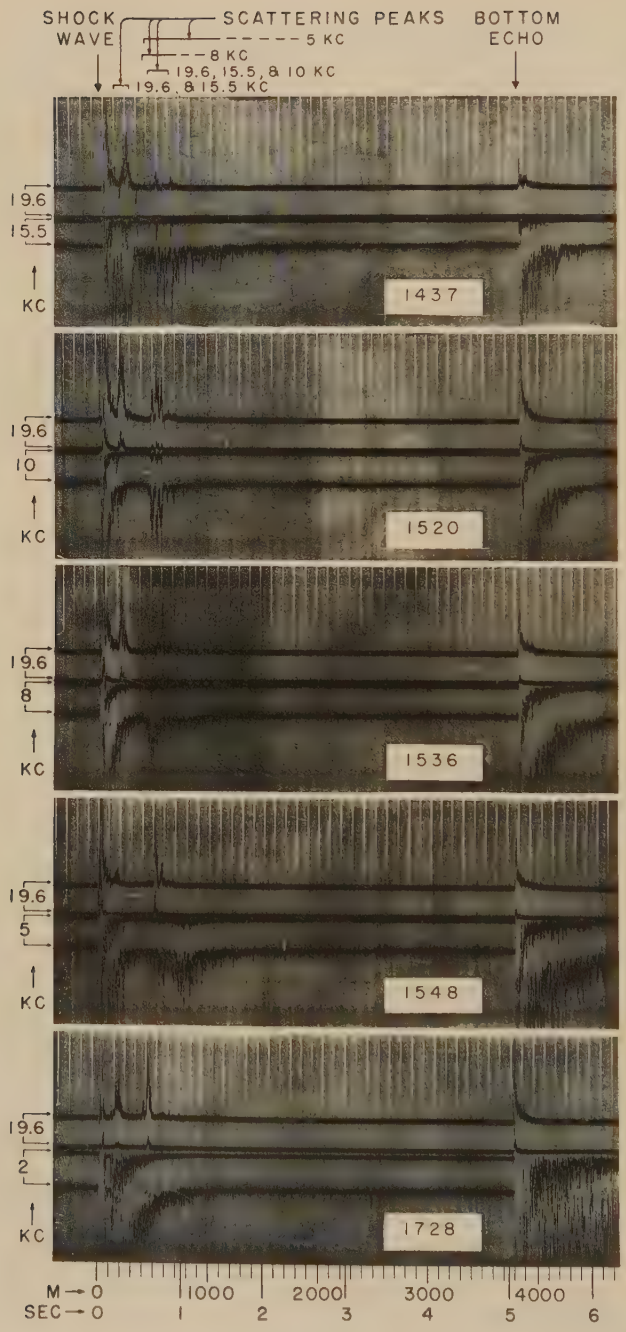

Figure 2. Sound scattering at various frequencies at Lat. 38°30'N, 71°55'W.

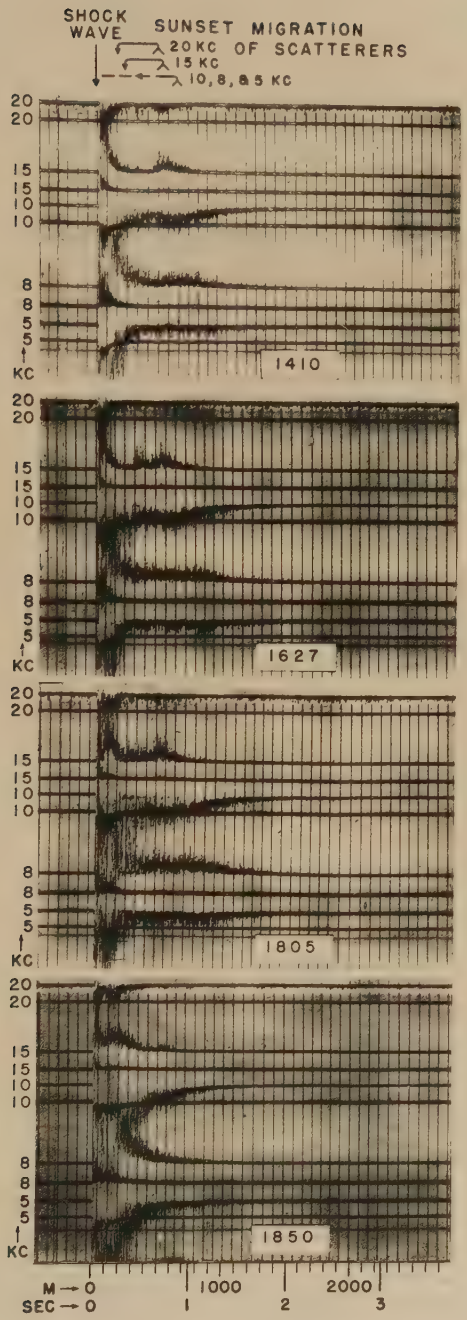

Figure 3. Sunset scattering record sequence.

(14) Morse, P. M.
1948. Vibration and sound. McGraw-Hill Book Co., New York.
(15) Raitt, R. W.
1948. Sound scatterers in the sea. J. Mar. Res., 7 (3): 393–409.
(16) Strutt, J. W., Lord Rayleigh
1945. The theory of sound. Dover Publications Edition.

THE GROWTH AND VIABILITY OF SIXTY-THREE SPECIES OF MARINE BACTERIA AS INFLUENCED BY HYDROSTATIC PRESSURE[1]

By

CARL H. OPPENHEIMER AND CLAUDE E. ZOBELL

Scripps Institution of Oceanography
University of California
La Jolla, California

ABSTRACT

The hydrostatic pressure of sea water, which increases approximately 0.1 atmosphere per meter of depth, was found to affect the viability, reproduction, and morphology of 63 stock cultures of marine bacteria representing several genera. Many of the cultures were killed at 27° C by pressures ranging from 200 to 600 atm, although some few reproduced at 600 atm. Initial inoculum concentrations of the various bacteria appeared to influence their ability to reproduce or to tolerate high pressures. Pressures exceeding 400 atm inhibited the fission of certain bacteria without stopping their growth, thereby resulting in bizarre cells, some of which formed long filaments.

INTRODUCTION

The precursory observations of Certes (1884), Regnard (1891), ZoBell and Johnson (1949), and ZoBell and Oppenheimer (1950) indicate that hydrostatic pressures of the order of 200 to 600 atm have a pronounced effect on the vertical distribution and activities of bacteria in the sea. The significance of these observations is suggested by the fact that pressures exceeding 200 atm prevail in more than 90% of the area of the oceans. Approximately half of the oceans of the world are deeper than 4,000 m, at which depth the hydrostatic pressure is about 400 atm.

From the illustrative data in Table I it will be observed that the pressure of sea water increases with depth by approximately 0.1 atm/m, the pressure-depth gradient being influenced somewhat by latitude, temperature, and salinity. One atmosphere is equivalent to 14.696 lb/in^2, 760 mm Hg, 1.0332 kg/cm^2, or to 1.0133 bars.

Living bacteria have been found in virtually all samples of marine sediments examined for their presence regardless of water depth (ZoBell, 1946). Until recently the greatest depth at which bacteria

[1] Contribution from the Scripps Institution of Oceanography, New Series No. 558. This investigation was supported in part by a grant from the American Petroleum Institute, Research Project 43A.

TABLE I. Selected Pressure-depth Gradients in Atmospheres Per Meter in the Sea for Different Depths, Salinities, Temperatures, and Latitudes (Adapted From Data Given By Bjerknes and Sandström, 1910)

Dynamic depth (m)	*Salinity* °/₀₀	*Temperature* °C	*Latitude 30°* atm/m	*Latitude 60°* atm/m
0	32	0	0.099,414	0.099,403
0	32	20	0.098,831	0.099,092
0	35	0	0.099,375	0.099,638
0	35	20	0.099,052	0.099,314
5,000	35	0	0.101,757	0.102,026
5,000	35	5	0.101,660	0.101,929
10,000	35	0	0.103,952	0.104,225

had been found was 5,800 m, but during the last year the Galathea Deep Sea Expedition extended the lower limits of the biosphere to 10,460 m. In several samples of sediments collected from depths exceeding 10,000 m in the Philippine Trench, ZoBell (1952) demonstrated the presence of bacteria that were physiologically active at pressures of the order of 1,000 atm. In fact, the well being of many bacteria collected from abyssal oceanic depths appears to depend upon high pressure. The purpose of this paper is to record the effect of pressure upon the activities of 63 different species of marine bacteria, all of which were taken from depths of less than 6,000 m.

EXPERIMENTAL METHODS

The bacteria were subjected to pressures up to 600 atm by means of apparatus described by ZoBell and Oppenheimer (1950). Essentially the apparatus consisted of thick-walled steel cylinders which have an inside diameter of 1 ⅜ inches and which are long enough (11 inches) to accommodate two dozen small culture tubes. The latter were fitted with no. 000 neoprene stoppers which functioned as pistons to subject the aqueous contents of the tubes to virtually the same pressure as the hydraulic fluid filling the steel cylinder. Preliminary experiments proved that pressure up to 1,000 atm could be applied and released ten times successively by means of the connecting hydraulic pump without the contents of the closed tubes becoming contaminated.

The culture medium consisted of sea water enriched with 0.5% peptone, 0.1% yeast extract, and 0.01% ferric phosphate. Following autoclave sterilization the pH of the medium was 7.6. Sufficient volume of such sea water medium was inoculated with bacteria in their logarithmic phase of growth to fill the number of culture tubes required

for any one experiment. This ensured having comparable numbers and kinds of bacteria at the beginning of each experiment. The inoculated medium was pipetted aseptically into sterile culture tubes, leaving approximately 0.5 ml of air at the top. The tubes were closed with sterile stoppers preparatory to placing them in pressure cylinders. After displacing the air from the cylinders by filling the space between the culture tubes with water, the cylinders were closed and immersed in a water bath at 27° C. Sufficient time (about 10 minutes) was allowed for the contents of the cylinders to attain this temperature. Then each cylinder in turn was connected to the hydraulic pump and the desired pressure applied. The valve was closed, the pump disconnected from the pressurized cylinders, and the latter were returned to the water bath to provide for the incubation of the bacterial cultures at 27° C.

Following four days' incubation the cylinders were reconnected to the hydraulic pump and gauge for checking the terminal pressure. After releasing the pressure, the culture tubes were removed from the cylinders for examination for evidence of growth as indicated by increased cloudiness or turbidity of the medium. Those tubes showing no evidence of bacterial growth under pressure were incubated an additional four days at room pressure in order to ascertain if the bacteria were still viable. The abundance and viability of bacteria in some tubes was estimated by standard plate count procedures. The contents of other tubes were examined by means of a phase microscope at a magnification of 970x.

RESULTS

In order to assess the effect of the abundance of bacteria in the inoculum upon the pressure tolerance of bacteria, four representative species were introduced into sea water medium to give initial populations ranging from 10 to 10^7 cells/ml. After four days' incubation at different pressures the bacterial population was determined by plate counts (Table II). When incubated at pressures of 1, 200, or 400 atm, the final bacterial population was not perceptibly affected by the initial number of cells present within the range of 10^2 to 10^6 cells/ml. Comparable results were not obtained when the initial bacterial population was less than 10^2 cells/ml. This suggests that an initial low bacterial population results in a more prolonged lag phase probably due to the presence of fewer pressure-tolerant cells in the smaller inocula. Therefore in subsequent experiments the medium was inoculated with enough cells to give initial bacterial populations of approximately 10^3 cells/ml.

As shown by the data in Table II, there was generally a decrease in

TABLE II. Numbers of Viable Cells per ml of (a) Culture No. 643, (b) *Serratia marinorubra*, (c) *Sarcina pelagia*, and (d) Culture No. 38:172 as Indicated by Plate Counts After Sea Water Broth Cultures Containing the Indicated Inocula Had Been Incubated at Different Pressures for Four Days at 27° C

Cultural organism	*Inoculum cells/ml*	*Hydrostatic pressures in atmospheres*			
		one	*200*	*400*	*600*
(a)	3×10^{0}	5×10^{7}	1×10^{7}	2×10^{8}	0
	3×10^{2}	2×10^{7}	5×10^{7}	9×10^{7}	8×10^{2}
	3×10^{4}	1×10^{7}	2×10^{7}	4×10^{7}	6×10^{4}
	3×10^{7}	3×10^{7}	3×10^{7}	7×10^{6}	4×10^{6}
(b)	2×10^{1}	5×10^{7}	9×10^{6}	6×10^{5}	7×10^{1}
	2×10^{3}	6×10^{7}	3×10^{7}	5×10^{6}	8×10^{4}
	2×10^{5}	9×10^{7}	5×10^{7}	7×10^{6}	8×10^{4}
	2×10^{7}	5×10^{7}	3×10^{7}	7×10^{7}	7×10^{6}
(c)	2×10^{-1}	1×10^{7}	3×10^{3}	1×10^{5}	0
	2×10^{1}	3×10^{7}	7×10^{7}	4×10^{7}	1×10^{3}
	2×10^{3}	1×10^{8}	5×10^{7}	3×10^{7}	3×10^{4}
	2×10^{5}	3×10^{7}	4×10^{7}	4×10^{7}	7×10^{6}
(d)	6×10^{0}	4×10^{7}	4×10^{7}	6×10^{3}	2×10^{1}
	6×10^{2}	9×10^{7}	4×10^{7}	5×10^{5}	2×10^{2}
	6×10^{4}	5×10^{7}	4×10^{7}	7×10^{7}	2×10^{3}
	6×10^{6}	1×10^{8}	5×10^{7}	5×10^{7}	6×10^{6}

the bacterial population of medium incubated at 600 atm. Employing turbidity as a criterion of growth or reproduction, it was found that only seven out of a total of 63 species tested reproduced at 600 atm. The pressure tolerance of the 63 species, representing 10 different genera, recorded in Table III, is summarized as follows:

Number of bacterial cultures which:	*Hydrostatic pressure at 27° C*			
	1 atm	*200 atm*	*400 atm*	*600 atm*
Reproduced	63	48	35	7
Showed no change	0	10	17	33
Were killed	0	5	11	23

In interpreting these results, it should be noted that the organisms had been maintained in the laboratory for several years since their isolation from the sea. Whether their pressure tolerance changed during this period is problematical, although significantly those tolerating the highest pressures in general are species commonly found at greater depths in the sea. Most of the organisms, described by ZoBell and Upham (1944), were originally isolated from shallow water

TABLE III. Multiplication of Marine Bacteria as Indicated by Relative Turbidity in Sea Water Broth After Eight Days' Incubation at Different Hydrostatic Pressures at 27° C

	Hydrostatic pressures in atmospheres			
*Name or number of culture**	*one*	*200*	*400*	*600*
Achromobacter stenohalis	++++	−	−	K
Achromobacter aquamarinus	++++	++++	+++	−
Achromobacter stationis	++++	++++	++++	−
Achromobacter thalassius	++++	K	K	K
Actinomyces halotrichis	++	−	−	−
Actinomyces marinolimosus	++++	++++	−	−
Bacillus imomarinus	++++	−	−	−
Bacillus cirroflagellosus	++++	++	−	−
Bacillus epiphytus	+++	++	++	K
Bacillus submarinus	++++	+++	+++	−
Bacillus thalassokoites	++++	+++	+	−
Bacillus filicolonicus	++++	−	K	K
Bacillus abysseus	++++	++++	+++	−
Bacillus borborokoites	++++	++++	++++	+++
Flavobacterium marinotypicum	++++	++++	++++	−
Flavobacterium marinovirosum	++++	++++	++	−
Flavobacterium neptunium	++	+	−	−
Flavobacterium okeanokoites	++++	++++	+	−
Micrococcus aquivivus	++++	++++	++++	++++
Micrococcus sedimenteus	++++	++++	++++	K
Micrococcus maripuniceus	++++	++++	−	−
Micrococcus infimus	+++	++++	−	−
Micrococcus sedentarius	++++	++++	++++	−
Micrococcus euryhalis	++++	K	K	K
Pseudomonas enalia	++++	+++	−	K
Pseudomonas neritica	++++	++++	+++	K
Pseudomonas azotogena	++++	K	K	K
Pseudomonas vadosa	++++	++++	++++	−
Pseudomonas oceanica	++++	+++	++++	−
Pseudomonas felthami	++++	++++	++	−
Pseudomonas aestumarina	++++	−	K	K
Pseudomonas membranula	+	−	K	K
Pseudomonas stereotropis	++++	+++	+	K
Pseudomonas coenobios	++++	++++	++++	−
Pseudomonas obscura	++++	++++	++	−
Pseudomonas pleomorpha	++++	++++	++	−
Pseudomonas marinopersica	++	K	K	K
Pseudomonas periphyta	++	−	K	K
Pseudomonas hypothermis	++++	K	K	K
Pseudomonas perfectomarinus	++++	++++	+++	+++
Pseudomonas xanthochrus	++++	−	−	−

TABLE III. (*Continued*)

*Name or number of culture**	*Hydrostatic pressures in atmospheres*			
	one	*200*	*400*	*600*
Sarcina pelagia	++++	+++	+++	–
Serratia marinorubra	++++	++++	+++	–
Vibrio marinopraesens	++++	++++	+++	–
Vibrio algosus	++++	++++	++	+
Vibrio adaptatus	++++	+++	+++	K
Vibrio marinoflavus	+++	+++	+	K
Vibrio ponticus	++++	+++	++	K
Vibrio phytoplanktis	++++	++++	++++	+++
Vibrio haloplanktis	++++	++++	++++	+
Vibrio marinovulgaris	++++	+++	–	–
Vibrio marinofulvus	++++	++++	++	–
Vibrio marinagilis	++++	+	–	–
Vibrio hyphalus	++++	++++	K	K
Number 516	++++	++++	++	K
Number 549	++++	++++	+++	K
Number 595	++	–	–	–
Number 623	++	++	–	–
Number 632	++++	–	–	–
Number 633	++++	++++	–	–
Number 639	++++	++	K	K
Number 643	++++	++++	++++	++++
Number 689	++++	+++	–	K

* All except the numbered cultures have been described by ZoBell and Upham (1944).

++++ = good multiplication
+++ = fair multiplication
++ = less multiplication
\+ = poor multiplication
– = no multiplication, but organisms not killed
K = all bacteria in culture killed

TABLE IV. Morphological Variations of Marine Bacteria Induced by Hydrostatic Pressures Ranging from 200 to 600 atm After Four Days' Incubation at 27° C

Organism	*Morphological variations*
Bacillus abysseus	Increase in cell size and spore formation
Bacillus borborokoites	General increase in cell size
Micrococcus aquivivus	General increase in cell size
Sarcina pelagia	Increase in size and marked pleomorphism
Serratia marinorubra	Formation of long filaments and loss of motility
Vibrio phytoplanktis	Longer pleomorphic rods, granular, loss of motility
Culture no. 643	Long filament formation

environments and none of them came from depths exceeding 6,000 m where pressures are greater than 600 atm.

Examination of the bacteria with a phase microscope shortly after the cultures were removed from the pressure cylinders showed that many had undergone morphological alterations (Table IV). The commonest change in organisms that failed to reproduce at elevated pressures was an increase in cell size, especially in length. Pressure to the limit of tolerance nearly always induced marked pleomorphism and rendered the cells nonmotile. Several seemed to grow in size or length without any evidence of cell fission or reproduction.

DISCUSSION

Although our knowledge of the effects of pressure on organisms is still woefully scant, data summarized by Cattell (1936) show that pressures such as those that occur in the sea may have multiple physiological effects. Slightly increased pressures may be stimulatory, whereas higher pressures cause the attenuation or death of organisms. According to literature reviewed by Bridgman (1946), pressure affects the rate and direction of many chemical reactions. By virtue of its effect on solubilities and dissociation constants, the pH and Eh values of complex solutions may be affected by pressure. These and other properties of solutions affected by pressure may combine to influence the physiology and ecology of marine organisms in many ways.

Very little is known about the ability of organisms to adjust themselves to higher pressures. In the marine environment, where pressures range from one to somewhat more than 1,000 atm, organisms may become acclimatized to the pressures of their habitat range. The results presented in this paper substantiate the observations of ZoBell and Johnson (1949) that the pressure tolerance of marine bacteria is related to their depth habitat. The intolerance of certain bacteria for pressures exceeding 200 atm, for example, suggests that such organisms are not active in the sea at depths exceeding 2,000 m. On the other hand, finding bacteria at depths of several thousand meters that grow at atmospheric pressure but not at pressures isobaric with the environment where they are found raises the question whether such bacteria were active in situ or were in a state of dormancy.

Such questions must be answered before the marine microbiologist can hope to appraise the importance of bacteria as biochemical or geochemical agents in the deep sea. The effect of temperature must be taken into account in seeking the answers to such questions, because there is evidence that the pressure tolerance of organisms is

partly a function of the temperature. Although data to be detailed elsewhere show that the pressure tolerance of some bacteria is increased at elevated temperature, others seem to exhibit maximum pressure tolerance at the lowest temperature at which they are physiologically active.

While submarine pressures undoubtedly affect the distribution and physiological activities of bacteria, at no place in the sea will pressures prohibit the presence of bacteria, because mixed cultures have been shown to be alive and active at presssures higher than those characteristic of the most abyssal deeps.

SUMMARY

The optimal initial bacterial population in nutrient medium to give comparable results in pressure tolerance tests proved to be approximately 10^3 viable cells per ml.

Pressures ranging from 200 to 600 atm inhibited the normal growth of nearly all of the 63 different species of marine bacteria tested, although a few cultures of mixed microflora from deep sea sediments reproduced at pressures exceeding 1,000 atm. Out of 63 pure cultures tested, 15 failed to reproduce when subjected to a pressure of 200 atm at 27° C and 5 were killed in four days. Of the 28 that failed to reproduce at 400 atm 11 were killed, and of 56 that failed to reproduce at 600 atm 23 were killed by pressure.

The morphology of bacteria was affected by pressures ranging from 400 to 600 atm.

The distribution and physiological activities of bacteria in the sea are probably influenced by the hydrostatic pressures which increase per meter of depth by approximately 0.1 atm.

BIBLIOGRAPHY

Bjerknes, V. L. and J. W. Sandström
1910. Dynamic meteorology and hydrography. Part I. Statics. Publ. Carneg. Instn., No. 88: 3–146.

Bridgman, P. W.
1946. Recent work in the field of high pressures. Rev. mod. Phys., *18:* 1–93.

Cattell, M.
1936. The physiological effects of pressure. Biol. Rev., *11:* 441–476.

Certes, A.
1884. Sur la culture, a l'abri des germes atmosphériques, des eaux et des sédiments rapportés par les expéditions du "Travailleur" et du "Talisman." C. R. Acad. Sci., Paris, *98:* 690–693.

Regnard, M. P.
1891. Recherches expérimentales sur les conditions physiques de la vie les eaux. G. Masson, Paris. 500 pp.

ZoBell, C. E.
1946. Marine Microbiology. Chronica Botanica Co., Waltham, Mass. 240 pp.
1952. Bacterial life at the bottom of the Philippine Trench. Science (in press).
ZoBell, C. E. and F. H. Johnson
1949. The influence of hydrostatic pressure on the growth and viability of terrestrial and marine bacteria. J. Bact., *57:* 179–189.
ZoBell, C. E. and C. H. Oppenheimer
1950. Some effects of hydrostatic pressure on the multiplication and morphology of marine bacteria. J. Bact., *60:* 771–781.
ZoBell, C. E. and H. U. Upham
1944. A list of marine bacteria including descriptions of sixty new species. Bull. Scripps Inst. Oceanogr., *5:* 239–292.

THICK SOURCE ALPHA ACTIVITY OF SOME NORTH ATLANTIC CORES[1]

By

J. LAURENCE KULP, HERBERT L. VOLCHOK, H. D. HOLLAND, AND DAVID B. ERICSON

Lamont Geological Observatory
Columbia University
Palisades, New York

ABSTRACT

Six representative deep sea cores have been analyzed for their thick source alpha emission at about every 20 cm. Some correlation can be made with a calcium carbonate content but not with absolute surface area. The range of relative alpha activity is 2–3 counts/cm²/hr for sand, 2–4 for globigerina ooze, 4–6 for foraminiferal green clay, and 5–10 for fine white to red clay with low foram content. It appears that total alpha activity cannot be correlated simply with age as might be suggested from the Urry ionium vs. depth curves.

INTRODUCTION

Reconnaissance measurements of the radioactivity of deep core material have been carried out by several workers (Piggot and Urry, 1941, 1942a, b; Urry, 1949; Urry and Piggot, 1942; Evans, Kip and Moberg, 1938; Sanderman and Utterback, 1941; Utterback and Sanderman, 1948). Piggot and Urry determined the radium content of several North and South Atlantic cores; from their data they interpreted the radium vs. depth curve in terms of ionium decay and suggested some tentative dates for various depths. Since radon measurements (from which the radium content is calculated) are more difficult and time-consuming to use than direct alpha-counting, it was thought worthwhile to apply the latter technique to several representative cores. Provided the excess ionium and its decay products contribute a significant fraction of the total activity and provided the uranium and thorium series concentration in the bulk sediment is reasonably constant, a curve of total alpha activity vs. depth would show a maximum due to radium accumulation and ionium decay. Such a curve would permit age estimates to be made. As the following

[1] Contribution No. 45. Lamont Geological Observatory. The research reported in this document has been made possible through support and sponsorship extended by the U. S. Navy, Office of Naval Reseearch, under Contract n6onr 271 Task Order 18. This work is being used by H. L. Volchok as partial fulfillment for the degree of Master of Science at Columbia University.

results show, this simple picture is not observed in any of the cores measured. In spite of the negative result with regard to age determination, it is considered worthwhile to make these quantitative data available for other purposes such as stratigraphic correlation and sedimentation studies.

EXPERIMENTAL

The alpha activity was measured on thick sources by the scintillation method. The scintillation counting technique, developed in this laboratory for low level alpha activity measurement, is described elsewhere (Kulp, Holland and Volchok, 1952). By this method the reproducibility for the counting intervals used is about 2%. Duplicate analyses were made on a large portion of the samples included in this report, and in several cases three or four repeat measurements were made. The results are reported in counts/cm^2/hr. Conversion of this value to α/mg/hr involves a number of uncertainties, including the nature of the distribution of the radioelements, the uranium-thorium ratio, and the mineral densities. On this particular type of sediment, it is not considered likely that the surface contamination around grain boundaries, observed by Hurley (1950) for granites, is a major problem. However, there are other equally difficult things to consider, especially particle size and mineral distribution. Thin source and radon studies are in progress which will make it possible to determine the exact uranium-thorium ratio and the activity per unit mass.

The core samples were dried at 110° C, powdered to less than 200 mesh and placed in a circular tray within 0.5 mm of the silver activated zinc sulfide phosphor which is coated on the window of an RCA 5819 photomultiplier tube. Absolute calibration is obtained with thick sources containing known amounts of the uranium and thorium series in a silicate matrix obtained from the National Bureau of Standards (B. S. No. 11, No. 12).

Calcium carbonate determinations by standard gravimetric procedure were carried out on certain samples. Surface area determinations on some of the samples were made as described by Kulp and Carr (1952). Estimates of surface water temperature changes at the various core stations were made by Ericson. These are based on variation in the planktonic or floating species of foraminifera and therefore apply only to the uppermost few hundred meters of water.

RESULTS

Fig. 1 shows the location of the six cores investigated in this work and of one Kelvin core measured by Urry. Table I summarizes the geographical and depth data of each core. All of the cores except

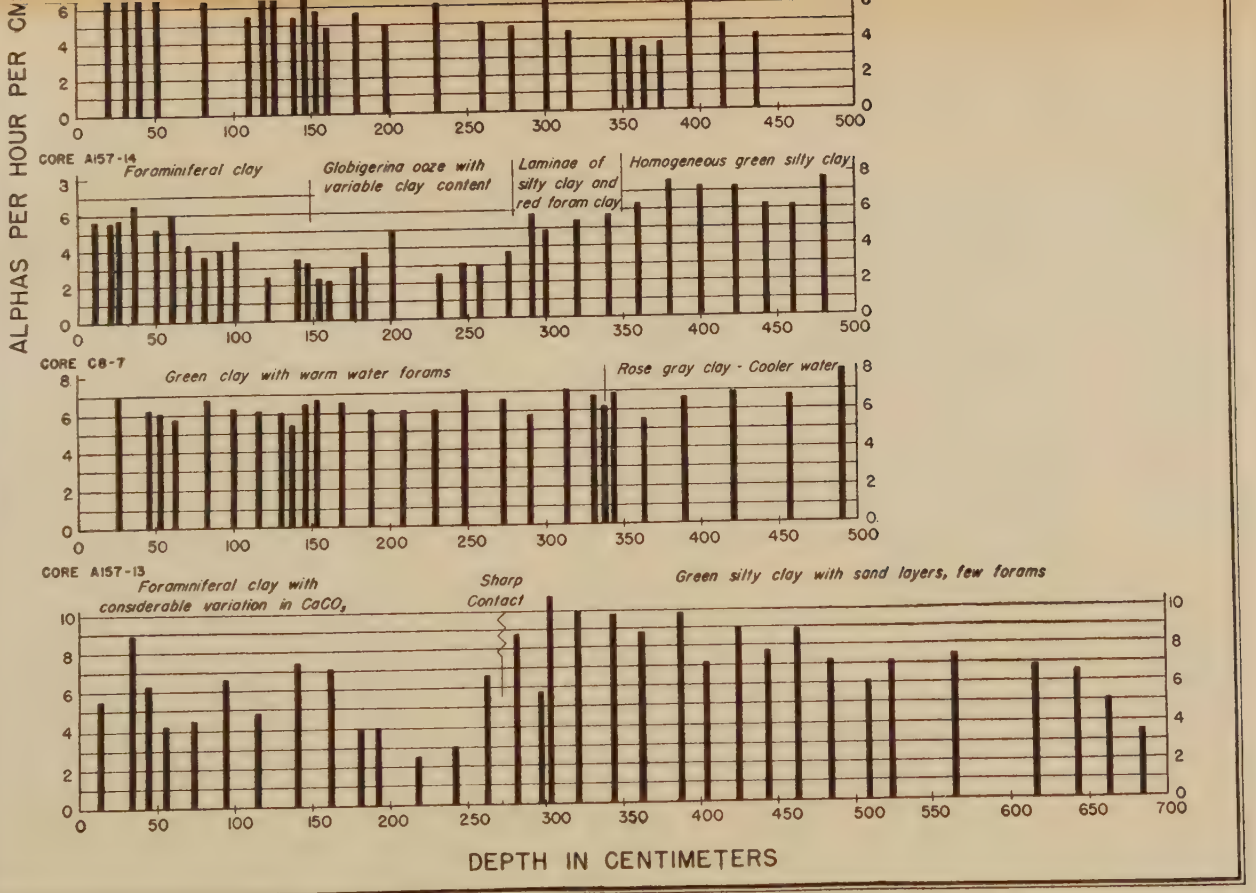
ALPHAS PER HOUR PER CM
CORE A157-14
Foraminiferal clay
Globigerina ooze with variable clay content
Laminae of silty clay and red foram clay
Homogeneous green silty clay
CORE C8-7
Green clay with warm water forams
Rose gray clay - Cooler water
CORE A157-13
Foraminiferal clay with considerable variation in $CaCO_3$
Sharp Contact
Green silty clay with sand layers, few forams
DEPTH IN CENTIMETERS

Figure 2. Bar graph of the thick source alpha activity.

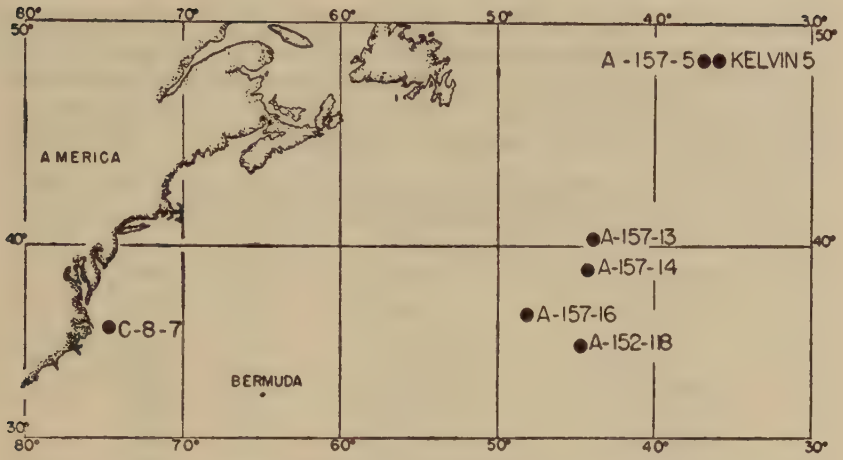

Figure 1. Location of cores.

TABLE I. Geographical and Depth Data of the Cores.

Core No.	*Lat.* (*N*)	*Long.* (*W*)	*Water Depth* (*m*)	*Core Length* (*cm*)	*Remarks*
C–8–7	35° 56′	74° 41′	1370	495	NE of Hatteras; 100 mi. off shore; shelf
A–157–5	48° 35′	36° 51′	4500	320	43.5 km W of Urry's core Kelvin 5
A–157–13	40° 30′	43° 50′	4680	720	167 km N of A–157–14; SW Grand Banks
A–157–14	39° 0′	44° 15′	4775	490	SW Grand Banks
A–157–16	36° 45′	48° 5′	5230	317	S of Grand Banks; 480 km S of Gulf Stream; SE of A–157–14
A–152–118	35° 07′	44° 40′	4340	645	Due S of A–157–14; NW Flank of Mid-Atlantic Ridge

C-8-7, which is a continental shelf core, are from the broad and relatively flat expanse of the central North Atlantic. Core A-157-5 was taken from a locality that is close geographically and similar topographically to the location of the Kelvin No. 5 core to which the Ionium Age Method has been applied by Piggot and Urry (1942b). If long-range stratigraphic correlation is possible, it should show up in these cores.

Fig. 2 shows bar graphs of the thick source alpha activity and a generalized lithologic description. This representation was chosen because the nature of sediment deposition does not necessarily follow smooth changes in composition.

Core C-8-7. Constancy in radon content for continental shelf sediment has already been reported by Urry and Piggot (1942). Core C-8-7, containing typical continental shelf sediments indicative of fairly rapid deposition, gives a total alpha activity that is remarkably constant, ranging from 4.15 to 6.23 $\alpha/cm^2/hr$. The average

TABLE II. Relation of Total Alpha Activity to Surface Area for Specimens from Core C–8–7.

Depth (cm)	*Surface Area* (m^2/gm)	$\alpha/cm^2/hr$
26	10. ± 0.4	5.35
53	12.7 ± 0.5	4.68
99	12.1 ± 0.5	4.85
130	11.7 ± 0.5	4.65
145	12.5 ± 0.5	4.96
188	10.3 ± 0.7	4.73
227	11.1 ± 0.4	4.68
330	14.0 ± 0.5	5.20
340	15.5 ± 0.5	5.33
343	10.7 ± 0.4	5.33
361	17.3 ± 0.5	4.20
487	12.6 ± 0.5	6.21

alpha activity is 5.00 $\alpha/cm^2/hr$. The top two-thirds of the core consists of rather homogeneus green mud with warm water forams. At a depth of 335 cm there is a sharp change from green mud to rose-gray clay that corresponds to a warm-to-cold surface water temperature transition. However, this abrupt change is not reflected in the alpha activity. Such a situation may be expected if the detrital material is from a constant source and if the major fraction of the activity is from the interior of the mineral grains. The color change was superficial, therefore, so far as the major mineral composition is concerned. Table II shows the relation of total alpha activity to surface area for selected specimens of this core.

It is clear from the data in Table II that there is no correlation of surface area of the sediment with alpha activity, which suggests that the major fraction of the activity lies within the particles rather than on the surface. This in turn indicates that any adsorption process makes a second order contribution to the total activity of this type of sediment unless some minor constituent adsorbs most of the radioelements, which is considered unlikely. Such an adsorption process is probably occurring (Holland and Kulp, 1952) but is masked by the bulk activity.

Core A-157-5. This is the northernmost of the remaining five cores from the North Atlantic basin, and it was chosen for study due to its

proximity to a core studied by Piggot and Urry (1941). The first 75 cm consist of a reasonably homogeneous foraminiferal gray clay in which the total alpha activity appears to be related to the surface water temperature during deposition (see Table III). Around 100 cm the rapid variations in alpha activity appear related to the sand

TABLE III. Alpha Activity in Samples of Core A-157-5, Arranged in the Order of Increasing Temperature as Estimated from the Faunal Array

Depth (cm)	$\alpha/cm^2/hr$
15	5.42
65	5.09
55	4.92
10	4.92
30	4.60
40	4.51
45	4.51

concentration. At this depth the washed sediment consists of about 95% heterogeneous sand, with granules up to 4 mm in diameter, whereas mechanical analyses of washed samples showed 50% sand at 90 cm and 40% at 110 cm. While these mechanical analyses were not obtained for samples from exactly the same depths as the alpha counts, the general trend is considered significant. From 120 cm to the bottom of the core the sediment consists of a reasonably uniform foraminiferal clay with minor variations. It seems that this core is relatively homogeneous in broad aspect and should therefore be usable for age determination by the ionium method. Radon measurements are now being carried out on this core to study this possibility.

Some surface area data are also available for this core, and in Table

TABLE IV. Relation of Total Alpha Activity to Surface Area for Specimens from Core A-157-5

Depth (cm)	*Surface Area* (m^2/gm)	$\alpha/cm^2/hr$
10	18.8	5.16
23	27.8	4.35
43	22.5	4.60
63	24.5	5.06
84	28.8	5.28
112	32.7	4.85
155	18.3	4.16
186	14.2	4.13
222	31.1	4.80
248	17.8	4.06

IV they are compared with the alpha activity. Again the correlation of surface area with alpha activity is negative, although the surface areas are considerably higher on the average than those in core C-8-7.

Core A-157-13. This sample was taken 1520 km SW of A-157-5, and in general the alpha activity is double that in core A-157-5. Core A-157-13 is relatively nonhomogeneous down to 270 cm. From

TABLE V. Sand Concentration and Alpha Activity in Core A-157-13

Depth (cm)	*Sand concentration (%) in washed samples*	$\alpha/cm^2/hr$
180	95	3.91
60	85	4.18
160	20	6.25
40	15	7.10
140	1–2	7.37

200 cm down the sediment is a foraminiferal clay with varying sand concentration, and it appears that the alpha activity in this zone may be correlated with sand content, as is shown by the data in Table V. In this section also there are two thin layers of globigerina ooze, but these were not alpha counted. The sample at 215 cm lies in a globigerina ooze layer and thus might be expected to show a low activity. The sample at 240 cm consists largely of foram shells and sand grains. From 273 cm down the core consists primarily of a green silty clay with a few sandy layers such as those at 295, 400, 505, 660, and 680 cm. Again it appears that the total thick source alpha activity is reasonably constant for a constant sediment type but that it is directly affected by the concentration of carbonate shells and sand. The extent of the effect can be predicted qualitatively.

The contact between the two sediment types at 273 cm is so sharp that it could represent an unconformity. This break is also distinct in the alpha activity (see Fig. 2). There is no apparent correlation in alpha activity or lithologic type between cores A-157-5 and A-157-13.

Core A-157-14. This core was taken 201 km directly south of A-157-13. The top 10 cm consists of globigerina ooze with an alpha activity below 5 $\alpha/cm^2/hr$. The 10-150 cm section consists of a fairly homogeneous foraminiferal clay which shows a suggestion of an Urry-type curve. At 150 cm the sediment becomes a globigerina ooze with considerable variation in clay content until the green silty clay begins to appear at 275 cm alternating with thin layers of red foraminiferal clay. At 340 cm an impure sand occurs with an activity of 5.23 $\alpha/cm^2/hr$; this compares closely with the activity of similar sand

layers (295 and 660 cm) in the green silty clay section of core A-157-13. Below 350 cm the core consists of a homogeneous green silty clay that is similar to the lower part of A-157-13 and is probably correlative with it; this part of A-157-14 contains more forams than the similar sediment in A-157-13, which suggests why the alpha activity ranges from 6.5–7.3 $\alpha/cm^2/hr$ instead of 6.5–9.5 $\alpha/cm^2/hr$, as in A-157-13.

Core A-157-16. This core appears to have been taken south of the glacial zone, since it is long enough to be Wisconsin but contains no glacial marine layers. It consists of a pink to gray foraminiferal clay.

TABLE VI. Carbonate Data for Core A-157-16

Depth (cm)	*% $CaCO_3$*	*$\alpha/cm^2/hr$*
5–6	15	5.56
11–12	26	5.40
16–17	28	5.18
23–24	26	5.75
27–28	19	8.47
31–32	26	7.75
36–37	29	6.85
44–45	28	6.46
52–53	6	7.66
64–65	8	6.78
71–72	22	6.55
84–85	10	6.80
91–92	9	5.95
103–104	13	6.78

Some inhomogeneity is observed in the first 30 cm, but at 30 cm there is a lithologic break which is reflected in the alpha activity. Another such break, which is not as evident in the alpha activity, occurs at about 53 cm. The alpha activity ranges from 5–8 $\alpha/cm^2/hr$, and there is a downward trend from 30 cm to the bottom of the core which suggests an ionium decay curve. Compared to A-157-13 and A-157-14, this core is quite homogeneous.

In this core it is evident that other factors are more important in determining the total alpha activity than the fluctuation of calcium carbonate content from 6–29%. See Table VI for carbonate data obtained for this core.

Core A-152-118. This was located 501 km south of A-157-14. The top 30 cm consist of a clayey globigerina ooze, and from 30–80 cm the sediment is a reddish calcareous clay which changes to a gray-white clayey ooze to 270 cm. A similar clay with a faint pink color occurs from 270–300 cm and then turns gray from 300–340 cm. From

TABLE VII. $CaCO_3$ Content and Alpha Activity of Core A-152-118

Depth (cm)	*% $CaCO_3$*	*$\alpha/cm^2/hr$*
	Red Calcareous Clay (few forams) (30–80 cm)	
30	48	4.00
80	30	4.41
40	25	4.93
	Gray-white clay ooze (80–270 cm)	
263	45	2.89
162	45	2.77
180	35	3.25
200	32	3.40
	Pink Calcareous Clay (abundant forams) (350–442 cm)	
370	52	2.00
360	45	2.23
350	45	2.39
442	40	2.42
420	35	2.78
400	25	3.59

TABLE VIII. Surface Area and Alpha Activity for Core A-152-118

Depth (cm)	*Sample Area (m^2/gm)*	*$\alpha/cm^2/hr$*
30	34.1	4.00
40	29.7	4.95
52	27.1	4.3
75	32.5	3.8
147	23.3	7.0
162	——	2.7
181	21.7	3.1
200	23.7	2.9
263	25.3	3.0
283	22.1	2.8
305	18.0	3.8
321	——	2.4
350	——	2.2
360	15.8	2.2
380	18.8	2.0
400	30.1	3.7
410	24.2	2.8
442	——	2.4

340–490 cm the core is a pink to red calcareous clay with an abundance of forams. In these sections a correlation can be shown between the calcium carbonate content and the alpha activity (Table VII), providing samples of identical lithology are compared. Again it appears that the total alpha activity is determined by the radioactive elements within mineral grains, not on the surface. Table VIII shows some surface area data for this core.

CONCLUSIONS

The alpha activity of samples from six representative deep sea cores has been determined. The thick source alpha count ranges from 1.6–3.2 $\alpha/cm^2/hr$ for sand and globigerina ooze, from 4.0–5.6 $\alpha/cm^2/hr$ for foraminiferal green clay, and 6.5–9.7 $\alpha/cm^2/hr$ for fine red clay with low foram content.

Although certain sediment types have distinct total thick source alpha activity ranges, there is considerable overlap. The actual alpha activity measured is determined to a large extent by such variables as the per cent of foraminiferal shells, the concentration and radioactivity of the sand grains, and the composition of a particular clay type. It appears that the greatest determinant of activity is the mineral composition of the particles. However, it is possible that coprecipitation brings in considerable alpha activity to the sediment. Limited qualitative correlation is possible between the total alpha activity and $CaCO_3$ content or sand content, both, however, being limited to zones of similar lithology. In the cases of A-157-13, A-157-14 and of A-152-118, A-157-16, comparison of the sediment type and the alpha activity at certain depths does not appear to yield stratigraphic correlation except for the distinctive green silty clay which appears at 339 cm in A-157-14 and at 273 cm in A-157-13. This may be due to the fact that the cores were taken at too great a distance from each other. It should be noted, however, that since the alpha activity varies considerably outside of the experimental error it would seem that stratigraphic correlation by such a method might be possible if cores sufficiently close in geographic location were studied.

It may be concluded from this study that total thick source alpha counting is inadequate for age determination of the sediment layers by the ionium method.

LITERATURE CITED

Evans, R. D., A. F. Kip and E. G. Moberg
1938. The radium and radon content of Pacific Ocean water, life and sediments. Amer. J. Sci., (5) *36:* 241–259.

Holland, H. D. and J. L. Kulp
1952. Mechanism of the removal of radioelements from the ocean (in preparation).
Hurley, P. M.
1950. Distribution of radioactivity in granites and possible relation to helium age measurement. Bull. geol. Soc. Amer., *61:* 1–7.
Kulp, J. L. and D. R. Carr
1952. Surface area of deep sea sediments. J. Geol. (in preparation).
Kulp, J. L., H. D. Holland and H. L. Volchok
1952. Low level alpha counting on rocks and minerals by the scintillation method. Trans. Amer. geophys. Un. (in preparation).
Piggot, C. S. and W. D. Urry
1941. Radioactivity of ocean sediments. III. Radioactive relations in ocean water and bottom sediment. Amer. J. Sci., *239:* 81–91.
1942a. Radioactivity of ocean sediments. IV. The radium content of sediments of the Cayman Trough. Amer. J. Sci., *240:* 1–12.
1942b. Time relations in ocean sediments. Bull. geol. Soc. Amer., *53:* 1187–1210.
Sanderman, L. A. and C. L. Utterback
1941. Radium content of ocean bottom sediments from the Arctic Ocean, Bering Sea, Alaska Peninsula, and the coasts of southern Alaska and western Canada. J. mar. Res., *4:* 132–141.
Urry, W. D.
1949. Radioactivity of ocean sediments. VI. Concentrations of the radioelements in marine sediments of the southern hemisphere. Amer. J. Sci., *247:* 257–275.
Urry, W. D. and C. S. Piggot
1942. Radioactivity of ocean sediments. V. Concentrations of the radioelements and their significance in red clay. Amer. J. Sci., *240:* 93–103.
Utterback, C. L. and L. A. Sanderman
1948. Radium analyses of marine sediments in northern Pacific and adjacent waters. J. mar. Res., *7:* 635–643.

MARINE LEPTOPEL, ITS RECOVERY, MEASUREMENT AND DISTRIBUTION[1]

By

DENIS L. FOX, JOHN D. ISAACS AND EUGENE F. CORCORAN

University of California
Scripps Institution of Oceanography
La Jolla, California

ABSTRACT

Leptopel, the colloidally or otherwise finely particulate organic and inorganic detritus suspended in natural bodies of water, varies in chemical composition and in relative quantities with reference to depth, latitude and proximity to land. The leptopelic material may be quantitatively recovered by passing the water through an ultrafilter of inert, insoluble adsorptive powder. Apparatus has been designed to so recover such samples *in situ* at various depths.

Leptopelic organic matter is present in rich concentrations in the feces of filter-feeding animals, which rely upon a constant supply of it as a source of nutrition; it is present also in marine slicks, especially in association with the surfaces of temporarily entrapped fine silt particles. Fine bottom deposits in regions near shore adsorb considerable quantities of organic detritus as well, while larger inorganic particles, such as sand, furnish less surface per unit of mass for physical attachment. Far smaller quantities of suspended organic matter have been recovered from deep water samples than from those near the surface. Feces from the California mussel, a detritus-feeding filterer, and leptopel from coastal slicks have yielded considerable proportions of organic nitrogen.

Emphasis is given to the significance of organic leptopel in biochemical cycles of the sea, involving the release of inorganic nitrogenous and phosphatic molecules by bacteria, the reassimilation of these soluble molecules by phytoplankton, and the *a priori* correlation between amounts of leptopel and populations of living communities.

INTRODUCTION

Oceans, estuaries and inland bodies of water contain varying amounts of suspended *leptopel*, which is composed of finely particulate dispersed mud or sludge of organic and inorganic composition (λεπτο-, fine, thin: πηλος, mud or clay). Such materials, ranging in size from finely colloidal micelles to minute visible particles and including intimately associated micro-organisms such as bacterial cells, will vary in quantity and in chemical constitution with reference to latitude, depth, season and proximity to land.

[1] Contribution from the Scripps Institution of Oceanography, University of California, New Series No. 568.

Leptopel may be properly regarded as an attenuated hydrosol, the colloidal micelles of which, due to their constituent organic matter, may readily become somewhat concentrated at the water surface and at water-solid interfaces, there reducing the interfacial tension in accordance with the important principle first delineated by Willard Gibbs. At the surface of relatively quiet waters, the aggregations of leptopelic material may constitute extensive thin floating scums or slicks, readily observable by their contrasting optical properties. These effects are generated through diminution of the surface tension, rendering the water surface more elastic and resulting in substantial reduction in the height of the capillary waves (Ewing, 1950; Schmidt, 1936; Hardman, 1941).

The marine colloidal matter, when adsorbed to solid surfaces, such as those of submerged rocks, pilings, ships' hulls, sand or finer sediments, may assume the form of curds or of a more or less continuous semiliquid gel, muddy slime, or *pelogloea* (from πηλος + γλοια, slime, gum or oil). Sapropel is a special accepted term applied to the soft thin carpet of sludge or mud, rich in organic matter, lying upon some areas of the ocean floor.

It is manifest that the chemical, biological and sedimentational features, as well as the optical and surface studies in the realm of hydrography, must of necessity include serious consideration of leptopelic substances. The richness of bacterial flora, the production of soluble compounds of nitrogen, phosphorus and sulphur and their availability as plant nutrients, and indeed the level of general biological productivity, all must be intimately associated with the quantities of unorganized organic matter present in surrounding waters (cf. Keys, Christensen and Krogh, 1935). The physical and chemical character of sediments and the biochemical reactions occurring in them must vary greatly in accordance with the amounts of organic detritus adsorbed to the component silt, clay or sand.

Of salient interest to the marine biochemist is the direct utilization of finely particulate organic matter as a food by countless species of animals, whether by filtering the leptopel from the water with cilia, mucus-sheets, sieves, setae, or combinations of any of these, by scraping or sucking the pelogloea from solid surfaces, or by swallowing masses of whole sand, mud or sapropel at the shore line or at greater depths. Regions of relatively high leptopel concentration (e. g., near areas of river mouths, of sewage outfalls or of terrestrial run-off, or at gradually sloping rocky shores) will be expected to harbor the more dense populations of animals, including not only those species which subsist directly upon the finely divided organic matter but various

predatory forms as well (e. g., sea-stars, larger crustaceans, carnivorous mollusks and fishes) which devour the whole bodies or the gametes of herbivores and detritus-feeders (Fox, 1950).

Inorganic materials, suspended in the sea or floating on its surface, carry attached organic substances. For example, in tide pools formed in the sand about the pier pilings at the Scripps Institution and open to intermittent exchange of water at low tide, flakes of mica and other sand components float upon the water surface. Such material, collected upon a fine filter-membrane and dried overnight in an oven at temperatures reaching 120°, has shown, on ashing, that there are losses of from 1.07 to 1.32% in weight, representing the approximate amount of adsorbed organic matter (cf. beach-sand; Fox, Crane and McConnaughey, 1948).

Again, analyses of feces from a marine detritus-eating filter-feeder, the California mussel (*Mytilus californianus*), throw further light upon the composition of leptopelic marine detritus. Such material has shown an average ash content of 69.1%. Organic nitrogen (by Kjeldahl analysis) shows an average value of 1.1% which, when multiplied by the conventional factor of 6.25, gives approximately 6.9% protein in the whole feces or some 22.3% protein in the total organic matter in the feces. Lipids may amount to as much as 12%, or 38.7% of the organic fraction, leaving about 39% as carbohydrates or other components (cf. Fox and Coe, 1943).

Kalle (1946) has reported that yellow, blue-fluorescing ulmic acid-like derivatives, arising from such materials as decaying wood, peat, etc., reflect, by their relative concentrations, the quantities of terrestrial organic matter introduced by runoff into coastal waters.

Suspended materials in the English Channel have been studied by Armstrong and Atkins (1950). Some of the suspended solids were recovered by collecting water in wooden vessels and by passing large volumes of it through filter paper and through "Gradocol" membranes. The coarser particles retained in typical analyses yielded about 1 mg/l. Residual colloidally dispersed material yielded traces of ash, involving about 60% SiO_2 and some 13% Fe_2O_3. The Tyndall beam was observed to persist in filtrates which had passed membranes of 0.2μ average pore diameter.

Dried, ignited residues reportedly ranged from 2.77 to 0.45 ppm, while the organic matter, measured in a few analyses by drying at 100°, amounted to about 1.5 ppm. While the porosity of the filters used by Armstrong and Atkins suggest that recovery was incomplete, the persistence of the Tyndall beam in the filtrates bearing out such a conclusion, the data agree rather well with the results obtained at La

Jolla. The British workers found in the ash of their recovered solids the following components in respective proportions: SiO_2, 17 to 55%; Fe_2O_3, 3 to 28%; Al_2O_3, 1 to 20%; and $CaCO_3$, 9 to 70%.

Comparative turbidimetric measurements of sea water samples have been conducted by Jerlov (1951), who employed the relative intensity of Tyndall scattering for following water movements in estuaries and through straits.

Investigations of marine leptopel are being pursued with the expectation that quantitative data may be gathered relative to the amounts and variations in colloidal and other particulate organic matter according to depth, latitude, season, and proximity to shore. Such data, it is hoped, may afford a correlative parameter that will supplement surveys of microplankton populations, studies of concentrations of dissolved oxygen, phosphate, nitrate and silicate, and observations of similar factors associated with marine biological productivity.

The presence of leptopel may be demonstrated by the gray or bluish Tyndall cone that is produced when a glass vessel (preferably a Florence flask) filled with sea or tap water is illuminated in a darkened room by a bright light (e. g. from a carbon arc) which passes through an adjustable slit or iris diaphragm and which is brought to a focus within the body of the fluid by means of a supplementary lens. The Tyndall cone is intensified by minimizing stray light and by placing the flask against a dark background; or better, black paint may be applied to the outer half of the flask's surface opposite the viewer.

After all colloidal and other finely suspended matter has been removed by passing the water through a sufficiently fine ultrafilter and collecting it in a scrupulously clean container, under appropriate illumination the water now manifests only the quality of a barely perceptible, soft blue-violet Tyndall cone which is given by twice-distilled water, as described by Lord Rayleigh and by Wood (1934, Chap. XIII). This so-called Rayleigh scattering is characteristic of pure air, pure water, and other homogeneous fluid molecules.

MATERIALS AND METHODS

(a) *Collection by Adsorption.* The finely suspended matter may be quantitatively removed by passing the aqueous system through a short layer of finely powdered adsorptive inorganic material. Selection of an insoluble and relatively inert adsorbent permits quantitative investigations to be carried out on the particulate materials. For this purpose, various finely powdered or somewhat gelatinous compounds have been employed, including MgO, $MgCO_3$, Fe_2O_3, $CaCO_3$, $Mg(OH)_2$, kaolin, talc and cellite (or Hyflo Super-cel, a refined diatoma-

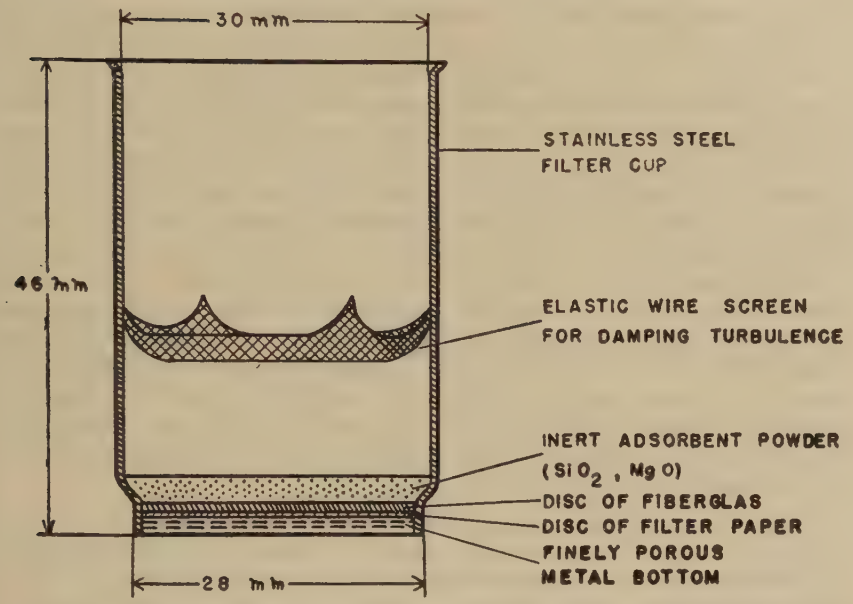

Figure 1. Diagram of stainless steel filter crucible, containing glass-cloth pad supporting inert adsorbent powder; ready for use.

ceous earth, substantially pure SiO_2). Repeated investigations have been carried out on the complete adsorptive removal of finely dispersed protein micelles from aqueous systems, e. g., dilute sols of gelatin, egg albumin, hemoglobin, the latter two forming micelles of very small size (McBain, 1950: 128–129), or mixed fresh materials such as breis of mussel tissues. A separate report by Fox, Kittredge and Oppenheimer will deal with the quantitative adsorption achieved with the use of a mixture of equal weights of pure MgO and SiO_2 (Hyflo Supercel).

It is necessary to employ amounts of the adsorbent in such excess as to assure quantitative adsorption of all particulate materials. Since most natural waters are extremely dilute disperse systems, the required excess of adsorbent is easily achieved by the method outlined below.

One or two grams of powder (equal weights of MgO and cellite) packed into a filter-cup (30 mm diameter) provide an operating column of adsorbent material some 6 to 8 mm high, which is sufficient to adsorb in a thin layer (1 to 2 mm) all colloidal material commonly encountered in large volumes of sea water. Standard glass crucibles with fritted glass bottoms are suitable in the laboratory, but for work at sea, similar cups of stainless steel are used because of their ruggedness (Fig. 1).

The clean porous cup is fitted into its adaptor, which is then inserted into the mouth of a filter-flask, preferably a Fisher filtrator (see below). To keep the fine powder from clogging the pores, a loosely fitting disc of No. 50 Whatman filter paper is laid on the floor of the cup, after which the paper is moistened with distilled water and drawn to a smooth coverage of the fritted area by applying gentle suction. No wrinkles should be allowed to remain in the paper, since they may serve as channels for the escape of some of the adsorbent. A disc of clean glass cloth (Fiberglas) of equal diameter is then placed over the paper disc in order to isolate the powder from this potential source of organic contamination; the glass disc is dampened and drawn by suction uniformly against its substrate in the manner previously described. Equal parts (usually 0.5 g each) of floury Hyflo Super-cel and pure finely powdered MgO are intimately mixed in a small quantity of pure distilled water (or in previously filtered, colloid-free sea water if necessary), and the suspension is poured carefully down a stirring rod onto the bottom of the filter-cup.[2]

The system is allowed to stand for about five minutes, thus providing time for most of the suspended powder to settle, after which some of the water is slowly drawn through by gently opening the vacuum line. Drawing through *all* of the water, thus exposing the filter-bed directly to the atmosphere, commonly leads to the formation of cracks and channels and to shrinkage from the walls of the cup. Should such channels occur through inadvertent exposure of the powder-cake, these should be filled with additional absorbent powder in suspension before conducting the ultimate filtration.

The preliminary filtration of reagent-water should proceed until a clear filtrate is obtained; this is frequently achieved at the outset or after only a small volume has been delivered within the first few minutes. Filtration is then halted *gently*, i. e., by gradually opening an intake valve in the vacuum line to avoid jarring the filter-pad loose from its firm seating. The design of the Fisher filtrator provides against such a contingency.

The prepared filter is permitted to stand, filled with water and undisturbed until ready for use. When collections are to be made

[2] In this operation a saturated solution of $Ca(OH)_2$ may be employed instead of water alone in order to provide sufficient traces of alkali to coat the adsorbing surfaces with $Mg(OH)_2$, which is generated at once upon introduction of sea water. Excessive $Ca(OH)_2$ gives rise to sufficient $Mg(OH)_2$ to clog the filter; use of the powdered lime itself is therefore to be avoided. Even the saturated $Ca(OH)_2$ solution should be omitted if a balanced sea-water filtrate is desired for a biological medium.

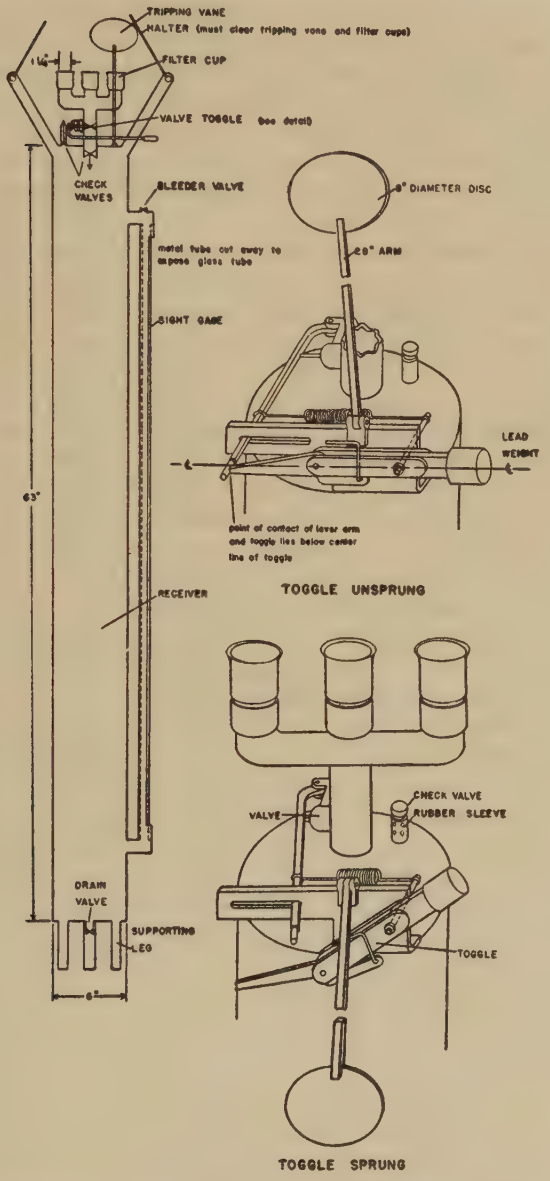

Figure 2. Diagrammatic sketches of the Scripps Subsurface Autofiltrator and of detailed parts.

from aboard ship with the use of the subsurface autofiltrator (developed by J. D. Isaacs; see Fig. 2), a stiff elastic screen of stainless steel wire is pressed into the mouth of the cup for a short distance. This is to preclude possible disturbance of the filter-bed by inrushing water following any spillage of the resident water from its cup while the gear is being lowered away. The buffering screen is omitted during laboratory operations, where cautious procedures may be assured.

Water to be transferred to the laboratory for analysis is best collected directly into clean bottles of inert water-repelling plastic material. This procedure provides against accidental breakage, affords a degree of lightness, and should minimize adsorption of the colloidal materials to the walls of the container. Such potential sources of loss may be further reduced by adding one or two grams of the powdered adsorbent to the container before or at the time of collection, provided the sample in each collecting vessel is destined for quantitative adsorptive recovery upon a single filter.

Should a delay of some hours be anticipated before water samples can be analyzed, mercuric chloride may be added to give a dissolved concentration of about 0.1 g/l; such procedure serves as a preservative against bacterial degradation of the organic matter.

(b) *The Subsurface Autofiltrator.* In operations at sea, an important requirement in the quantitative sampling of leptopelic material *in situ* at any desired depth is to minimize contact of the raw water with any save the actual filtering surface. With this in mind, several alternative operations may be considered briefly before we describe the means which have been adopted as best satisfying requirements.

(1) Pumping water from selected depths through long tubes to a filter on deck, or collecting it in wooden, glass or metallic containers for subsequent filtration aboard ship. These devices are undesirable because: The adsorption of interfacially active colloidal materials to the extensive solid surfaces would create errors; later, after repeated operations, a degree of sloughing (or desorption) of accumulated films from such devices might substantially contaminate the samples to be filtered and analyzed.

(2) The alternative use of a pump aboard ship, drawing water through a filter installed at the end of a hose paid out overside. This procedure would involve several disadvantages: It would limit the pressure gradient to a low value, i. e., the prevailing barometric pressure, minus the height of the pump above the sea surface, minus the ambient vapor pressure of the water; the additional difficulties involved in storing and handling long tubes of fairly large diameter

would limit such a system to the use of relatively coarse filters at shallow depths.

(3) Subsurface collections made with a submerged pump, designed to draw the water directly through the juxtaposed filtering medium by providing a high gradient *in situ*. Such apparatus would possess the manifest advantage of minimizing time and area of prefiltering contact for processing large quantities of water at gradients limited only by the absolute hydrostatic pressure at the depth of operation. Disadvantages in such a design include not only the necessity of supplying a source of power and a metering system but the practically unavoidable risk of contaminating the collected residues with droplets of lubricating oil from the pump. However, a unique system may be applicable to filtration of samples while the ship is underway. This would involve submergence of the instrument to desired depths with a depressor (Isaacs, 1951) and the employment of the Venturi principle to obtain the required pressure gradients. The comparatively slow rates of water passage through a fine adsorptive powder filter would permit a multiplication of Venturi units, i. e., a small unit operating in the region of high velocity produced by a larger unit. Preliminary calculations have yielded promising indications for the application of such devices.

The subsurface autofiltrator which has been developed at the Scripps Institution is of reasonably simple and rugged design and is shown in Fig. 2. It utilizes a large heavy cylindrical receiver which permits the gradient between its interior (at atmospheric pressures or evacuated if necessary) and the ambient hydrostatic pressures outside to effect filtration of the water at the desired depth. The device is not lubricated, and it requires no mechanical metering system, since the filtered water is retained and can be measured directly at the end of the operation in a calibrated sight gauge. The factors of large size and bulkiness are relatively minor, since modern oceanographic gear is adapted for ready manipulation of large and heavy equipment.

The tripping mechanism is of somewhat unique design and deserves some detailed description. The toggle is designed to preserve its balance under conditions of severe linear shock, provided there be no actual contact with the tripping device itself. This design is achieved by balancing the first moment of mass about the fixed pivot.

It is to be remembered that the moment of the notched outer arm of the toggle is only its reaction at the central pivot. Having calculated this value, we then affixed an equivalent mass at the central pivot and balanced the mechanism against gravity around the fixed pivot. With a trapezoidal outer arm of thickness t, of density ρ, of length L and of major and minor altitudes A and B respectively, the reaction of the central pivot (R_1) is:

$$R_1 = L^2 t \rho \left(\frac{A + 2B}{6}\right).$$

With an equivalent mass suspended at the central pivot, the lead counterweight is adjusted to produce a balance about the fixed pivot (see Fig. 3). The mechansim in current use has received heavy

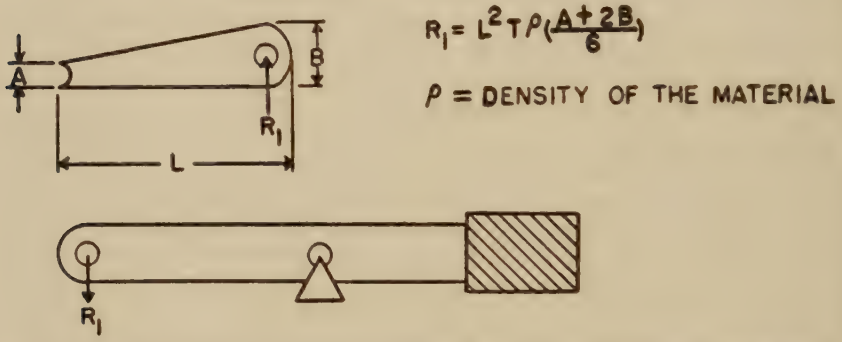

Figure 3. Representation of the forces involved in the tripping mechanism of the Scripps Subsurface Autofiltrator.

mechanical shocks without resultant tripping of the cocked toggle.

Accidental tripping of the toggle through premature falling of the vane (e. g., due to the roll of the ship or to wave action) is precluded by the length of the vane arm. The force of the arm against the toggle trigger should exceed by three- or four-fold that which is necessary to produce tripping. This requirement is readily calculated from the force relationships in the toggle (see Fig. 4).

The required thickness of the cylinder wall is calculated from the relationship:

$$P = \left(\frac{2E}{1-\mu^2}\right)\left(\frac{(t)}{D}\right)$$

where P = collapsing pressure, μ = Poisson's ratio, t = thickness of wall, D = diameter to neutral axis, and E = Young's modulus.[3]

The thickness of the glass walls of the sight gauge may be selected in accordance with similar analysis, but adequate strength is to be found in any boiler gauge material adapted to meet high pressures.

In operations at sea, the stainless steel filter cup (or each of these if two or three are employed in order to shorten the filtration time) is furnished with the powdered filtering material in the manner previ-

[3] From "Implosion of cylinders," W. H. O. I. Report (unpublished).

ously described. An elastic stainless steel wire screen is pressed firmly into position at about half the depth of each cup, which is then filled with water. The toggle is cocked and the tripping vane is attached and held in a nearly vertical position with a single band of glued paper tape (a weak junction of paper readily torn apart when wet is preferable). To preclude the filtration of any sea water before the gear has

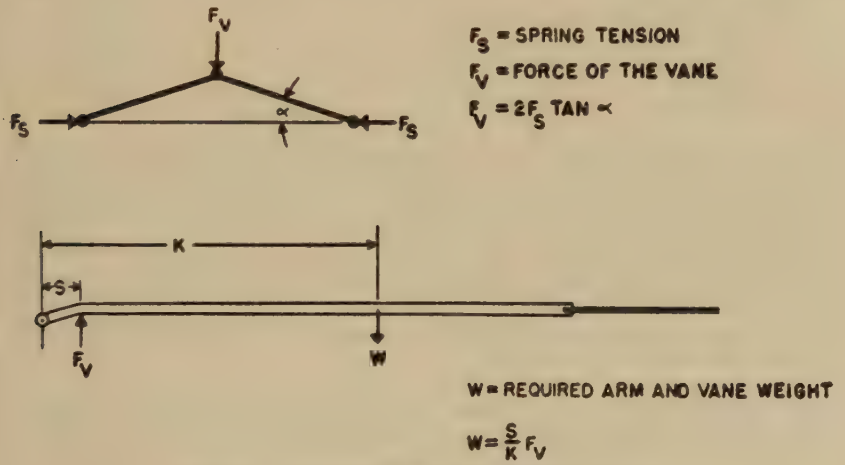

Figure 4. Diagram of force relationships in toggle.

been lowered to the desired depth, the short tube or filter manifold above the valve is filled with water until very little air space remains in the adaptors.

The prepared filter cups are now fitted into the open adaptors, which are supplied with rubber sleeves. With the tripping vane held in position by hand or by weak tape, depending on the amount of freeboard of the vessel and on the rapidity of lowering, the assemblage is lowered over the ship's side and the supporting cable is paid out to permit rapid sinking until the required depth has been achieved.[4]

When the cable meter indicates the required depth, lowering is abruptly halted, whereupon the tripping vane rotates into its downward position and its arm trips the toggle; thus the valve beneath the filter manifold is opened and the passage of water is initiated through the adsorptive powder and into the reservoir below. The time re-

[4] If lowering is accomplished rapidly enough, the vane arm will not fall sufficiently to trip the toggle before immersion and descent of the apparatus serves to prevent this; should the freeboard be too great to risk abortive tripping, the single lashing with paper tape may be applied, since this will come free shortly after submergence

quired for the collection of adequate samples (ca. 20 l of filtered water in the current model) will depend upon the hydrostatic pressure of each sampling depth and upon the fineness of the powder and the length of the powder column. Suggested intervals for the collection of from 15 to 20 l are as follows:

Depth	*Time Interval*
On surface (with evacuated chamber)	30 min.
50 m (unevacuated chamber)	20 min.
100 m	15 min.
300–1000 m	10 min.

As the instrument is raised the pressure of the expanding air within the top of the cylinder closes a check valve in the filtering manifold, thus halting filtration and precluding passage of air with destruction of the filter pad. The air now escapes through another check valve on the top of the cylinder. At the surface the volume of filtered water is recorded from the calibrated sight gauge. The filter cups are removed and the filtrator reservoir is emptied by opening the drain and bleeder valves (see Fig. 2).

(c) *Chemical Analysis.* Once the colloidally dispersed substances have been adsorbed upon a pad of inert inorganic powdered material, it is possible to determine approximate concentrations of numerous constituents in terms of milligrams per liter of water filtered. Lipid materials may be extracted with organic solvents; chlorophyll or its porphyrin derivatives, as well as carotenoids, may be similarly recovered and measured photometrically; colloidal iron oxides and colloidal phosphate may be recovered and measured by special methods. Retained organic carbon and organic nitrogen may be determined. Preliminary reports of the methods and findings regarding the latter two components are given in this paper. Discussion of other constituents will be reported elsewhere.

The organic nitrogen content of adsorbed leptopel was determined by the Kjeldahl method; the sample was completely digested with boiling conc. H_2SO_4, and the resulting NH_3 was distilled from the alkalized system into a saturated boric acid solution and measured volumetrically (from a semimicroburette in this work) by titration with dilute standard HCl, using methyl orange as indicator.

The organic carbon content was measured by a rapid titration method outlined by Waksman (1936: 404–405). The reagents used are: (1) about 0.4 N chromic and sulphuric acid solution prepared by dissolving 40 g of $K_2Cr_2O_7$ (or 32 g CrO_3) in 1 l of H_2O, to which is added

conc. H_2SO_4 (sp. gr. 1.84) to give 2 l of solution when cool; (2) about 0.2 N acidic ferrous ammonium sulphate, prepared with 80 g of the salt $(Fe(NH_4)_2\ (SO_4)_2 \cdot 6H_2O)$ and 20 ml of conc. H_2SO_4/l of solution, which is ultimately standardized with 0.1 N $KMnO_4$ solution; 1 ml of the ferrous ammonium sulphate solution is taken as equivalent to 0.6 mg of organic carbon, or to 1.034 mg of humus. (3) Diphenylamine indicator prepared with 0.5 g dissolved in 100 ml conc. H_2SO_4 + 20 ml water.

Each sample (i. e., the powdered filter pad) is transferred to a 100 ml Erlenmeyer flask; to each flask is next added a considerable excess (usually 10 ml) of the chromic acid solution. After either a small funnel or a Pyrex "cold-finger" (a short round-bottomed tube of cold water, fitting the opening of the flask and covering its mouth with a flanged rim) is inserted into each flask, the contents are heated to the boiling point and kept moderately boiling for five minutes. The contents of each flask, after cooling, are transferred quantitatively into a beaker or a large flask of about 400 ml capacity which contains about 250 ml of distilled water. Care is taken to rinse into the receiver any material that adheres to the funnel or cold finger or remains in the boiling flask. Ten drops of the indicator commonly suffice to impart a distinct violet-blue color to the solution, which is now titrated with the ferrous reagent until there is a sharp change to grayish green which becomes a deeper green on standing.

Multiplying the factor 0.6 by the difference between the observed titration figure and that of the control (i. e., 10 ml of chromic-sulphuric acid solution alone, previously boiled and diluted in the same manner) yields the empirical figure for the organic carbon content of the sample.

It is to be emphasized that the quantity of chromic acid reduced will naturally vary somewhat in accordance with the condition of the organic carbon involved, e. g., the degree in which it may already have been combined to some extent with oxygen, as in carbohydrate material $(CH_2O)_n$ or alternatively in a more reduced state, as in fatty acids, hydrocarbons, long-chain alcohols, and the like (CH_3-CH_2-CH_2 . . .). The factor adopted applies to humic materials in general and has been retained throughout in the present work, since a part of our program deals with the determination of organic carbon of marine humus in sediments; it is highly probable that most samples of suspended leptopel will contain varying amounts of the relatively refractory humic material.

Table I shows a summary of quantitative findings relative to the amounts of leptopelic organic matter in marine waters and in other

TABLE I. Results of Quantitative Studies of Leptopelic and Pelogloeal Organic Matter, Collected and Analyzed in Various Ways.

Material	*Method of Collection*	*Method of Analysis*	*Organic C*	*Organic N*	*Other Material*	*Total Organic Matter*
1. Beach sand	Manual	Dry combustion				0.7%*
2. Floating mica	By aspiration	Dry combustion				a. 1.07% b. 1.32% av. = 1.2%
3. Mussel feces	Voided by freshly collected mussels	Organic matter by combustion; organic N by Kjeldahl; lipid-soluble matter by extraction with organic solvents		a. 1.02% b. 1.06% c. 1.19% d. 1.13% av. = 1.1% or 1.1 × 6.25 = 6.87% protein	Lipid-sol matter 3.7% (or ca. 12% of total organic matter)	a. 36.2% b. 30.7% c. 25.7% d. 31.1% av. = 30.9%†
4. Sedimentary component of a marine slick	In bottles, from surface, by G. C. Ewing	Wet chromate combustion of sediment				27.65%
5. Water from a slick area near shore in San Diego Harbor a. turbid water from slick surface b. clear water 6″ beneath slick c. clear water from rippled surface	In bottles, from surface, by G. C. Ewing	Organic C by wet chromate combustion of adsorbed filter residues; organic N. by Kjeldahl analysis of similarly recovered material	a. 6.77 mg/L b. 4.16 mg/L c. 5.9 mg/L C/N a. = 9.55 C/N b. = 9.25 C/N c. = 9.42	a. 0.71 mg/L = 4.44 b. 0.45 mg/L = 2.78 c. 0.63 mg/L = 3.94 } mg protein/L		C × 1.8 N × 17 a. 12.20 12.05 b. 7.48 7.58 c. 10.70 10.54 av. a. 12.12 mg/L av. b. 7.53 mg/L av. c. 10.61 mg/L
6. Water from various oceanic depths off San Diego a. 9 l from 150 m, 32° 37′ N, 120° 29′ W b. 20 l from 600 m c. 20 l from 300 m d. 20 l from 100 m (all 3 samples from station at 33° 02′ N, 118° 59′ W)	Subsurface autofiltrator	Organic C by wet chromate combustion of adsorbate on Super-cel + M_gO, 1:1	a. 0.47 mg/L b. 0.14 mg/L c. 0.16 mg/L d. 0.17 mg/L			C× 1.8 a. 0.85 mg/L b. 0.25 mg/L c. 0.29 mg/L d. 0.30 mg/L
7. Water from slick areas San Diego Channel a. from surface b. from near bottom (ca 10 m deep) c. from surface d. just beneath surface	In bottles, by G. C. Ewing and M. W. Johnson; preserved with H_gCl_2 at time of collection	Wet chromate combustion of adsorbate on Super-cel + $Ca(OH)_2$, 1:1	a. 17.66 mg/L b. 19.64 mg/L c. 11.61 mg/L d. 6.71 mg/L			Org. C × 1.8 a. 31.7 mg/L b. 35.3 mg/L c. 20.9 mg/L d. 12.1 mg/L
8. Oceanic bottom mud, from station 32° 37′ N, 120° 29′ W (cf. item 6 in this table) a. 0–1 inch depth of mud b. 3–4 inch depth of mud c. 10–11 inch depth of mud	In coring sampler	Wet chromate combustion			Ash (%) H_2O (% in dried samples by difference) a. 88.29 7.73 b. 85.59 11.32 c. 85.64 10.74	Org. C. (%) Org. matter (%) (C × 1.7) 1.88 3.20 1.56 2.65 2.01 3.42

* Fox, Crane and McConnaughey, 1948.

† Fox and Coe, 1943; Fox, Updegraff and Novelli, 1944.

marine materials. It will be observed that concentrations of organic matter are relatively high in shallow waters near shore, especially in the vicinity of marine slicks (e. g., from about 7.5 to as high as 35 mg/l), while in water from considerable depths far from shore the values are relatively low (from 0.25 to 0.85 mg/l). In the data at hand there are higher concentrations of organic matter in the former than in the latter environment by some 40-fold.

Solid materials such as mussel feces or silt from a floating slick are relatively rich in organic matter, while beach sand and fine bottom sediments adsorb quantities of organic materials that yield intermediate values which are in rather good agreement with data presented by Revelle and Shepard (1939: 245–282).

It is also to be observed that the organic material recovered from both mussel feces and from a slick (items 3 and 5 respectively in Table I) were relatively rich in nitrogenous material. The four analyses of mussel feces yielded 17.6, 21.5, 28.9 and 22.7%, with an average value of 22.6% "protein," while the material from the slick gave 36.6, 36.9 and 37.1% respectively or an average figure of 36.9% "protein."

DISCUSSION

A brief review of relative masses of animate and unorganized colloidal or otherwise particulate organic matter in the sea may be of interest. The fact has been emphasized that "in any area of biological productivity, the total quantity of unorganized, raw material must considerably exceed the mass of organized living matter." (Fox, 1950; cf. also Keys, Christensen and Krogh, 1935).

Sverdrup, et al. (1942: 250–251, 912) have emphasized this point, citing the work of Krogh and of Bond (1933). While Krogh estimated that the "dissolved" organic material exceeds the "particulate" organic matter by some 300-fold, Bond's figures indicate a preponderance of only 76.9%, or some 3.3-fold of such "dissolved" organic matter over the combined amounts of net plankton and nannoplankton. Bond's investigations, carried out in waters near Friday Harbor, which are characteristically rich in phytoplankton, yielded average figures of 0.03, 0.03 and 0.20 mg-at C/l of water in net plankton, nannoplankton and dissolved organic matter respectively. These figures, multiplied by 12 to give mg of carbon, and by the factor of 2 to convert to organic matter, are 0.72, 0.72 and 4.8 mg/l. Bond's term "dissolved" naturally refers to colloidal and other suspended matter as well as such materials as may have been in true solution.

Reviewing the data obtained at La Jolla (including those presented here and by Fox and Coe, 1943) and those of Brandt (1898), we arrive

at some interesting approximate ratios of living phytoplankton to unorganized organic detritus in local waters. Living phytoplanktonic organisms in waters off La Jolla may supply average amounts of organic matter such as the following:

Dinoflagellates (ca.10,000/L; 2×10^{-5} mg organic matter/cell)	0.2 mg/L
Diatoms (ca.20,000/L; 1.5×10^{-6} mg organic matter/cell)	0.03 mg/L
Bacteria (ca.45,000,000/L; 5×10^{-11} mg organic matter/cell)	0.002 mg/L
	ca. 0.23 mg/L

Now, if we take 5 mg/l as an average value for total colloidal or otherwise finely particulate organic matter, the living fraction would appear to be only some 4% of the total; but if we should adopt the figure of 15.3 mg/l (the average value of collective data in items 5 and 7, Table I), then the proportion of living cells would appear to be only about 1.5% of the total.

Marine biochemical cycles undoubtedly entail close parallelism between fluctuations in populations of microplankton and concentrations of suspended organic detrital materials. It would be unlikely that the mass of living cells, even of phytoplankton, should exceed that of suspended detritus in any area, save for relatively brief periods.

ACKNOWLEDGMENTS

The authors gladly acknowledge the cooperation of the following: Dr. Roger Revelle for advice, encouragement, and for aid in making available the deep oceanic samples; Dr. Gifford C. Ewing and Dr. Martin W. Johnson for collection of certain water samples in the vicinity of slicks; Mr. Wheeler J. North for helpful advice and for preparing the drawings; the Rockefeller Foundation for a grant in aid of this research, and the Bureau of Ships of the United States Navy for supporting the development of the activating mechanism of the autofiltrator.

SUMMARY

The nature, methods of quantitative recovery, chemical measurements, and distribution of organic materials in marine leptopel are discussed.

Marine detrital organic matter is relatively concentrated in solid material such as the feces of filter-feeding animals, in finer sediments on the ocean floor or in fine silt temporarily suspended in surface slicks. It shows intermediate concentrations in waters removed from

the vicinity of slicks and is recoverable in relatively low concentrations from water a few hundred meters in depth, at some distance from shore.

The quantitative determination of organic leptopel is discussed as a useful parameter in studying marine biochemical cycles, and discussion is given to the general ratio between the weight of organic matter in living microplankton and the total mass of organic substances in suspended marine detritus.

REFERENCES

Armstrong, F. A. J. and W. R. G. Atkins
1950. The suspended matter of sea water. J. Mar. biol. Ass. U. K., *29:* 139–143.

Bond, R. M.
1933. A contribution to the study of the natural food-cycle in aquatic environments. Bull. Bingham oceanogr. Coll., *4* (4): 1–89.

Brandt, K.
1898. Beiträge zur Kenntnis der chemischen Zusammensetzung des Planktons. Wiss. Meeresunters., Abt. Kiel. N. F. *3:* 45–90.

Ewing, Gifford
1950. Slicks, surface films and internal waves. J. Mar. Res., *9:* 161–185.

Fox, D. L.
1950. Comparative metabolism of organic detritus by inshore animals. Ecology, *31:* 100–108.

Fox, D. L. and W. R. Coe
1943. Biology of the California sea mussel (Mytilus californianus). II. Nutrition, metabolism, growth and calcium deposition. J. exp. Zool., *93:* 205–249.

Fox, D. L., S. C. Crane and B. H. McConnaughey
1948. A biochemical study of the marine annelid worm, Thoracophelia mucronata. Its food, biochromes and carotenoid metabolism. J. Mar. Res., *7:* 567–585.

Fox, D. L., D. M. Updegraff and G. D. Novelli
1944. Carotenoid pigments in the ocean floor. Arch. Biochem., *5:* 1–23.

Hardman, Yvette
1941. The surface tension of Wisconsin Lake waters. Trans. Wis. Acad. Sci. Arts Lett., *33:* 395–404.

Isaacs, J. D.
1951. Homogeneous Depressor. Progress Report, Bureau of Ships. Rep. Scripps Inst. Oceanogr., 51–10. Aug. 1, 1951. 5 pp. plus 3 plates.

Jerlov, N. G.
1951. Optical measurement of particle distribution in the sea. Tellus, *3:* 122–128.

Kalle, Kurt
1946. Fluoretzung und Gelbstoffgehalt im Bottnischen und Finnischen Meerbusen. Unpubl. Sci. Rep., Serial No. 28 from Deutsch. Hydrogr. Inst., U. S. Hydrographic Office.

Keys, A., E. H. Christensen and A. Krogh
1935. The organic metabolism of sea-water with special reference to the ultimate food cycle in the sea. J. Mar. biol. Ass. U. K., *20:* 181–196.
McBain, J. W.
1950. Colloid Science. D. C. Heath and Co., Boston. 450 pp.
Revelle, Roger and F. P. Shepard
1939. Sediments off the California coast. In Recent Marine Sediments, Amer. Ass. Petrol. Geol., Tulsa, Okla. 736 pp.
Schmidt, W.
1936. Causes of 'oil patches' on water surfaces. Nature, Lond., *137:* 777.
Sverdrup, H. U., M. W. Johnson and R. H. Fleming
1942. The Oceans. Prentice Hall, Inc., New York. 1087 pp.
Waksman, S. A.
1936. Humus. Williams and Wilkins, Baltimore. 494 pp.
Wood, R. W.
1934. Physical Optics. MacMillan, New York. 846 pp.

ON THE STABILITY OF GAS BUBBLES IN SEA WATER[1]

By

JEFFRIES WYMAN, JR.,[2] P. F. SCHOLANDER,[3]
G. A. EDWARDS[4] AND L. IRVING[5]

ABSTRACT

Laboratory experiments have been performed to determine the rate of solution and the change in composition of air bubbles in stirred sea water as a function of depth (0–200 m) and temperature (1–27° C). At each depth the shrinking of the diameter is nearly linear. This rate of solution increases with increasing pressure up to a limiting value which is almost reached at a depth of 20 m. The rate of disappearance of a bubble is only imperceptibly influenced by temperature. When a bubble of air dissolves at a given depth it becomes richer in nitrogen until a final constant composition is reached. This final nitrogen percentage increases with increasing depth. Equations have been developed, based on the theory of diffusion, which satisfactorily account for the observed facts.

INTRODUCTION

There are many biological processes known where free gases are produced under water: gas bubble formation as a result of decomposition of organic material in lakes and swamps and in the sea, and gas bubbles from water plants as a result of photosynthesis. In many cases gases are carried by plants and animals either externally or internally or both. Gas bubbles also appear in the blood of higher organisms as a result of sudden decompression, giving rise to what is commonly called "bends." The mechanisms of gas bubble formation have been admirably treated by E. N. Harvey and coworkers (1944). The present study deals mainly with the fate of a bubble after it has been formed.

When gas is produced in the form of free bubbles, the partial pressures of the components within the bubbles are likely to be different from the partial pressures of the same components in the water, and hence gas exchange takes place. In sea water the partial pressures of the dissolved atmospheric gases are usually close to those in the atmosphere. This holds true very exactly for nitrogen at all depths

[1] Contribution No. 600 from the Woods Hole Oceanographic Institution. This investigation was made in 1943 under contract with the Navy Department, which has given permission for its publication.

[2] Now at the Department of Biology, Harvard University.

[3] Now at the Marine Biological Laboratory, Woods Hole.

[4] Now at the Department of Biology, Tufts College.

[5] Now at the Arctic Health Research Center, Anchorage, Alaska.

(Rakestraw and Emmel, 1938; Hamm and Thompson, 1941). Any bubble in water will be at a total pressure of one atmosphere plus the prevailing hydrostatic pressure; hence it will finally dissolve. Since different gases have different solubility and diffusion characteristics, the composition of a bubble will change during the process. We have studied the rate of disappearance and the change in composition of dissolving gas bubbles at different depths by introducing bubbles into stirred sea water under pressures corresponding to depths as great as 200 m. Both disappearance rates and changes in composition have been found to follow simple physical laws that can presumably be applied also to other gases in less simple systems; the analysis we have given should be useful as a basis of calculation and interpretation to other investigators concerned with problems of gas exchange, respiration, and the like.

METHODS

Both low and high pressure systems were used to expose bubbles of gas to stirred water at different hydrostatic pressures and temperatures. The low pressure system is shown in Fig. 1B. A 300-cc glass bulb furnished with a vaccine stopper at one end and a piece of pressure tubing at the other is suspended on two bearing posts in a waterbath. The pressure tubing leads to a mercury leveling bulb which is suspended from a swivel so that the bulb can be elevated to any desired height. Through the injection port an air bubble can be introduced into the 300-cc bulb completely filled with water; the bulb is rotated by a simple drive so as to keep the bubble close to the center. The diameter of the bubble is measured through an ocular micrometer after stopping the rotation. The corresponding volume is found from an empirical calibration involving introduction of bubbles of known volume from a capillary syringe analyzer furnished with a hypodermic needle (Scholander and Roughton, 1942). The bubble is then withdrawn and analyzed with the same instrument. Pressures up to 20 m can be handled by this system.

For pressures corresponding to those at depths of 20 to 200 m, a pressure cylinder was employed which was fitted with a window and pressure gauge (see Fig. 1A). A large centrifuge tube containing about 300 cc of sea water is wedged into the cylinder. This tube is closed with a rubber stopper containing two holes, one for introduction of bubbles, the other connected with a syringe. The syringe ensures an anaerobic, sensitive pressure transmission between the nitrogen gas in the cylinder and the water containing the bubble. The desired pressure is furnished from a nitrogen cylinder. The instrument is rotated horizontally in a waterbath at a speed sufficient to keep the bubble

near the center of the water column. After stopping the rotation, the diameter of the bubble is measured through the glass window by means of an ocular micrometer, using an empirical calibration as described for the low pressure system. The sea water used in the experiments was filtered and equilibrated with air at the desired waterbath temperature.

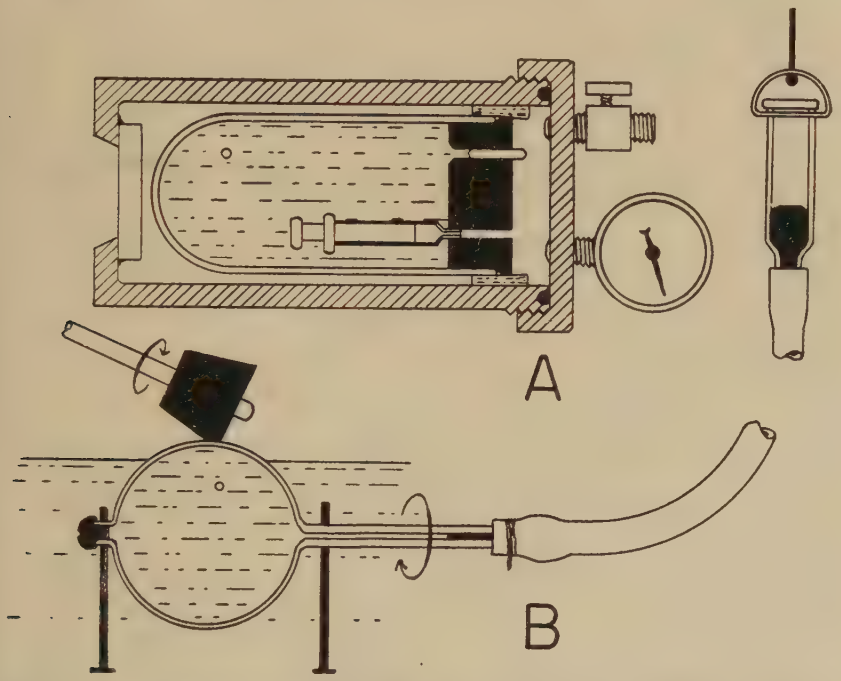

Figure 1. Methods for studying disappearance rate and changes in composition of bubbles under various hydrostatic pressures. A. The high pressure system. B. The low pressure system.

It should be pointed out that the amount of water used in both types of apparatus is so large that the solution of the bubble does not increase the concentration of dissolved gas enough to change the diffusion gradient by as much as one per cent.

RATE OF SOLUTION OF AIR BUBBLES IN RELATION TO PRESSURE

The first experiments were made to determine the rate of solution of a single bubble of air as a function of pressure. The results obtained are summarized as follows:

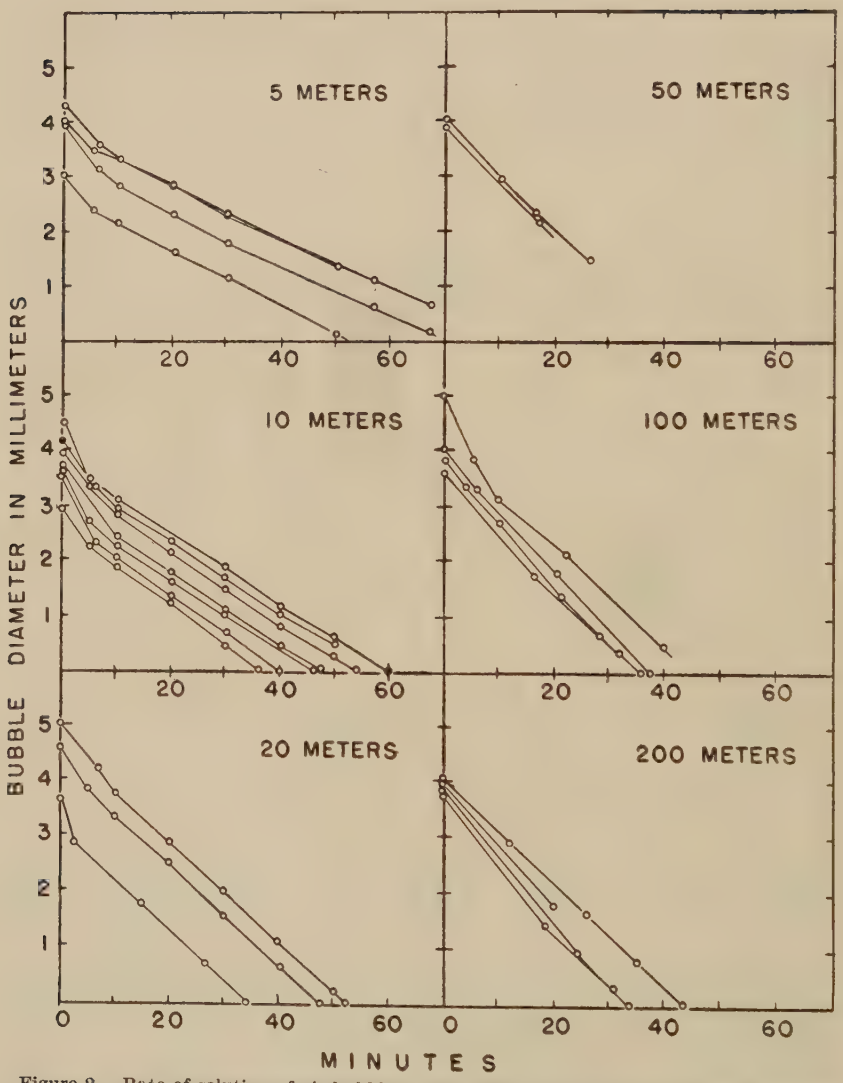

Figure 2. Rate of solution of air bubbles in sea water in relation to hydrostatic pressure (depth). Sea water was saturated with air at normal atmospheric pressure.

(a) As a bubble dissolves there is, at any given pressure, a nearly linear decrease in its diameter with time until it is too small to be seen. Actually the initial rate of shrinkage is always somewhat greater than the subsequent rate (Fig. 2).

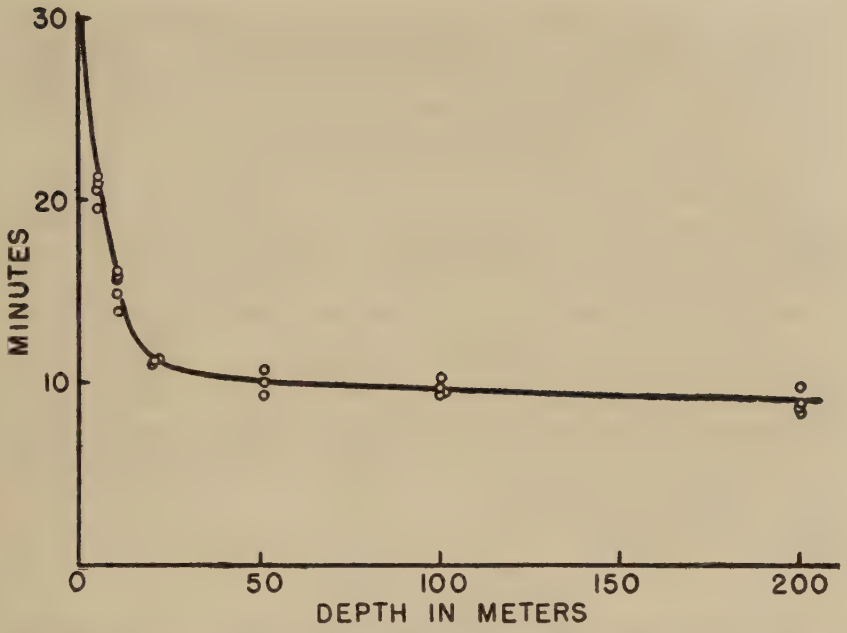

Figure 3. Minutes required to diminish bubble diameter 1 mm at various depths. Sea water was saturated with air at normal atmospheric pressure.

(b) The rate of solution increases with pressure but approaches an upper limiting value at high pressures. In Fig. 3 the average rate of disappearance of the bubbles is represented in relation to pressure.

(c) The rate of disappearance of a bubble does not vary significantly with temperature in the range from 1 to 27° C. Table I shows the figures obtained at a total pressure of 2 atm. (depth, 10 m).[6]

TABLE I

Temp., °C.	*Decrease of Bubble Diameter (mm/min.)*
1	.065–.068 (4 observations)
15	.065–.069 (7 observations)
27	.068–.069 (2 observations)

These results indicate that below 10–15 m the lifetime of an air bubble of given size should not vary much with depth and should be nearly proportional to the diameter. A bubble 2 mm in diameter would last about 20 minutes.

[6] Of course the total pressure includes the pressure of one atmosphere which prevails at the surface.

This very simple behavior of a bubble can be accounted for, as a first approximation, by a correspondingly simple treatment based on the principles of diffusion. Due to the relative motion of the water and the bubble, we assume that the composition of the water in respect to dissolved gas is everywhere uniform except in a thin shell surrounding the bubble and that the gas in the bubble is uniform right up to the gas-water interface. The inner layer of water in the shell will be in equilibrium with the gas, and the whole of the diffusion gradient which causes the gas to pass from the bubble to the water will be supported by the shell. We assume further that this gradient is uniform throughout the shell. Also, we ignore the fact that the gas actually consists of oxygen and nitrogen, and we treat the situation as if only one kind of molecule were present with a single diffusion constant.[7] We introduce n to denote the number of moles of gas in the bubble; p, the pressure in the bubble; r, its radius; p_o, the partial pressure of the gas in the water everywhere outside the thin shell; t, the time; R, the gas constant; and T, the absolute temperature. Then, from the gas law:

$$n = \frac{1}{RT}\frac{4}{3}\pi r^3 p \,. \qquad (1)$$

Also, from Fick's first law, which relates the amount of material which diffuses through unit area to the product of the concentration gradient and the diffusion constant:

$$\frac{dn}{dt} = -\,\delta 4\pi r^2 (p - p_o) \,. \qquad (2)$$

In this expression δ is a proportionality constant which depends on: d, the thickness of the shell; on Δ, the diffusion constant of the gas in the water: and on α, the solubility of the gas in the water, in accordance with the relation

$$\delta = \frac{\Delta\alpha}{d} \,;$$

α is involved because of the necessity of converting the expression $(p - p_o)$ on the right of (2) into a concentration difference. By

[7] The uniformity of the gradient is a necessary consequence of Fick's second law of diffusion in any situation involving a steady state. In the present case the pressure of the gas within the bubble, which is the same as the hydrostatic pressure, remains constant, and the concentration of gas in the surrounding water is likewise constant. Therefore there must be a steady state as regards the concentrations of gas on the two sides of the diffusion layer except for changes of composition.

differentiating (1) with respect to time and combining the result with (2) we obtain the following expression for the rate of change of the radius of the bubble with time:

$$\frac{dr}{dt} = - RT\delta \frac{(p - p_o)}{p}. \tag{3}$$

The underlying basis for this result is that the pressure in the bubble depends on its volume whereas the amount of gas which escapes by diffusion depends on its surface.

Equation (3) accords with the results summarized above.

(a) It shows that for any value of p, corresponding to any given depth,[8] the value of $\frac{dr}{dt}$ should be constant. That is, the radius or diameter of the bubble should decrease uniformly with time.

(b) It describes the effect of pressure on the rate of disappearance of the bubble, at least as a first approximation. For example, at the surface $p = p_o = 1$ atm., and $\frac{dr}{dt} = 0$, as we know it must. At a depth of 10 m, $p \cong 2$ atm. At this depth

$$\frac{dr}{dt} = - \frac{RT\delta}{2}.$$

At 200 m, where $p = 21$ atm.,

$$\frac{dr}{dt} = - RT\delta \frac{20}{21},$$

or about twice this. The limiting value of $\frac{dr}{dt}$ for very great depths is of course $-RT\delta$, or twice that at 10 m. This is close to what is observed (see Fig. 2 and Table II).

(c) It accounts for the fact that the rate of solution of a bubble is essentially independent of temperature. It will be seen that this rate is proportional to the absolute temperature and to the product of the

[8] It should be emphasized that p is the total pressure of the gas in the bubble: i.e., 1 atm. at the surface. We take no account of the slight additional pressure due to surface tension. This is equal to $\frac{2\gamma}{r}$, in which γ is surface tension (for water, $\gamma = 72.8$ dynes/cm at 20°). For the smallest visible drop, of diameter say 0.1 mm, this will amount to 30,000 dynes/cm^2 (= 0.03 atm. = 30 mm water), which is too small to be of consequence. (Below 0.1 mm the pressure due to surface tension mounts rapidly and soon becomes the dominant factor.)

diffusion constant Δ times the solubility α of the gas. Of the latter quantities the first (Δ) increases while the second (α) decreases with temperature, so that their product may be expected to remain roughly constant. No data appear to be available on the diffusivities of oxygen and nitrogen as a function of temperature, but the figures given in International Critical Tables show that from 10 to 21° the diffusivity

TABLE II

Meters	$-\frac{dr}{dt}$ *(cm/sec)*	$\frac{p - p_o}{p}$	$\delta\left(\frac{moles}{cm^2\ sec\ atm}\right)$
	(observed)		*(calculated)*
5	4.0×10^{-5}	1/3	5.0×10^{-9}
10	5.4×10^{-5}	1/2	4.5×10^{-9}
20	7.6×10^{-5}	2/3	4.8×10^{-9}
50	8.3×10^{-5}	5/6	4.1×10^{-9}
100	8.8×10^{-5}	10/11	4.0×10^{-9}
200	9.2×10^{-5}	20/21	4.0×10^{-9}

of hydrogen in water increases from 4.3 to 5.2 cm^2sec^{-1}. Over the same range the solubility coefficient of nitrogen decreases from .0186 to .0152. If the proportional change in the diffusivity of nitrogen were the same as that of hydrogen, the product $\Delta\alpha$ would change by only about one per cent between 10 and 21° and could be regarded as essentially independent of temperature. As a first approximation, the same conclusion may be applied to air. Since the range of absolute temperature covered by the experiments is small, we should therefore expect the rate of solution of the bubble to be nearly independent of temperature, as it is.

A more quantitative indication of the essential correctness of this interpretation is afforded by the constancy of the values of δ calculated by equation (3) from the experimental data, taking RT as 2.4×10^4 cc atm./mole, which corresponds to 20°. The constancy of the values of δ so calculated is shown in Table II, where the values listed for $\frac{dr}{dt}$ are those obtained by averaging the results of the various experiments, taking the final constant value of the rate in each case. It is seen that the values of δ are indeed fairly constant but that they show a real decrease with p. In all probability this is to be correlated with the fact that the bubble consists of two gases, oxygen and nitrogen, which, under the conditions of the experiment, leave the bubble at different rates and that the percentage of nitrogen in the bubble during the majority of its life is higher at the higher pressures. In the next sec-

tion we shall deal with the question of the composition of the bubble and its effect on the rate of solution.

Added confirmation of the simple picture given above is provided by observations on the rate of disappearance of an air bubble at 2 atm. (10 m) into degassed sea water. The observed rate is $\frac{dr}{dt} = 0.06$ mm/min. This is the same, within the limits of error, as the observed value for 100 or 200 m (0.055 mm/min.). This is as it should be, for in the case of degassed water, $p_o = 0$ and (3) reduces to

$$\frac{dr}{dt} = - RT\delta ,$$

which is the same as the limiting form approached by the equation for great depths ($p \rightarrow \infty$) when $p_o = 1$.

Before we conclude this section it is important to point out that the results on the rate of disappearance of an air bubble in water are in general agreement with much cruder results on the rate of accumulation of gas in a cavity produced by suddenly and forcibly withdrawing and briefly holding back the piston of a syringe while the nozzle is kept closed. The amount of gas which would be expected to enter the cavity produced under these conditions may be roughly estimated by means of equation (3). For this purpose we set $p = 0$ and $p_o = 1$. Then, if we denote the surface area of the cavity by A, the number of moles of gas which enter it in time t should be given by

$$\int_o^t \frac{dn}{dt}\, dt = A\delta p_o t . \tag{4}$$

The volume which these molecules would occupy at a pressure of 1 atm., corresponding to the condition when the piston of the syringe is released, is

$$RTA\delta p_o t . \tag{4.1}$$

On the basis of Table II, $RT\delta$ may be taken as 10^{-4} cm/sec. Several experiments were made to test this prediction under conditions for which A was estimated to be in the neighborhood of 16 cm^2, though this figure was probably too low due to the irregularity of the cavity associated with the splashing of the liquid. From the figures just given, the calculated volume of gas which should have entered the cavity per second turns out to be approximately 1.6×10^{-3} cm^3. The observed amount is about twice this, but in view of the uncertainties involved in the calculations, the agreement may be regarded as satis-

factory and may be taken as evidence in support of the fundamental correctness of the interpretation. These results on the accumulation of gases in a cavity by diffusion from the surrounding medium are of interest in connection with various respiratory problems.

CHANGES IN COMPOSITION ACCOMPANYING SOLUTION OF GAS BUBBLES

When the gas obtained from freshly formed cavities is analyzed it contains significantly more oxygen than the 21% characteristic of air. In fact, analyses made as soon as possible after formation of a cavity yield values up to 35% oxygen.[9] Correspondingly it is found that as bubbles of air introduced into water diminish in size under excess pressure they become poorer in oxygen and richer in nitrogen. These two observations really represent the same phenomenon, namely the different rates of passage of oxygen and nitrogen across the diffusion layer at the surface of the bubble (cavity). As we have already suggested, certain small discrepancies between the observations and theory encountered in the preceding section are probably attributable to this phenomenon. In order to explore this subject, experiments were carried out to determine the changes in composition accompanying the solution of gas bubbles in water, and, in particular, the effect of pressure on the phenomenon.

The bubbles, consisting either of air or of an arbitrary mixture of oxygen and nitrogen, were placed in either one of the pressure chambers previously described and were allowed to dissolve for a given time before being withdrawn for gas analysis. The initial size of the bubble used varied somewhat, but it was in the neighborhood of 3.5–4 mm in diameter. The results are shown in Fig. 4, which illustrates quantitatively the way in which the bubbles always become richer in nitrogen as they diminish in size. By the time they are disappearing they ap-

[9] In accordance with considerations to be developed presently we should expect the amount of oxygen in a freshly formed cavity to be half that of nitrogen; in other words, the gas should be 33⅓% oxygen. This follows from the same line of reasoning involved in equations (4) and (4.1). We should expect the ratio of oxygen to nitrogen in the cavity, before any gas has had a chance to escape, to be given by

$$\frac{\delta_1}{\delta_2}\frac{p_{1o}}{p_{2o}} = 2 \times \frac{0.2}{0.8} = \frac{1}{2}.$$

(Subscripts 1 and 2 refer to oxygen and nitrogen respectively.) The value 2 for the ratio $\frac{\delta_1}{\delta_2}$ is based on considerations given later in this section.

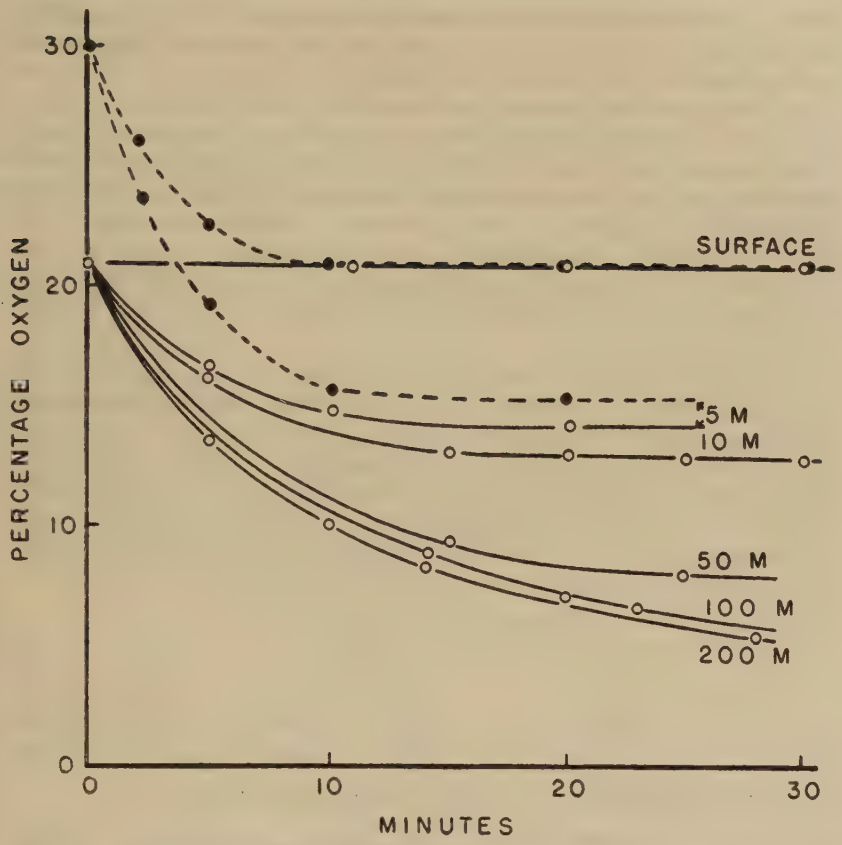

Figure 4. Change in composition of bubbles as they dissolve at different pressures (depths) in sea water saturated with air at normal atmospheric pressure. The initial diameter of the bubbles studied varied from approximately 3.4 to 4 mm.

pear to have attained a nearly constant composition. This composition is the richer in nitrogen the higher the pressure.

The physical explanation of the phenomenon is simple. It rests on the fact that the diffusion constants of oxygen and nitrogen are nearly the same but that the solubility of oxygen is about twice that of nitrogen.[10] Let us consider the case of an air bubble suspended in

[10] At 19° the diffusivity of nitrogen in dilute aqueous solution is close to 1.9 and at 18° that of oxygen is also close to 1.9 $cm^2\ sec^{-1}$ (International Critical Tables). The solubility coefficient of N_2 is .0155 and that of O_2 is .0310 in H_2O. These figures refer to volumes of gas (measured at 0 and 1 atm.) dissolved by 1 volume of water when the partial pressure of the gas is 1 atm.

water saturated with air at atmospheric pressure. If the pressure in the bubble is one atmosphere, as at the surface, no gas will pass into the liquid phase, for the system is at equilibrium (see Fig. 2). There will be no concentration gradient anywhere to produce diffusion. However, if the pressure is raised, the concentration of oxygen at the air-water interface, and consequently the concentration gradient across the diffusion layer, will increase more in proportion to the amount of gas in the bubble for oxygen than for nitrogen, owing to the greater solubility of oxygen. Consequently, since the diffusion constants of the two gases are the same, the percentage loss of oxygen from the bubble will exceed that of nitrogen and the bubble will become richer in nitrogen.

It is worth-while to formulate the situation mathematically in terms of our simplified hypothesis. On the whole the result agrees so well with the facts that it suggests that our picture of the physical factors involved is correct and lends confidence to any inferences based on that picture. In this formulation, subscript 1 refers to oxygen and 2 refers to nitrogen, and x is introduced to denote the mole fraction of oxygen in the bubble. Otherwise we use the same notation as before. The situation is governed by the following equations:

$$n_1 = \frac{1}{RT}\frac{4\pi r^3}{3} xp, \quad n_2 = \frac{1}{RT}\frac{4\pi r^3}{3}(1 - x)\, p\,, \tag{5}$$

$$\frac{-dn_1}{dt} = \delta_1 4\pi r^2(xp - p_{1o}), \quad \frac{-dn_2}{dt} = \delta_2 4\pi r^2[(1 - x)p - p_{2o}]\,. \tag{6}$$

If we differentiate (5) with respect to time we obtain:

$$\begin{aligned} \frac{dn_1}{dt} &= \frac{4\pi r^2}{RT} xp\frac{dr}{dt} + \frac{4\pi r^3}{3RT} p\frac{dx}{dt}\,, \\ \frac{dn_2}{dt} &= \frac{4\pi r^2}{RT}(1 - x)p\frac{dr}{dt} - \frac{4\pi r^3}{3RT} p\frac{dx}{dt}\,. \end{aligned} \tag{7}$$

Equations (6) and (7) provide four relations between the five infinitesimals dn_1, dn_2, dt, dx, and dr. They may be combined to eliminate any three of these, leaving an equation between the remaining two. Our interest is of course limited to t, x, and r. If the two infinitesimals are chosen as dr and dx, we obtain, after taking account of the fact that $\delta_1 = 2\delta_2$,

$$\frac{-3dr}{r} = \left[\frac{xp + p - p_{2o} - 2p_{1o}}{x^2p - x(p + p_{2o} + 2p_{1o}) + 2p_{1o}}\right] dx. \tag{8}$$

Similarly, if they are chosen as dr and dt, we obtain

$$-dr = RT\delta_2 \left(\frac{xp + p - p_{2o} - 2p_{1o}}{p} \right) dt. \tag{9}$$

Finally, if they are chosen as dx and dt, we obtain

$$dx = \frac{3RT\delta_2}{rp} \left[x^2 p - x(p + p_{2o} + 2p_{1o}) - 2p_{1o} \right] dt. \tag{10}$$

Of these three equations only (8) is suitable for integration, and it is apparent that the significant variable in determining x is r, not t. Nevertheless (9) and (10) are of interest also. For example, (10) makes it possible to calculate the limiting steady value of the composition of a bubble as it dissolves $\left(\frac{dx}{dt} = 0,\ r \neq 0 \right)$ and to see how this varies with p, p_{2o}, and p_{1o}. If we assign to p_{1o} and p_{2o} the values corresponding to atmospheric air, we verify that the equilibrium composition of the bubble is richer in nitrogen the greater the pressure p, as we find it to be.

If equation (8) is written in the form

$$\frac{3dr}{r} = \left(\frac{x + a}{b^2 - (x + c)^2} \right) dx, \tag{11}$$

it may be integrated to give

$$\log r = \frac{1}{6} \left[\frac{(a - c)}{b} \log \left(\frac{b + c + x}{b - c - x} \right) - \log \{b^2 - (x + c)^2\} \right] + \text{const.} \tag{12}$$

Since, according to definition, the quantities a, b, and c are known functions of p, p_{1o}, and p_{2o}, (12) may be used to calculate pairs of values of x and r/r_o for different conditions (r_o being the initial radius of the bubble). Of course these must include a specification of the value of x for $t = 0$ ($r/r_o = 1$), i.e., the initial composition of the bubble. If we are interested in the case of an air bubble dissolving at pressure p in water saturated with air at atmospheric pressure we may set $p_{1o} = 0.2$ atm. and $p_{2o} = 0.8$ atm. Theoretical curves calculated for this case are shown in Fig. 5, together with corresponding experimental points obtained by the methods already described. The agreement, on the whole, is satisfactory and there is little doubt that the interpretation we have given provides the essential explanation of the main phenomenon; i.e., the gradual increase in the nitrogen content of the

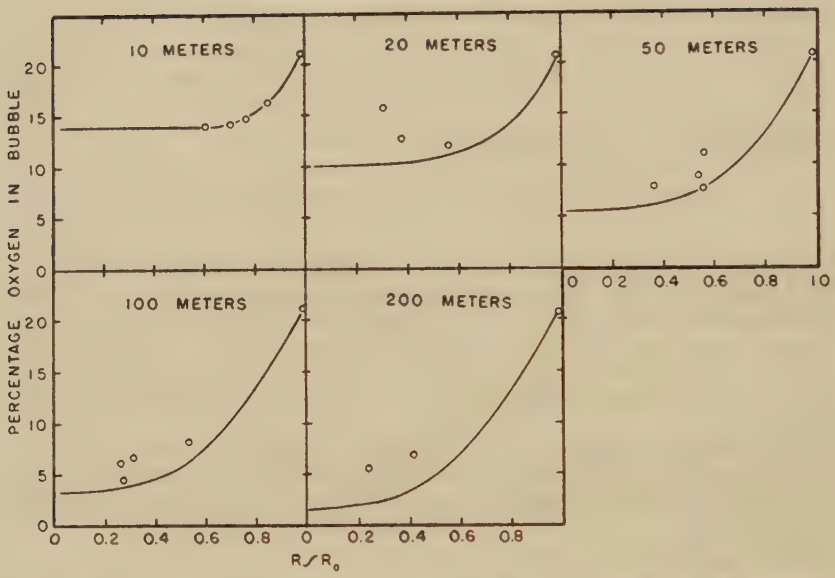

Figure 5. Changes in composition of air bubbles dissolving at different pressures (depths) in sea water saturated with air at normal atmospheric pressure. The abscissa gives the ratio of the radius of the bubble at the time the analysis was made to the initial radius of the bubble.

bubble as it dissolves towards a limiting steady value is greater as the pressure (depth) increases.

By joint use of equations (9) and (12) it is a simple matter to calculate how the rate of shrinkage of the bubble should vary with size and composition and depth. Such calculations are given in Table III, and they serve to explain the fact that at all pressures the initial value of $\frac{dr}{dt}$ is always greater than the later values, as shown by the data given in Fig. 2. They also explain why the values of $RT\delta$ calculated from (3) and shown in Table II are not constant but decrease with pressure. Physically, of course, this is explained by the fact that initially, when the bubble is relatively rich in oxygen, it shrinks more rapidly due to the fact that the rate of loss of oxygen is greater than that of nitrogen.

From the values of $-\frac{1}{RT\delta_2}\frac{dr}{dt}$ given in Table III and from the values of $\frac{dr}{dt}$ given in Table II (representing final rates), δ_2 (referring to nitrogen) may be calculated and then the thickness of the water shell

TABLE III

$\frac{r}{r_o}$	x	$-\frac{1}{RT\delta_2}\frac{dr}{dt}$	$\frac{r}{r_o}$	x	$-\frac{1}{RT\delta_2}\frac{dr}{dt}$
10 m			20 m		
1	.21	.61	1	.21	.81
0.5	.140	.54	0.5	.110	.71
0.0	.136	.54	0.0	.103	.70
50 m			100 m		
1	.21	1.01	1	.21	1.10
0.5	.072	.871	0.5	.055	.945
0.0	.058	.859	0.0	.033	.923
200 m					
1	.21	1.21			
0.5	.048	.99			
0.0	.018	.96			

surrounding the bubble. We first find that $RT\delta_2 = (10 \pm 0.5)^{-4}$ cm/sec. From this, taking $RT = 2.4 \times 10^4$ cc atm./mole, we obtain $\delta_2 = 4.2 \times 10^{-9}$ moles/cm²/sec./atm. (δ_1 is twice this, or 8.4×10^{-9}). However, $\delta_2 = \frac{\Delta_2 \alpha_2}{d}$. At 20°, $\Delta_2 = 2 \times 10^{-5}$ cm²/sec. and $\alpha_2 = 6.9 \times 10^{-7}$ moles/cc/atm. Consequently, $d = 3.3 \times 10^{-3}$ cm. It should be realized that the picture of a sharply defined water shell supporting a uniform diffusion gradient surrounding the bubble is artificial. The bubble behaves as if this were the case, but this simply means that the mixing of the water is practically complete up to a distance from the air-water interface of the same order of magnitude as the calculated thickness of the shell.

SUMMARY

Observations on the rate of solution of gas bubbles in water are described and are shown to be in close accord with equations based on the theory of diffusion. As an air bubble dissolves in water saturated with the atmosphere, the rate of decrease in diameter with time is nearly constant and increases with depth up to a limiting value. However, there is a slight decrease in the rate of solution with time, and this is associated with a change in composition, the bubble becoming richer in nitrogen as it approaches a limiting composition. When a bubble is formed in water saturated with air as a result of cavitation, it is initially much richer in oxygen than air, as would be predicted. Theoretically, the percentage of oxygen to be expected in such a bubble at the moment of formation is 33⅓%. Actually the highest observed value was 35%.

The equations developed in connection with these observations are of general applicability and should be of use in the analysis of various respiratory and other physiological problems involving aquatic organisms. They may also apply in certain problems of physical oceanography.

REFERENCES

Hamm, R. E., and T. G. Thompson
1941. Dissolved nitrogen in the sea water of the Northeast Pacific. J. Mar. Res., *4:* 11–27.

Harvey, E. N., D. K. Barnes, *et al.*
1944. Bubble formation in animals. I. J. cell. comp. Physiol., *24:* 1–22.

Harvey, E. N., A. H. Whiteley, *et al.*
1944. Bubble formation in animals. II. J. cell. comp. Physiol., *24:* 23–34.

Rakestraw, N. W., and V. M. Emmel
1938. The relation of dissolved oxygen to nitrogen is some Atlantic waters. J. Mar. Res., *1:* 207–216.

Scholander, P. F., and F. J. W. Roughton
1942. A simple microgasometric method of estimating carbon monoxide in blood. J. ind. Hyg. Toxicology, *24:* 218–221.

THE BALL-BREAKER, A DEEP WATER BOTTOM SIGNALLING DEVICE[1]

By

JOHN D. ISAACS AND
A. E. MAXWELL

Scripps Institution of Oceanography
La Jolla, California

ABSTRACT

A simple device for signalling the arrival of a deep cast on bottom has been developed and is now in routine use. The device is used either in line with corers or is suspended below as a pilot. When contact of either the ball-breaker or other apparatus is made with the bottom, a small glass sphere in the former is imploded and the resultant signal at the surface is amplified and reproduced over a loud speaker system. The device has been used successfully at depths to 2,700 fathoms.

General. With the present-day trend toward deep water oceanography, many difficulties have arisen which were not encountered in shallow water operations. Among these difficulties is the problem of determining the exact time when a piece of oceanographic equipment reaches bottom. This is not serious in shallow water, since sensitive dynamometers have been constructed which indicate to the observer aboard ship the moment that the tension on the cable is relieved. However, in deep water the weight of the equipment is often only a small fraction of the total weight of cable and of variable loads imposed by the ship's roll; therefore, no conclusive effect upon tension can be observed when the apparatus encounters bottom.

Obviously, the answer to this problem may be found by employing some device which is independent of both the ratio of equipment to cable weight and the depth of the water. To meet this need, an instrument was developed which imploded a small glass sphere when the apparatus hit bottom. The resulting implosion, picked up at the surface by a simple hydrophone, is amplified and reproduced audibly over a loudspeaker system.

Development. The original method used to trip the mechanism and to break the glass sphere is shown schematically in Fig. 1. The apparatus is very simple; it merely employs a piston fitted with a sharp point which is allowed to fall when the equipment contacts the bot-

[1] Contribution from The Scripps Institution of Oceanography, New Series, No. 565. This work represents results of research carried out for the Office of Naval Research and the Bureau of Ships under contracts with the University of California.

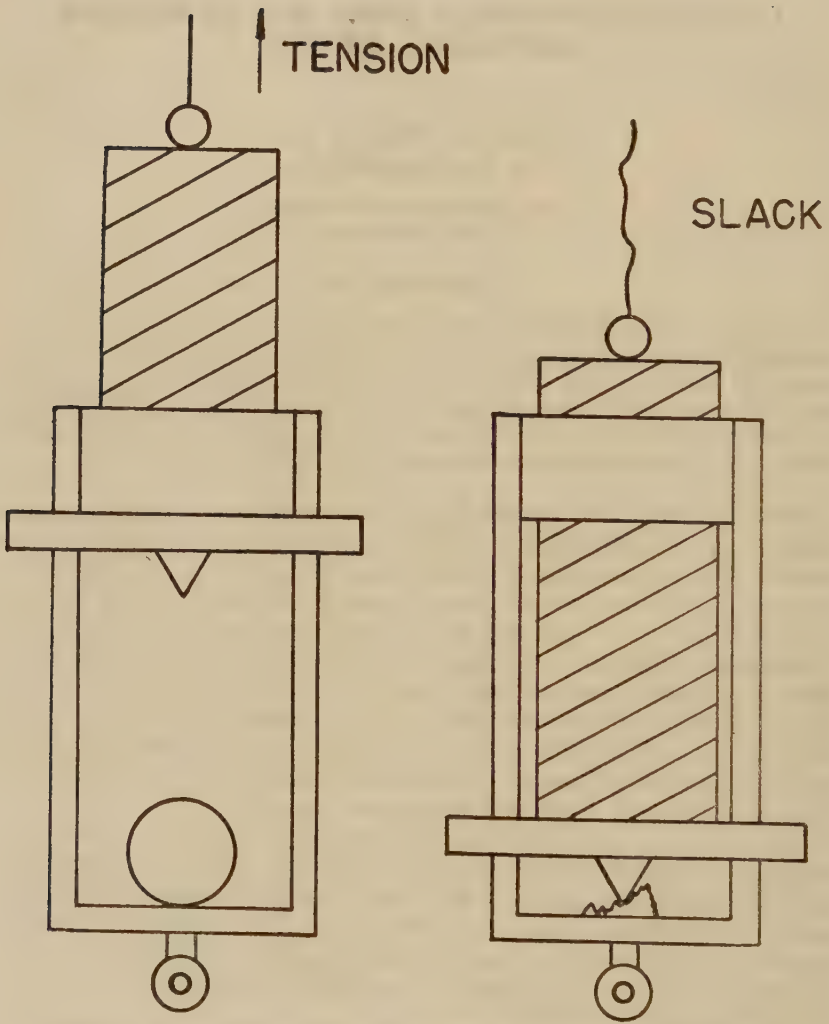

Figure 1. Schematic of early model ball-breaker showing method of tripping.

tom, thus imploding the glass sphere. Such a straight-forward device would seemingly present no problem in its initial design; however, as is often the case in oceanographic operations, equipment which appears to be encouraging on the drawing board and which works well in test tanks may fail entirely when lowered into the ocean. Such was the case with the early models of this device.

The first model functioned satisfactorily in shallow water, but in deep water the point succeeded only in chipping the glass ball and was therefore ineffective. It was thought that the cable stretched elastically under the loads and then contracted as the equipment reached bottom, thus allowing the piston to lower gently upon the glass sphere. This problem was solved by incorporating a tripping mechanism in the device to allow the piston to drop freely on contact with bottom.

However, with this new model a great many failures in breaking the ball were experienced, since some balls were entirely fractured but were held together by the pressure; thus they failed to implode. It became apparent that the glass balls acquired great strength under compression in much the same manner as an arch can carry greater concentrated loads under a large dead load than it can with a small dead load. To eliminate this difficulty, the chisel point tip was replaced with a conical tip in the hope of reducing the area of impact upon the sphere, but then the conical tip and the glass wedged together in a pressure tight seal as though the glass were plastic; again implosion was prevented. To avoid sealing, the tip was relieved in three places so that shearing and bending might occur in the glass to facilitate collapse. This proved successful in all subsequent trials.

Description and Techniques. Fig. 2 shows the instrument in its present form. The glass sphere is centered by three tips and is held into place by a turn of friction tape. A more complex holding device does not appear to be practical since projections are blown off by the implosion. Located inside the cylinder is the tripping mechanism which releases the piston upon contact of the device with the bottom. The ring on the bottom provides a means of securing other instruments below the ball-breaker if it is to be used as an in-line device.

There are several types of glass spheres which are available commercially and which appear to be satisfactory. Preliminary pressure tests of various samples have shown that some of these balls are capable of withstanding pressures up to 16,000 psi. The balls, made commercially for ornamental purposes from ordinary glass, are approximately two and one-half to three inches in diameter and have an average wall thickness of $\frac{1}{16}$ inch. The glass may contain a large number of air bubbles and may often be irregular as to size and shape; but these minor irregularities do not appreciably effect the efficiency of the balls. However, care must be taken to eliminate those balls that have a small hole at the point where they are sealed, since water in the balls render them ineffective. The balls are tested by securing several balls in a cloth sack and by lowering them a few hundred meters in the water. Experience has shown that the balls should be separated

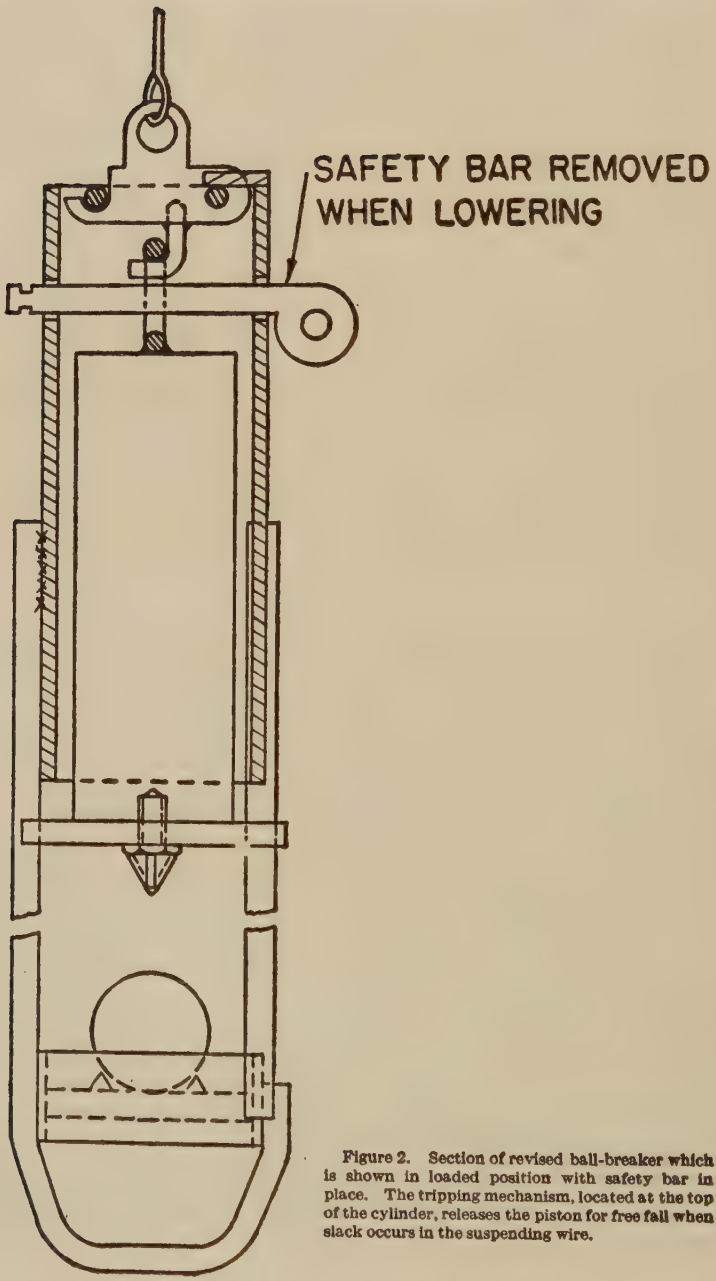

Figure 2. Section of revised ball-breaker which is shown in loaded position with safety bar in place. The tripping mechanism, located at the top of the cylinder, releases the piston for free fall when slack occurs in the suspending wire.

into two classes: thick spheres with about $\frac{1}{8}$-inch walls for use in depths greater than 3,000 fathoms, and thinner spheres with walls approximately $\frac{1}{16}$-inch thick for use in water less than this depth. In this way the balls are segregated into divisions which give maximum efficiency by avoiding premature failures.

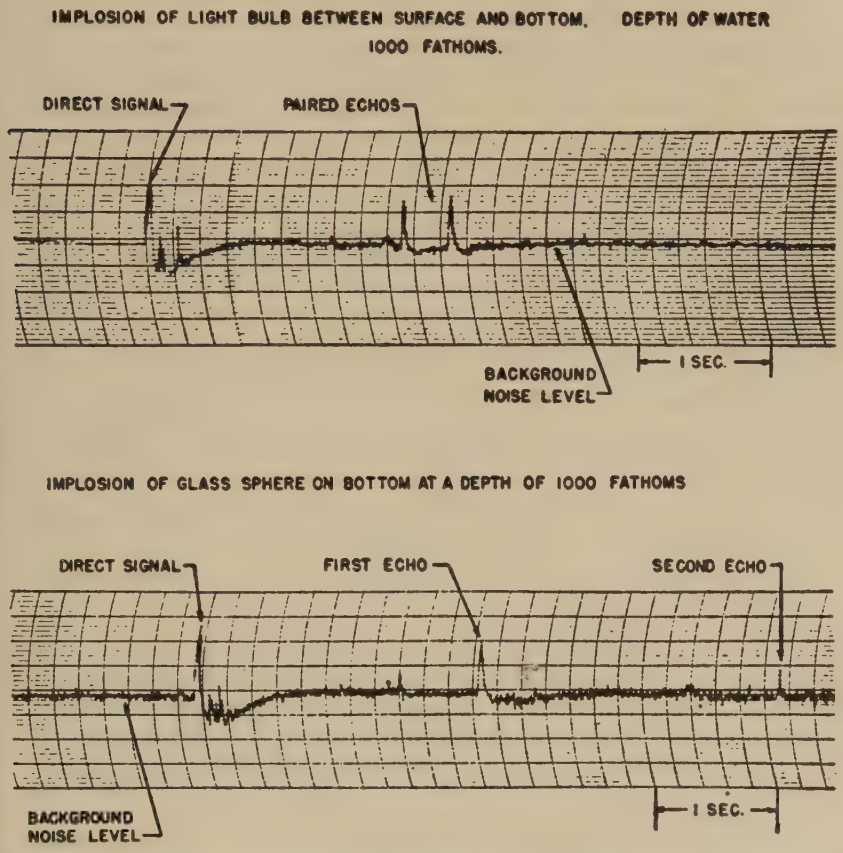
IMPLOSION OF LIGHT BULB BETWEEN SURFACE AND BOTTOM. DEPTH OF WATER 1000 FATHOMS.
DIRECT SIGNAL
PAIRED ECHOS
1 SEC.
BACKGROUND NOISE LEVEL
IMPLOSION OF GLASS SPHERE ON BOTTOM AT A DEPTH OF 1000 FATHOMS
DIRECT SIGNAL
FIRST ECHO
SECOND ECHO
1 SEC.
BACKGROUND NOISE LEVEL

Figure 3. Traces of two implosions illustrating the different types of echoes encountered.

Surprisingly, it is found that the peak intensity of the signal received from these implosions is practically independent of the depth of implosion; that is, the increase in attenuation is offset by the increase in *peak* energy obtained at greater depths. Such appears to be the case for signals which have originated at depths from 200 to 2,700 fathoms, although no quantitative measurements have been made. Although it might be expected that an increase in the diameter of the

sphere would result in a corresponding increase in the peak signal intensity, preliminary tests show that this is not the case. Possibly the larger air mass, corresponding to the larger volume, produces a cushioning effect which tends to reduce the peak energy released.

At the surface, the signal is picked up by a simple magnetostriction-type hydrophone which is lowered over the side about one hundred feet below the surface to reduce the background noise. The signal and echoes are very sharp and are easily distinguishable from the background noise, the signal above background noise being of the order of 20 d.b. The echoes act as a verification of the implosion, and further, the spacing of the echoes permits the determination of the relative depth of the implosion. If the ball breaks prematurely before hitting bottom, paired echoes are heard, while only single equally-spaced echoes are heard when the ball is broken on the bottom. The two traces in Fig. 3 were taken from a tape recording made of actual implosions at sea. Both implosions took place at the same ship's position. The upper graph is a recording of the sound from a common 25-watt light bulb which imploded under pressure at a depth of about 4,500 feet. The graph shows that the peak signal intensity is much higher than the background noise and, as would be expected, paired echoes are heard. In the lower graph a glass sphere is imploded on bottom by means of the ball-breaker device, and the resulting signal and two echoes are clearly discernible. These echoes are single and evenly spaced, thus verifying that the instrument reached bottom. Four echoes have been heard in depths of 2,500 fathoms, the number depending primarily upon the amount of background noise present and the state of the sea.

Remarks. This apparatus has been highly successful in deep-water operations where small cores have been taken, and it should be practical for a wide range of oceanographic operations. It should also be mentioned that a spring-loaded model has been designed which sacrifices the simplicity of the existing model for a reduction in total weight.

Acknowledgments. The authors are indebted to the Northwest Glass Company of Seattle, Washington and to the Blenko Glass Company of Milton, West Virginia for their cooperation and for the supply of glass balls used for the original development.

PHYSICAL OCEANOGRAPHIC INVESTIGATIONS IN THE EASTERN BERING AND CHUKCHI SEAS DURING THE SUMMER OF 1947

By

E. C. LaFOND and D. W. PRITCHARD[1]

U. S. Navy Electronics Laboratory
San Diego 52, California

ABSTRACT

New information on the physical properties of the waters in the eastern Bering and Chukchi seas is discussed. It shows that, in summer, the water masses of this area are complicated by the circulation and advective processes. In general, the southern Bering Sea water flows northward and is modified by warm low-salinity water from rivers along the Alaskan coast and from intrusions of cold high-salinity water from the western Bering Sea. This mixture of water funnels through the Bering Strait principally at the surface on the eastern side. In the Chukchi Sea this water continues northward, tending to follow the Alaskan coast, turning into Kotzebue Sound, and then heading around Cape Lisburne toward Point Barrow. Other water masses occur in the central Chukchi Sea opposite Kotzebue Sound and north of 70° N latitude. Near the Arctic ice pack boundary, unusual stratification of the water occurs, with subsurface temperature maximums in the form of tongues or pockets. This phenomenon is probably caused by mixing of water from melting ice cakes with the advected higher-salinity water from the Bering Strait.

INTRODUCTION

During a familiarization cruise on the USS Nereus to the Bering and Chukchi seas in the summer of 1947, geological, biological, and physical investigations of the sea floor and water were undertaken by oceanographers from the U. S. Navy Electronics Laboratory and the Scripps Institution of Oceanography. This paper reports studies of the physical properties of sea water; detailed results of all phases of the program have been reported elsewhere (LaFond, Dietz, Pritchard, 1949).

In the prosecution of the oceanographic programs, the ship hove to four times each day in the shallow areas of the Bering and Chukchi seas for vertical series of temperature, salinity, and other oceanographic observations. The locations of these serial oceanographic stations are shown in Fig. 1. Thirty-nine stations were located north of the Aleutian Islands, 22 of these being north of Bering Strait in the Chukchi Sea.

[1] Chesapeake Bay Institute.

Figure 1. Bathythermograph and hydrographic stations used for vertical sections.

Several previous cruises, notably those conducted by the U. S. Coast Guard in 1934 (Barnes and Thompson, 1938) and in 1937–1938 (Goodman, Lincoln, et al., 1942), have made fairly complete investigations of the eastern Bering Sea and Norton Sound. However, relatively few data have been obtained previously in the central Chukchi Sea area. The latter cruises, in the summers of 1937 and 1938, occupied a number of stations along the Alaskan Coast from Bering Strait nearly to Point Barrow, but the data obtained were not sufficient to show the lateral distribution of the physical variables.

Sverdrup, on the MAUD (Sverdrup, 1929), obtained considerable data between Herald Shoal and Wrangell Island, but he occupied only two serial stations east of 170° W in the Chukchi Sea. Thus, the data taken during this USS NEREUS cruise in the Chukchi Sea represent a considerable increase in the oceanographic information available for this area.

Also shown in Fig. 1 is the location of the line of bathythermograms obtained from Adak north to the southern edge of the extensive shallow water area of the Bering Sea. It was in this shallow water region, north from the area of the Pribilof Islands, that all of the serial observations in the Bering Sea were taken. At each hydrographic station, vertical water temperatures were obtained from both bathythermograms and reversing thermometers. The BT observations are extremely valuable from the standpoint of description of the thermal structure, since a continuous temperature trace with depth is obtained. Because of this greater detail given by the BT observations, all vertical cross sections are based on bathythermograms, and the isotherms are in degrees F. However, the more accurate temperatures obtained from reversing thermometers simultaneously with the water samples were used for computations of density and dynamic topography.

TEMPERATURE AND SALINITY

Adak to the Pribilof Islands. BT observations were made every hour along a section from Adak northward to 56° 03′ N, 176° 38′ W and then along a section east northeastward to 56° 36′ N, 173° 39′ W. These sections (Fig. 1, A and B) are over the eastern end of the deep Bering Sea basin, with the depth running at about 2100 fathoms at most stations. The BT, therefore, suffices in obtaining data on only a relatively small portion (300 to 400 feet) of the vertical thermal structure of this region. It has been shown, however, that the temperature and salinity structures of the Bering Sea basin below 100 m are very similar to those in the subarctic region of the North Pacific (Sverdrup, Johnson, and Fleming, 1946: 732–733). The mean flow is northward through the channels of the Aleutian chain, and the BT traces characteristic of most of these obesrvations in the southern Bering Sea are not unlike those found in the subarctic water south of the Aleutians.

The horizontal temperature structure at the surface, at 25 m and also at 40 m, is shown in Figs. 2, 3, and 4. It indicates the existence of a clockwise eddy at about 55° N, 175° W.[2] A study of the data

[2] A discussion of the relationship between thermal structure and currents is given by Sverdrup, et al., 1946: 394.

Figure 2. Horizontal distribution of temperature (°F) in Bering and Chukchi seas, at the surface.

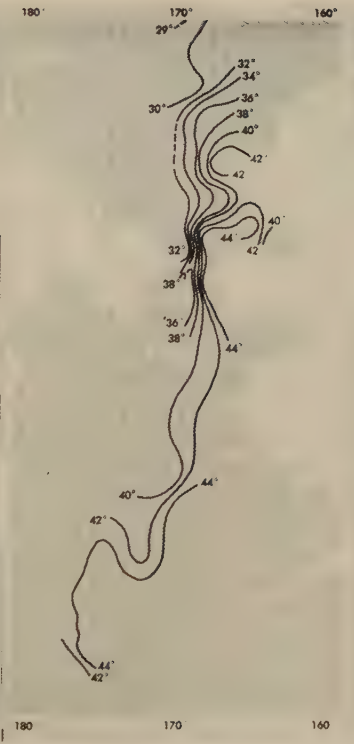

Figure 3. Horizontal distribution of temperature (°F) in the Bering and Chukchi seas, at a depth of 25 meters.

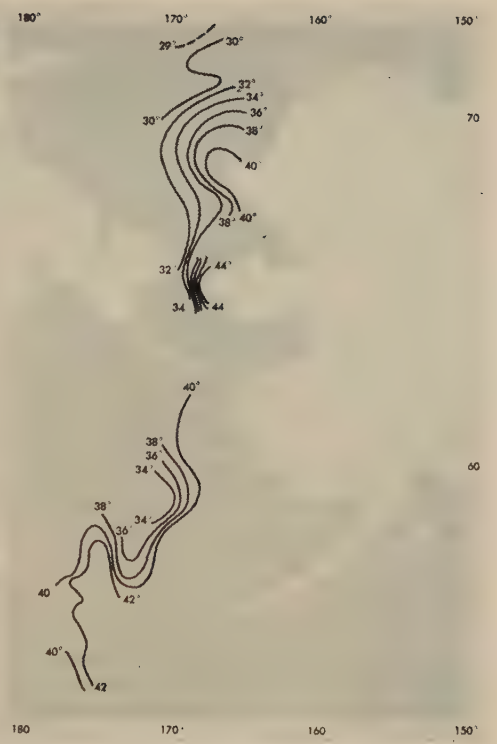

Figure 4. Horizontal distribution of temperature (°F) in the Bering and Chukchi seas, at a depth of 40 meters.

presented as a vertical section (figure not shown) further emphasizes the existence of this clockwise eddy.

The Bering Sea from the Pribilof Islands to Bering Strait. Nine hydrographic stations were occupied along a line running from a point just south of the Pribilof Islands to the eastern side of St. Lawrence Island and then north to Bering Strait; three more stations were occupied on a line southeast from Cape Prince of Wales toward Norton Sound (see Fig. 1).

As shown by the horizontal distribution of temperature and salinity at various depths (Figs. 2–7), the major change in these variables occurs in an east-west direction rather than along the line of stations running from the Pribilof Islands to the Bering Strait. In general, the warmer and less saline water is found near the Alaskan coast. The isotherms tend to run southwest-northeast in the region of the four southernmost stations; however, the ridge extending out from Cape Romanzof appears to deflect the warm coastal water west, so that the isotherms run southeast-northwest in the region south of St. Lawrence Island.

The isotherms and isohalines for the southernmost four stations are not parallel; the isohalines run from southeast to northwest, while the isotherms run approximately southwest-northeast. The protrusion of the isohalines to the west in the region of Cape Romanzof occurs somewhat south of the same protrusion of the isotherms. North of St. Lawrence Island the isotherms and isohalines run approximately parallel, converging toward Bering Strait.

The highest surface temperatures, 58° F, were encountered in Norton Bay. The lowest surface temperature obtained south of Bering Strait was 41° F, although the trend of the isotherms indicates that much lower temperatures exist off the Siberian coast opposite Seward Peninsula.

A study of temperature-salinity relationships provides a convenient method for determining water mass characteristics and origin. T-S diagrams, therefore, were plotted for all stations in the Bering Sea except for those in Norton Sound (see Fig. 8). Included in Fig. 8 is the T-S relationship for the upper layers of the subarctic water found to the south of the Aleutians, as given by the upper 100 m of Carnegie St. 120 (47° 02′ N, 166° 20′ E). The T-S curves for Nereus Sts. N1, N2, and N3 are similar in shape to that at Carnegie St. 120 but are 1‰ lower in salinity at equivalent temperatures. The shape of the T-S relationship remains about the same, but the average salinity decreases northward (Sts. N4, N5, N6, N7) to the region between St. Lawrence Island and Bering Strait. Here the water has a higher

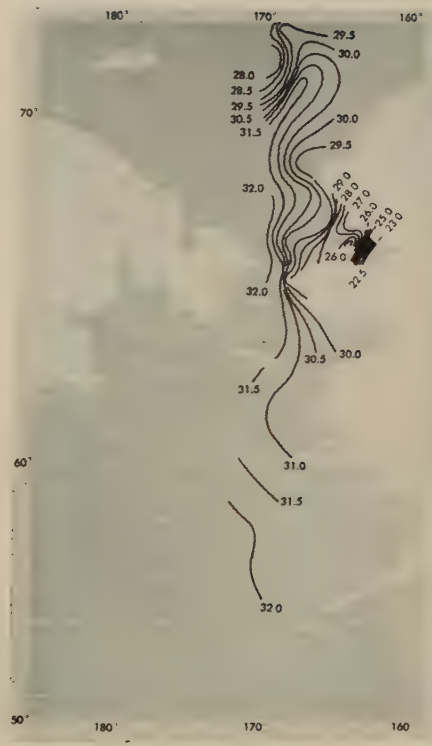

Figure 5. Horizontal distribution of salinity (°/₀₀) in the Bering and Chukchi seas, at the surface.

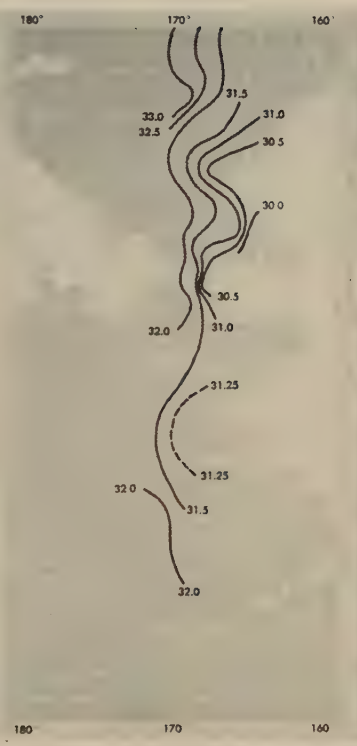

Figure 6. Horizontal distribution of salinity (°/₀₀) in the Bering and Chukchi seas, at a depth of 25 meters.

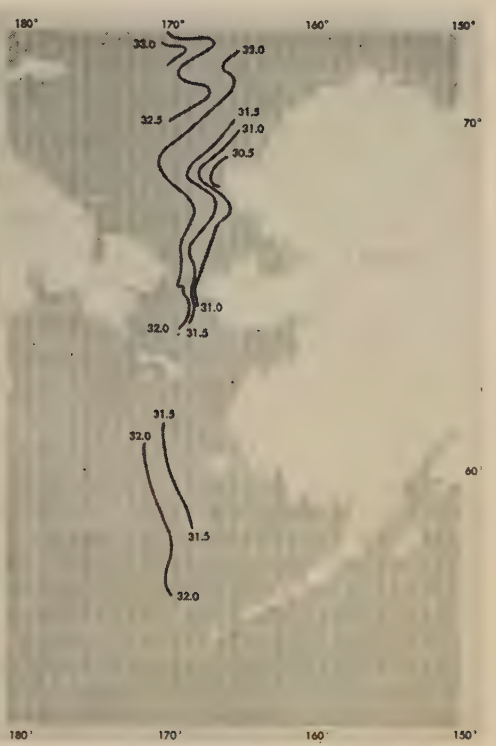

Figure 7. Horizontal distribution of salinity (°/₀₀) in the Bering and Chukchi seas, at a depth of 40 meters.

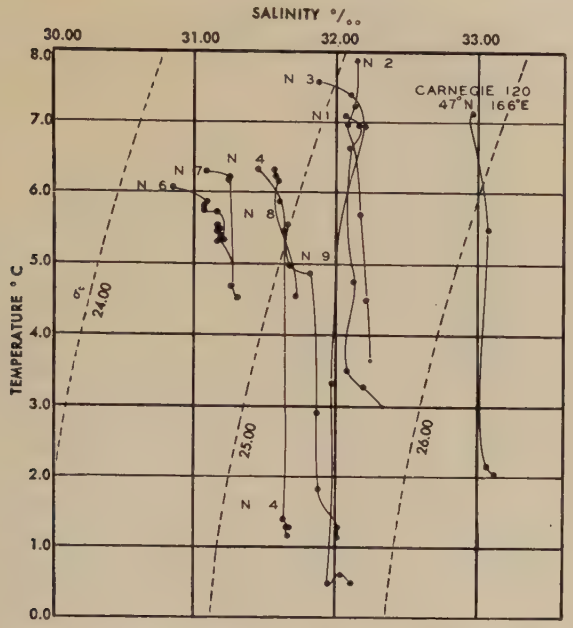

Figure 8. Temperature-Salinity diagrams from stations in the Bering Sea (see Fig. 1).

salinity because of the mixing with more saline water which apparently flows northward to the west of the line of the NEREUS stations (Goodman, Lincoln, et al., 1942).

Bering Strait. Five hydrographic stations were occupied across the eastern half of Bering Strait. Very large horizontal gradients of the physical variables were encountered here, the most extreme gradients occurring along the Alaskan side of the Strait. In this location, a surface temperature drop of 10° F in 30 miles was observed; 8° of this change occurred in the 10 miles between the two stations nearest to the Alaskan coast. The corresponding salinity change was 2.5 °/₀₀.

Vertical cross sections of temperature and salinity have been constructed for the five stations across the eastern part of Bering Strait. The temperature section (Fig. 9) shows the change from cold water on the western side of the section to relatively warm water near the Alaskan coast at all depths. The warm water overruns the cold water in the middle, producing fairly large vertical gradients in temperature. The salinity section (Fig. 10) shows the decrease in salinity from west to east. The greatest horizontal change at all depths occurs between the two stations nearest to the Alaskan coast. There the low-salinity

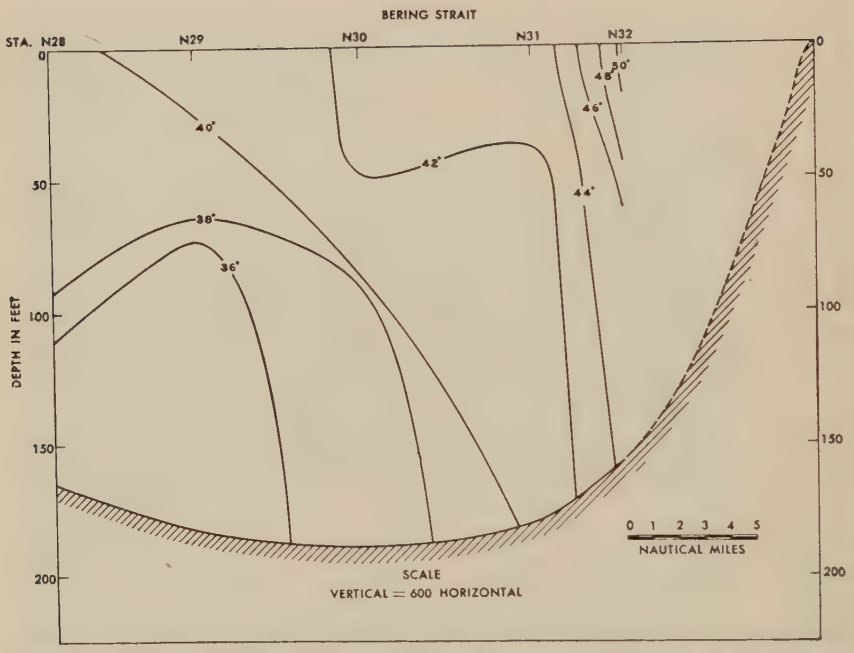

Figure 9. Vertical temperature section D (°F) across the eastern side of Bering Strait (see Fig. 1).

water is apparently related to runoff from Alaskan rivers. The mass field, as indicated by the distributions of temperature and salinity, must be associated with a relatively strong current running northward through Bering Strait.

The depth of the thermocline decreases from west to east, with the greatest gradients in the thermocline occurring at the central station. The vertical temperature gradients below the thermocline are small. The vertical salinity gradients increase from west to east. The layer of maximum vertical salinity gradient occurs just below the thermocline.

The T-S diagrams for this area are shown in Fig. 11. The stations on the western and middle portions of the section show the same T-S characteristics as those shown by the stations in the central Bering Sea (N28 to N30). However, St. N32, on the far eastern side of the Strait, shows water of different character. This water is warmer and less saline with a considerable salinity gradient. St. N31 is apparently a mixture of the western and eastern waters in the Strait. As will be seen later, the T-S relation at St. N32 is very similar to that of the

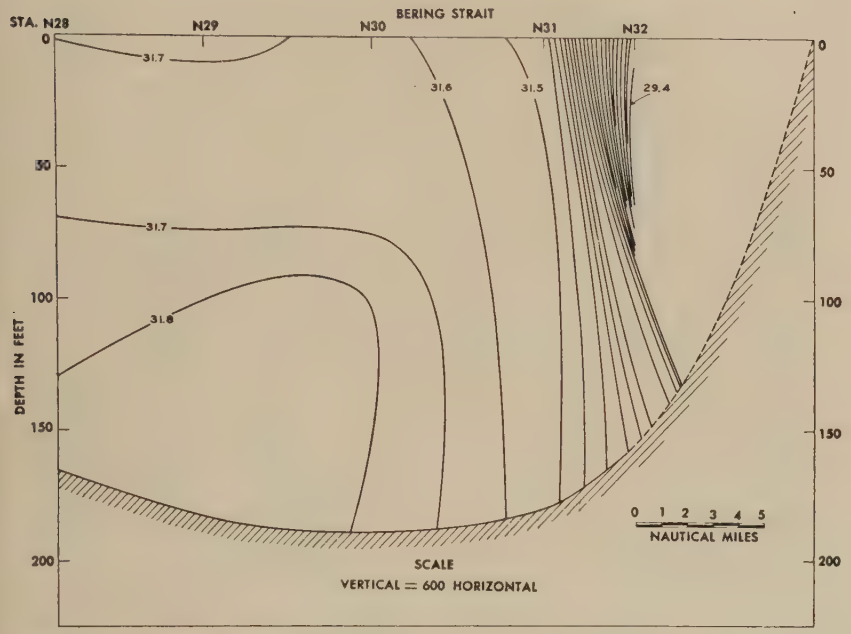

Figure 10. Vertical salinity section D (°/₀₀) across the eastern side of Bering Strait (see Fig. 1).

Alaskan coastal Sts. N33, N34, and N35 extending into Norton Sound, and to Sts. N26 and N27 in the Chukchi Sea, northeast of Bering Strait.

Chukchi Sea. Twenty-two serial stations were occupied north of Bering Strait in the Chukchi Sea: Seven in a north-south line from Bering Strait to the edge of the pack ice just north of 72° N; five stations, occupied over a 24-hour period while the ship was drifting southeastward, in the immediate vicinity of the ice pack; another eight stations from the ice pack into Kotzebue Sound, together with the two stations between the Sound and Bering Strait. These stations provide the most extensive data yet obtained in this area of the Chukchi Sea and provide a good network for the study of the distribution of physical properties.

The over-all distribution of temperature and salinity in the Chukchi Sea leads to horizontal contour charts which are remarkably similar for the various depths and for both temperature and salinity. Warm low-salinity water is found at all depths on the Alaskan side of the Chukchi Sea. The isopleths of both temperature and salinity tend to follow the contours of the coastline (Figs. 2–7).

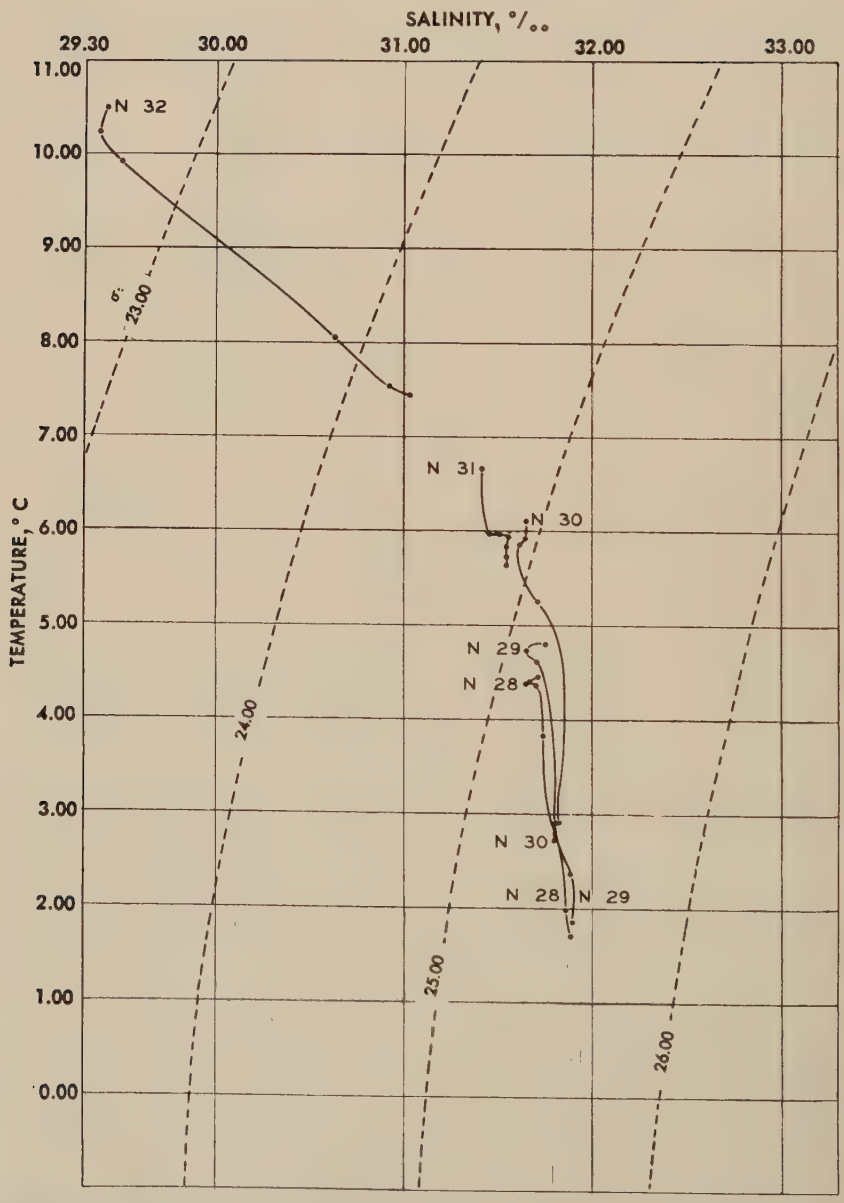

Figure 11. Temperature-Salinity diagrams from stations across the eastern side of Bering Strait (see Fig. 1).

The only marked departure from the similarity between the trend of the isopleths of temperature and salinity occurs at St. N15, where low-salinity surface water occurs in conjunction with the low-temperature water found on the westward side of the area. This region of cold low-salinity surface water may be explained as a pocket of

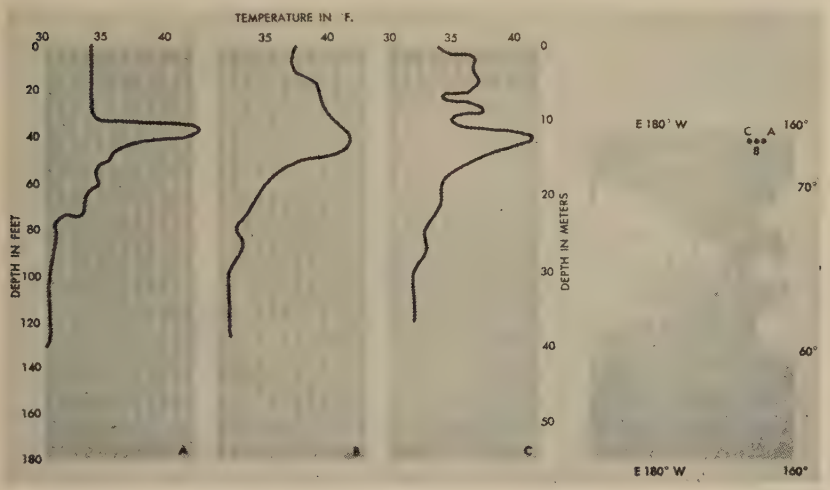

Figure 12. Bathythermograms taken in the ice pack region.

melt water which had drifted down from the ice area under the influence of the northwest winds which prevailed at this time. The similarity of St. N15 to the stations occupied in the ice area will be noted further in the discussion of the T-S relationship.

Several unusual features of these structures were shown by the BT observations. At several stations a subsurface maximum in temperature was observed. These maximums and their associated positive gradients were frequently observed north of 70° N near the boundary of the ice. Fig. 12 gives observations made in the region of the ice pack; these show pronounced positive gradients. The temperature in the warm subsurface layer was up to 9° F higher than the overlying isothermal layer (Fig. 12A). Repeated observations show that the layer may take on different characteristics. For example, the isothermal layer may be completely lacking, and a positive gradient may extend almost to the surface (Fig. 12B). In some cases multiple layers of positive temperature gradients were observed (Fig. 12C). The subsurface maximum occurred most often at a depth between 30 and 45 feet, and in all cases it occurred at a depth of less than 50 feet. In most cases the salinity gradient is large enough to counteract the

temperature gradient, and the vertical stability is maintained (Fig. 13A). At some stations, however, the increase in salinity in the layer of positive temperature gradients was not sufficient to compensate for the decreasing density caused by the temperature change, thus creating a condition of vertical instability. In some cases instability was ob-

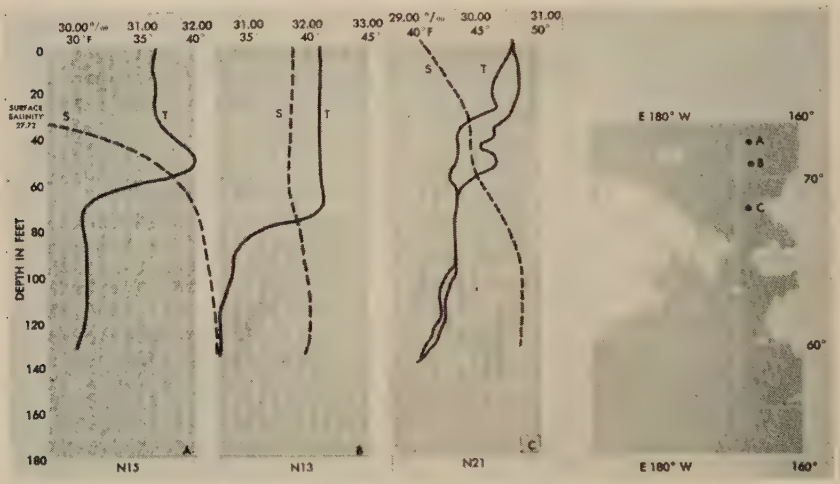

Figure 13. Bathythermograms (T) and salinity traces (S) taken in the eastern Chukchi Sea. Double trace in C represents the observed temperature when lowering and retrieving the bathythermograph.

served to be a result of vertical salinity gradients alone. At St. N13 (Fig. 13B), for example, the surface layers are isothermal, but the salinity decreases slightly with the depth in the upper 20 m.

The presence of instability is further substantiated by the bathythermogram at St. N21 (Fig. 13C). One of the traces shown is that made by the instrument while it was sinking through the water; the other trace was made by the instrument while it was being hauled in. If only one such bathythermogram had been obtained, it could be supposed that there was something wrong with the instrument; however, two BTs were lashed together at most of these stations, and nearly identical traces were obtained from both instruments. The rapid change in the thermal structure indicated here (the difference in time between the two traces is but 1 or 2 minutes) may well be explained as the result of vertical convection set up by recently established instability. Typical examples of vertical temperature and associated salinity plots (Fig. 13) indicate that the vertical gradients increase with increasing latitude. The layers near the bottom, especially at the northern stations, show low temperatures of approximately

29° F and high salinities of about 33 °/₀₀. A possible explanation of the formation of this bottom water is given in the discussion of the T-S relationships below.

The T-S relationships for Sts. N10–N15 are shown in Fig. 14. The T-S diagrams for N10, N11, N12, and N13 show characteristics similar

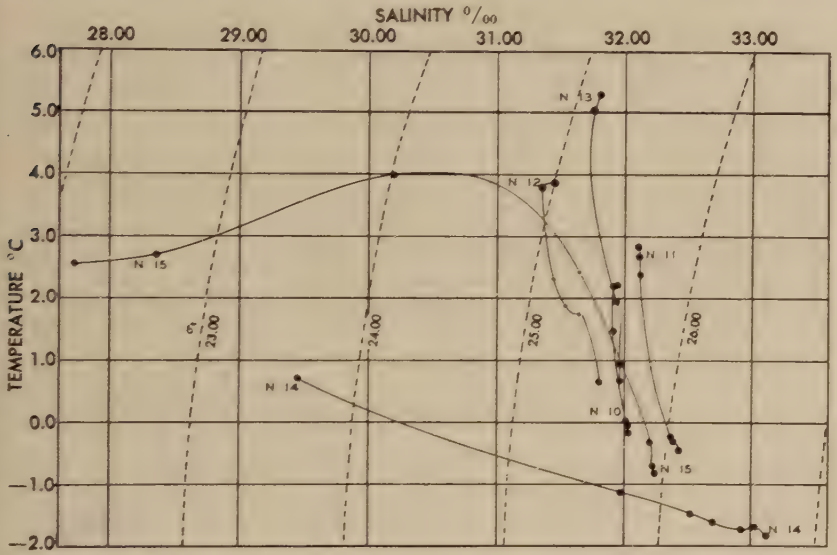

Figure 14. Temperature-salinity diagrams from stations in the central Chukchi Sea (see Fig. 1).

to those found at the central Bering Sea stations, though the temperatures at the Chukchi Sea stations are somewhat colder. It would seem apparent from this similarity in T-S relationship that the water at these Chukchi Sea stations results from a northerly flow at all depths from the Bering Sea.

The marked change in the T-S relationship at N14 and N15 is indicative of a change from water whose recent origin is the Bering Sea to water resulting from the melting of the ice in the northern Chukchi Sea. The elongation of the T-S relation for N14 and N15 toward low salinity in the surface layers is indicative of melt water.

The T-S relationships for N16, N17 (A–B), N18, and N19 appear in Fig. 15 with a repetition of the diagrams for N14 and N15. These stations show fairly similar T-S curves. The low-salinity surface water indicative of melting is present to a greater or less degree on all curves. The spread of the curves in the central portion of the diagram is related to the amount of mixing between the low-salinity melt water

and the more saline water. The more saline and relatively warm water found at mid-depths seems to have originated in the Bering Sea, and in this locality it appears as a wedge between the surface melt water and the uniform bottom water that is found on all of these T-S plots. The cold and relatively high-salinity water (33 °/₀₀), found on

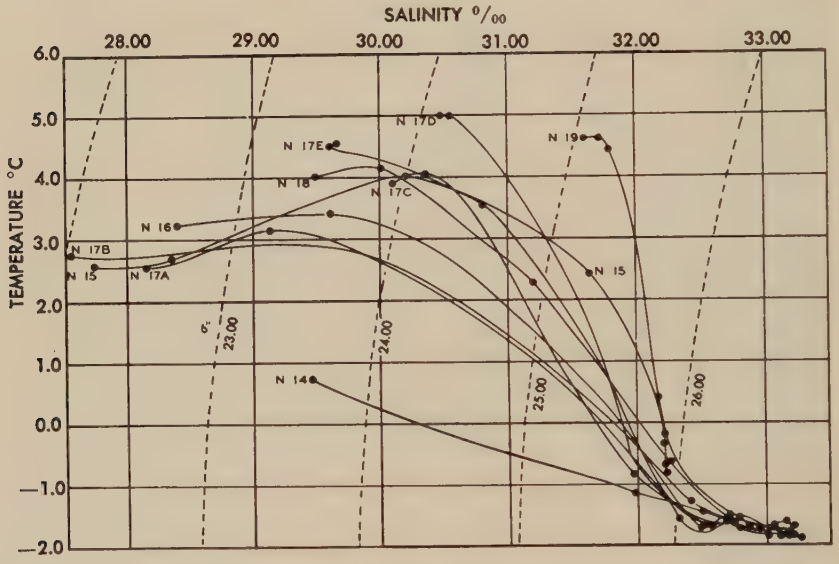

Figure 15. Temperature-Salinity diagrams from stations in the northern Chukchi Sea near ice pack (see Fig. 1).

the bottom at all of these stations, is probably the result of winter freezing. Because of the lower freezing point of salt water, relatively fresh water freezes first, especially when the rate of freezing is slow. Hence the water just below the freezing layer becomes more saline, and, since it is also being cooled, it becomes heavier than the underlying water and sinks to the bottom. Since this bottom water is probably formed in winter throughout the Chukchi Sea (probably in the northern part of the Bering Sea also), the failure of this high-salinity bottom water to appear farther south than N14 is indicative of a northward transport along the bottom at the stations in the southern and central Chukchi Sea.

Nearer the Alaskan coast the T-S plots show higher temperatures and lower salinities, as can be seen from the data for N20, N21, and N22 in Fig. 15. Also shown are the T-S relationships for N26 and N27, in the southeastern part of the Chukchi Sea, and for N33, N34,

and N35, located along the Alaskan coast south of Bering Strait and in Norton Sound. The similarity of the T-S plots between these latter stations in the northeastern Bering Sea and the stations in the southeastern section of the Chukchi Sea can be used to confirm the pattern of flow which will be discussed.

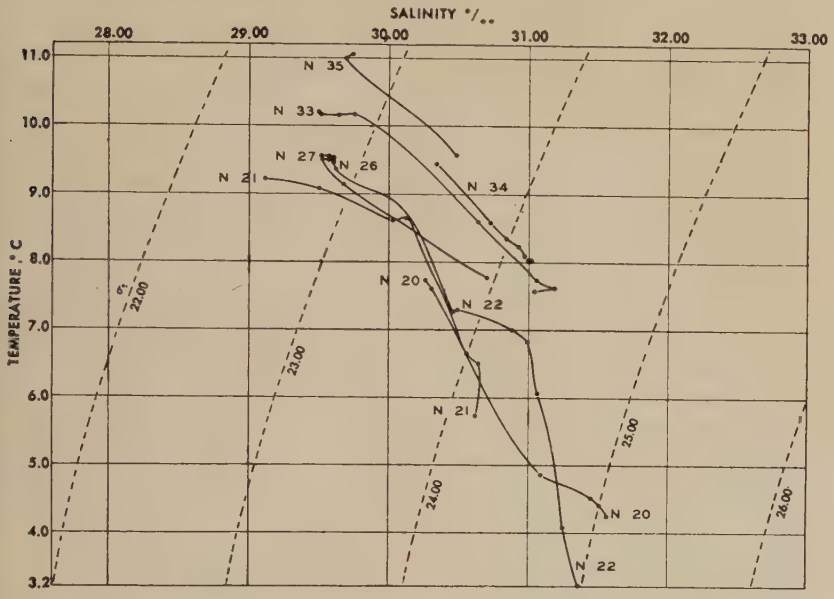

Figure 16. Temperature-Salinity diagrams from stations in Kotzebue and Norton sounds (see Fig. 1).

The vertical thermal structure in both Kotzebue and Norton sounds is characterized by large and sharp thermal gradients and by low-salinity water. The surface layer temperatures in these areas were the highest encountered on this cruise. Examples of temperature-depth and salinity-depth curves from Kotzebue and Norton sounds are shown in Fig. 16.

DENSITY

Because of the close relationship between the isopleths of temperature and salinity, contours of σ_t are very similar to the isotherms and isohalines. The general parallel character of the isopleths of these physical variables indicates that in general the conditions are stationary and that the current will flow parallel to the isolines of temperature, salinity, and density.

South of Point Hope the isopycnals run approximately parallel to the depth contours. The lower-density water is found at all depths along the Alaskan coast; very low-density water (σ_t = 16.8) is found in Kotzebue Sound. In the northern Chukchi Sea, regions of low density occur in the surface layer to the west of the line of stations (away from the Alaskan coast). This area of low surface density is related to melt water of low salinity. At greater depths (25 and 40 m) in the northern Chukchi Sea, the isopycnals again decrease toward the Alaskan coast.

DYNAMIC TOPOGRAPHY AND CURRENTS

Since the distribution of temperature and salinity is strongly indicative of the existence of generally stationary conditions throughout much of the area studied, it would be expected that quite satisfactory current determinations could be made from dynamic computation, providing a suitable level reference surface were found. This latter requirement cannot be met, however, for the area in general is less than 50 m deep and the pressure surfaces are apparently inclined relative to the level surfaces at all depths. Dynamic computations suffice only in indicating the flow of the surface relative to some deeper level, here taken at 45 m. However, the results indicate that the dynamic topography gives the direction and relative magnitude of the surface flow quite well, though the absolute magnitudes of the currents as obtained from the dynamic computations are lower than the magnitudes of the observed currents.

The dynamic topography, based on the dynamic height anomaly of the surface over 45 decibars, is shown in Fig. 17. In order to use 45 decibars as a reference level, it was necessary to extrapolate the data for several shallow stations, using several reference stations as guides. It was found that the final value for the dynamic anomaly was not greatly affected by the manner in which this extrapolation was performed.

The solid arrows on Fig. 17 show the direction of drift of the USS Nereus during several periods when the ship was allowed to drift with the current and the wind. Because the vessel has a high freeboard, it is likely that the drift is greatly affected by the wind. This is seen most clearly at the drift stations taken at the edge of the ice pack, where the ship drifted southeastward at about ½ knot although the dynamic topography indicates a northerly flow. This drift of the ship was related to the observed northwest wind of about 7 knots, for the drift was observed to be southward relative to the pieces of floating ice which surrounded the ship at the beginning of the drift.

Figure 17. Dynamic height contours (0/45 dynamic meters) in dynamic centimeters observed in the Bering and Chukchi seas with direction of calculated current flow indicated by arrowheads along the contours of dynamic height. Observed drift of ship is indicated by short heavy arrows.

The observed velocities of drift at Sts. N8, N9, and at the five stations in Bering Strait, gave directions which were very close to the direction of flow indicated by the dynamic topography. However, in every case the computed velocities were much smaller than the observed velocities (approximately 1/10 as large). This is to be expected since the bottom waters also have a northerly motion. Some

of the difference between observed and computed currents in Bering Strait can be related to wind drift of the ship, for the wind was blowing at an average speed of 17 knots from the south during this period of observation.

For the southern Bering Sea region the current streamlines, as deduced from the distribution of temperature alone, are shown on Fig. 17 as dashed lines. Previous investigators (Goodman, Lincoln, et al., 1942) have reported the existence of eddies similar to the one depicted here in this region of the Bering Sea.

REFERENCES

Barnes, C. A. and T. G. Thompson
1938. Physical and chemical investigations in Bering Sea and portions of the North Pacific Ocean. Univ. Wash. Publ., Oceanography, *3* (2): 35–39; also Appendix, pp. 1–164.

Goodman, J. R., J. H. Lincoln, et al.
1942. Physical and chemical investigations: Bering Sea, Bering Strait, Chukchi Sea, during the summers of 1937 and 1938. Univ. Wash. Publ., Oceanography, *3* (4): 107–169.

LaFond, E. C., R. S. Dietz and D. W. Pritchard
1949. Oceanographic measurements from the USS Nereus on a cruise to the Bering and Chukchi seas, 1947. Interim Report. Rep. U. S. Navy Electr. Lab., No. 91 (RESTRICTED).

Sverdrup, H. U.
1929. The waters on the North-Siberian shelf. Sci. Res. Norweg. N. Pol. Exped. "Maud," *4* (2): 34–40.

Sverdrup, H. U., M. W. Johnson and R. H. Fleming
1946. The Oceans. Prentice-Hall, Inc., New York. 1087 pp.

A NEW SPECTROPHOTOMETRIC METHOD FOR THE DETERMINATION OF NITRITE IN SEA WATER[1]

By

KENNETH BENDSCHNEIDER AND REX J. ROBINSON

Oceanographic and Chemical Laboratories
University of Washington
Seattle 5, Washington

ABSTRACT

A spectrophotometric method, employing sulfanilamide and N-(1-naphthyl)ethylenediamine, has been proposed for the determination of nitrite in sea water. The effect of the order of addition of reagents, acidity, reagent concentration, and temperature on the speed of color formation and maximum optical density has been discussed. It has been shown that salinity has no effect on the maximum color intensity. The color develops rapidly in either sea water or fresh water and is stable for approximately two hours. Calibration curves have been prepared which show that the concentration of nitrite is directly proportional to color intensity.

INTRODUCTION

The most widely accepted method for the determination of nitrite in sea water is based on the diazotization of sulfanilic acid by the nitrite, with subsequent coupling to α-naphthylamine to give a rose-colored dye whose color intensity is proportional to the nitrite concentration (Ilosvay, 1889; Robinson and Thompson, 1948). This method is rather slow, and spectrophotometrically the results are not as consistent as might be desired.

Shinn (1941) used sulfanilamide as the diazotizing agent and N-(1-naphthyl)ethylenediamine dihydrochloride as the coupling agent in the determination of nitrite in fresh water. Equation (1) represents the diazotization reaction. The product of the coupling reaction is not definitely known, but equations (2) and (2a) represent possibilities:

(1) $NH_2SO_2C_6H_4NH_2.HCl + HNO_2 \rightarrow NH_2SO_2C_6H_4N{\equiv}NCl + 2H_2O$;

(2) $NH_2SO_2C_6H_4N{\equiv}NCl + C_{10}H_7NHCH_2CH_2NH_2.2HCl \rightarrow NH_2SO_2C_6H_4N{=}NNHCH_2CH_2NH(C_{10}H_7).2HCl + HCl$;

(2a) $NH_2SO_2C_6H_4N{\equiv}NCl + C_{10}H_7NHCH_2CH_2NH_2.2HCl \rightarrow NH_2SO_2C_6H_4N{=}NC_{10}H_6NHCH_2CH_2NH_2.2HCl + HCl$.

Shinn claimed more rapid color development and greater color stability with these reagents than with the customary reagents.

[1] This work was partly supported by Office of Naval Research Contract Number N8onr-520/III, with the University of Washington.

Kershaw and Chamberlin (1942) modified the Shinn procedure which resulted in increased sensitivity and faster color development. The present paper reports the results of a spectrophotometric study of this method as applied to the determination of nitrite in sea water.

THE PROPOSED METHOD

Apparatus

A Beckman spectrophotometer, model DU, with Corex cells of 10 cm optical path, was used for optical density measurements in this investigation. A slit width of 0.10 mm was found to give satisfactory results. Distilled water was used in the reference cell except as otherwise noted.

Reagents

Sulfanilamide. Five grams of sulfanilamide, $NH_2SO_2C_6H_4NH_2$, are dissolved in 500 ml of 1.2 N hydrochloric acid. The solution should be stored in an amber glass-stoppered bottle.

N-(1-naphthyl)ethylenediamine dihydrochloride. A half gram of the compound, $C_{10}H_7NHCH_2CH_2NH_2.2HCl$, is dissolved in 500 ml of distilled water. The solution must be stored in an amber glass-stoppered bottle and kept out of direct sunlight.

Standard Nitrite Solutions

Standard Solution I. Pure sodium nitrite is dried at 110° C and cooled in a desiccator. Of the dried compound, 0.345 g is dissolved in distilled water and the solution is diluted to one liter. A few drops of chloroform are added to prevent bacterial growth. One ml contains 5 μg-at nitrite-nitrogen.

Standard Solution II. Five ml of Standard Solution I are diluted to 500 ml with distilled water. One ml contains 0.05 μg-at nitrite-nitrogen.

Standard Solution III. Standard solutions of the desired concentration are prepared, whenever needed, by dilution of Standard Solution II with distilled water over the range 0.05 to 1.00 μg-at nitrite-nitrogen/l of solution. Nitrite-free sea water or sodium chloride solution may be used for dilution of standard solutions, but it is not necessary, since the presence of these salts has little effect on the final color intensity.

Standard Solution I is usually stable for several weeks. Standard Solution II is usually quite stable, but variations in concentration occasionally occur in a few days, and therefore careful control is

necessary. Standard Solution III is not very stable and needs to be prepared fresh whenever used.

Method of Analysis

One ml of the sulfanilamide reagent is mixed thoroughly with 50 ml of sea water sample followed by 1 ml of N-(1-naphthyl)ethylenediamine dihydrochloride reagent within 2 to 6 minutes. The solution reaches its maximum color intensity in about 10 minutes and remains stable for approximately two hours. The optical density should be measured during this period by means of the spectrophotometer, with a wave length of 543 mμ. The nitrite concentration is determined from a calibration curve previously prepared by using standard nitrite solutions.

EXPERIMENTAL

Optical Density Curves at Various Wave Lengths. Absorption by the diazo compound was measured at various wave lengths on each of three solutions containing 0.1, 1.0 and 2.0 μg-at nitrite-nitrogen/l in a solution of S = 34.3 $^{\circ}/_{\circ\circ}$. Maximum absorption occurred at 543 mμ, as shown in Fig. 1. In all subsequent experiments with these reagents, optical density observations were made at this wave length.

Effect of the Order of Adding Reagents upon the Color Development. Various orders of adding the sulfanilamide, N-(1-naphthyl)ethylenediamine dihydrochloride and hydrochloric acid were investigated. It was determined that the maximum color development occurred when the sulfanilamide and hydrochloric acid were mixed with the sample before the coupling reagent was added. It is essential that the diazotization reaction, represented by equation (1), be completed before the coupling reagent is added, otherwise the undiazotized nitrite reacts with the amino group of the reagent with a resultant reduction in color intensity, according to Rider and Mellon (1946). A reagent containing all three reagents was found to be impractical, apparently because of the reaction of nitrite with the amino group of the coupling reagent.

Effect of Hydrogen Ion Concentration upon Color Development. A series of 1.0% sulfanilamide solutions was prepared with hydrochloric concentrations ranging from 0.03 to 6.0 N. One ml of each of these solutions was added to a 50 ml standard nitrite sample containing 1.0 μg-at/l. The sample was well mixed and 1 ml of a 0.2% solution of N-(1-naphthyl)ethylenediamine dihydrochloride reagent was introduced 60 seconds after the addition of the sulfanilamide reagent. The maximum color density and the pH of each sample were de-

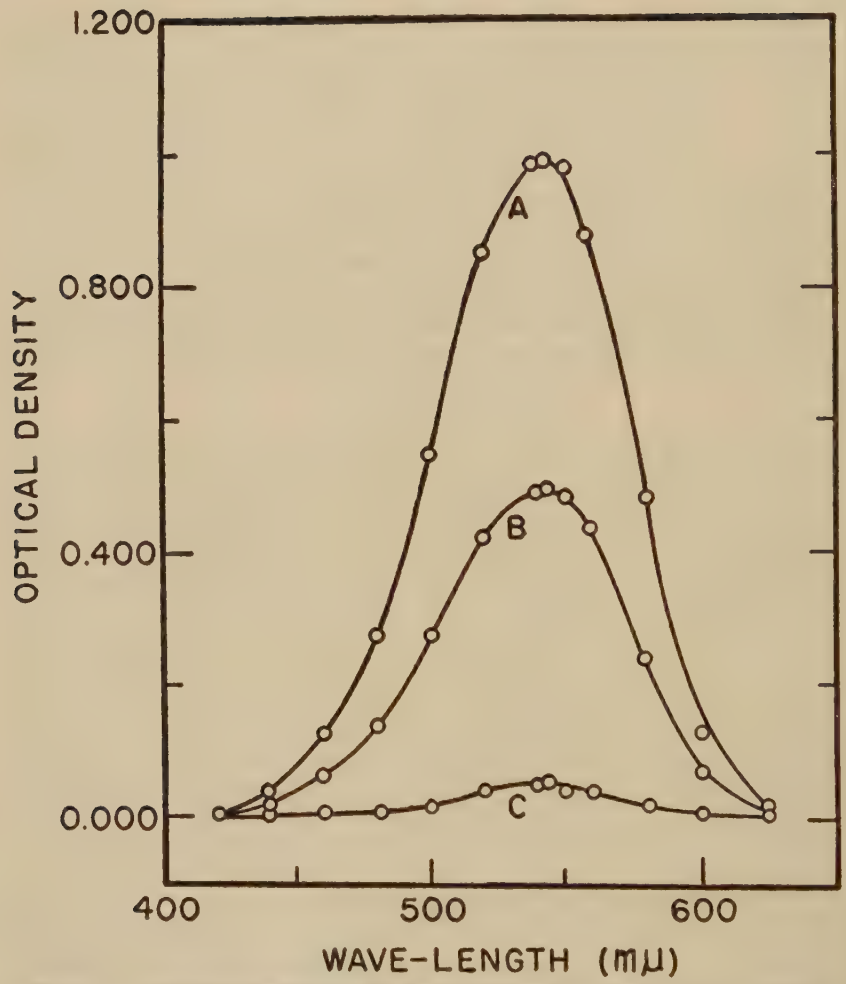

Figure 1. Absorption spectra of the diazo compound. Curve A: 2.0 μg-atoms of NO_2^-–N present per liter of solution. Curve B: 1.0 μg-atom of NO_2^-–N present per liter of solution. Curve C: 0.1 μg-atom of NO_2^-–N present per liter of solution.

termined. A plot of the results in Fig. 2 indicates that, with 1.0% sulfanilamide reagent and one minute diazotization time, a pH of 2.0 or less is required to produce maximum color intensity.

Effect of Reagent Concentration and Time Interval between the Addition of Reagents upon Color Development. The time required for complete diazotization was shown to vary with the sulfanilamide concentration

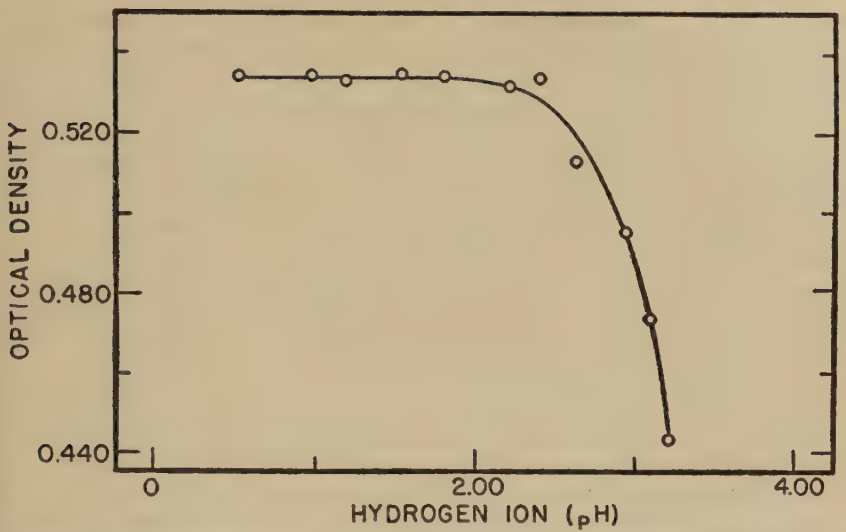

Figure 2. Effect of hydrogen ion concentration upon the maximum color intensity. 1.0 μg-atom of NO_2^-–N present per liter of solution.

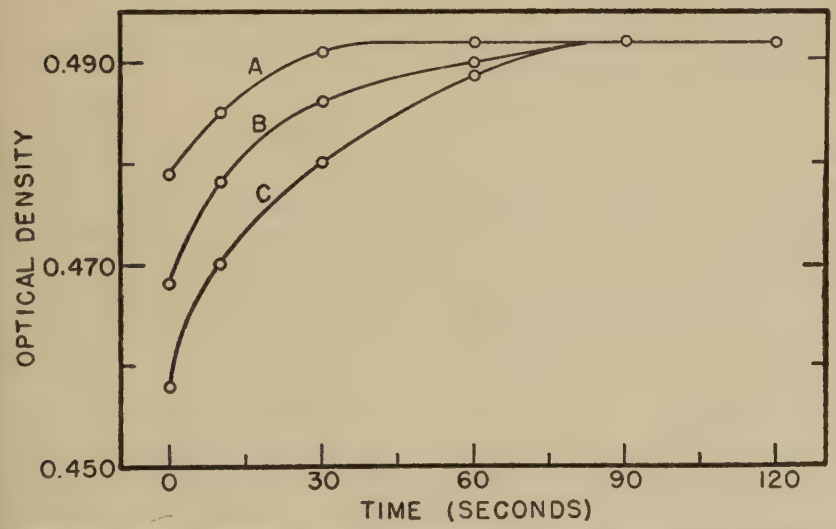

Figure 3. Effect of reagent concentration and time interval between the addition of reagents upon color development. Curve A: 2.0% sulfanilamide. Curve B: 1.0% sulfanilamide. Curve C: 0.5% sulfanilamide. 1.0 μg-atom of NO_2^-–N present per liter of solution.

when the pH is held constant. Three solutions were prepared with 0.5, 1.0, and 2.0% sulfanilamide and 80 ml of concentrated hydrochloric acid per liter of solution. One ml of each of these solutions was added to a corresponding 50 ml standard nitrite sample containing 1.0 μg-at/l. The sample was well shaken and 1 ml of 0.1% N-(1-naphthyl)ethylenediamine dihydrochloride was introduced 30 seconds after the addition of the first reagent. This procedure was repeated several times in the same manner except that the time interval between the addition of the reagents was varied. A plot (Fig. 3) of the maximum color density of each sample against time interval indicates the time required for complete diazotization with different concentrations of sulfanilamide. All optical densities below the highest value reveal incomplete diazotization.

The coupling reaction is bimolecular, and consequently the reaction velocity is dependent upon the concentration of either reacting substance. However, by using a rather large excess of N-(1-naphthyl)-ethylenediamine dihydrochloride, the reaction velocity can be made practically independent of the concentration of this reagent, and the reaction then becomes a pseudounimolecular one. One ml of a 0.04% solution of the coupling reagent, which represents a twenty-fold excess over the diazotized sample, was determined to be sufficient to transform the reaction into a pseudounimolecular one. Essentially the same reaction velocity was observed in the coupling reaction with one ml of either a 0.04 or 0.4% solution of N-(1-naphthyl)ethylenediamine dihydrochloride.

Velocity of Color Development. The velocity of color development is greater with the proposed method than with the method currently in use. Full color development is attained in about 10 minutes with the proposed reagents in the sea water medium, whereas about 30 minutes are required with sufanilic acid and α-naphthylamine. With the latter reagents about 90 minutes are required for full color development in the fresh water medium, whereas with the proposed reagents there is no difference in the velocity of color development in either the fresh or salt water medium. Typical kinetic curves are shown in Fig. 4.

Stability of the Reagents and the Color Produced by the Reaction. The acid-sulfanilamide reagent as used in the determination is very stable, no decomposition being evident in a period of three months, whereas the N-(1-naphthyl)ethylenediamine dihydrochloride reagent slowly decomposes but may be stored in an amber glass bottle for at least two weeks without appreciable discoloration. Direct sunlight greatly accelerates the formation of the brown decomposition product.

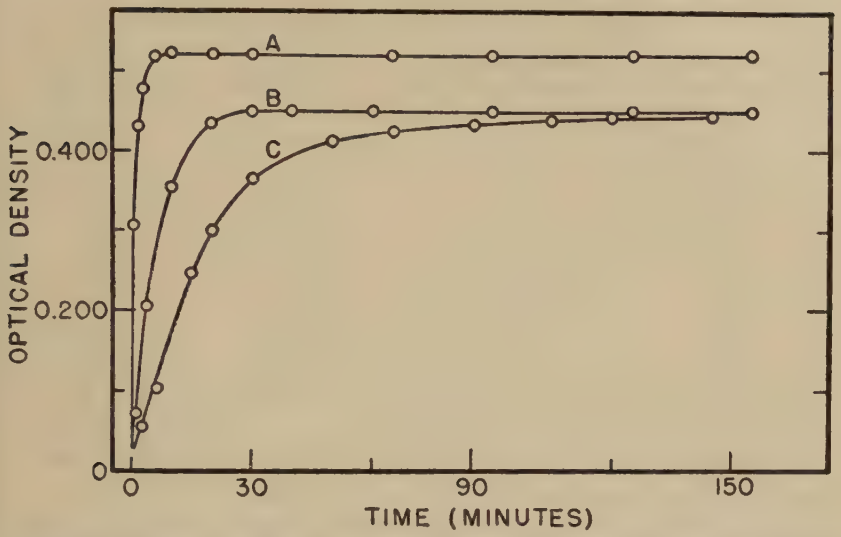

Figure 4. Velocity of the color development. Curve A: Proposed reagents in sea water medium. Curve B: Accepted reagents in sea water medium. Curve C: Accepted reagents in fresh water medium. 1.0 μg-atom NO_2^-–N present per liter of solution.

Under conditions of artificial light or bright daylight (but protected from direct sunlight) the color produced by the reaction is stable for about two hours, fading slowly thereafter. In direct sunlight the color changes rapidly to a redder hue with an increase in optical density; that is, the maximum absorption wave length shifts from 543 to about 530 mμ.

The diazotized sulfanilamide is also somewhat unstable, and therefore the time interval between the addition of reagents should not be prolonged. With a 15-minute time interval no decrease in maximum optical density occurs, but when the time interval is increased to 30 minutes, a 5% decrease in maximum optical density results.

Effect of Temperature upon Color Intensity. The color intensity is also dependent upon the temperature of the solution. In Table I are the results obtained when nitrite solutions containing 1.0 μg-at/l were heated to different selected temperatures, treated with the reagents and maintained at these desired temperatures. After the optical densities were determined, the solutions were slowly cooled to room temperature and the optical densities were redetermined. The color intensities varied inversely with temperature. When the solutions were again brought to the same temperature, the color intensities

TABLE I. The Effect of Temperature on the Maximum Color Intensity

Temperature of Coupling Reaction °C	*Optical Density at Reaction Temperature*	*Final Temperature* °C	*Final Optical Density*
13.0	0.510	29.0	0.505
30.0	.498	30.0	.498
30.0	.499	14.0	.510
38.8	.489	29.0	.498
		36.0*	.491
42.3	.492	29.5	.501
49.8	.483	29.5	.505
68.0	.474	29.0	.491
70.0	.444	29.0	.480

* Sample warmed from 29.0° to 36.0° C and the density redetermined. Solutions contained 1.0 ug-at nitrite-nitrogen/l of solution.

became essentially the same except for those which had been heated above 50° C when some decomposition apparently had occurred.

Effect of Salinity upon Color Intensity. Nitrite solutions were prepared in a distilled water medium and in various synthetic sea water media, prepared according to Lyman and Fleming (1940). Identical optical densities were obtained for nitrite solutions of equal concentration in either medium.

Likewise, salinity was found to have no effect with the reagents now currently used if the α-naphthylamine was added after the sulfanilic acid. However, if these reagents were added as a mixture, a slightly lesser optical density was noted at the lower salinities (see Table II). With the range of salinities normally encountered in marine work, this effect is practically insignificant except in very critical work.

Calibration Curve. Fig. 5 shows calibration curves with both the proposed and accepted reagents. Since Curve A is linear, the color produced is directly proportional to the nitrite concentration in conformity with Beer's law. Within the limits noted above, the slope of the curve is constant under the different conditions of pH, reagent concentration, time interval between reagents, and standard solutions prepared with distilled water or nitrite-free sea water.

As indicated in Fig. 5, some absorption occurs at zero nitrite concentration. This probably is due to nitrite impurity in the reagents or in the distilled water, since neither reagent causes absorption at wave length 543 mμ when added alone to distilled water. Redistillation of the water, made alkaline with sodium hydroxide, usually reduced the observed optical density. Distilled water plus the reagents may be used in the reference cell to compensate for the blank, but this

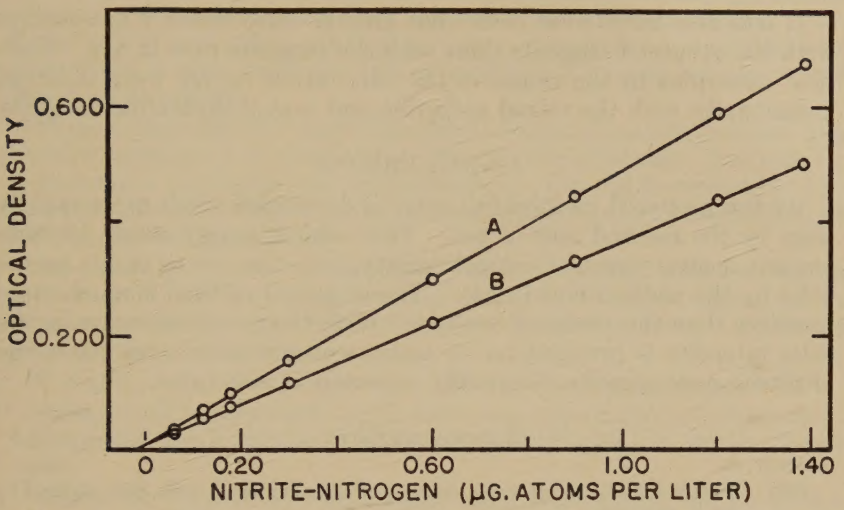

Figure 5. Calibration curves. Curve A: Proposed method at 543 mµ. Curve B: Accepted method at 520 mµ.

TABLE II. The Effect of Salinity upon the Maximum Color Intensity Produced by the Accepted Procedure

Sample Salinity °/₀₀	*Optical Density with Mixed Reagents*	*Optical Density with Separate Reagents*
34.3	0.208	0.210
24.0	.204	.209
17.2	.204	.209
10.6	.201	.209
3.5	.199	.209
0.6	.193	.208
0.0	.192	.209

Density observations at 520 mµ.
Samples contained 0.50 µg-at nitrite-nitrogen/l of solution.

is not recommended, since it introduces the possibility of variations in the absorption characteristics of the reference cell due to decomposition or contamination.

In Fig. 5 the greater slope of Curve A in comparison with Curve B indicates that the proposed reagents are more sensitive than those now used. Thus, with the proposed reagents, smaller amounts of nitrite may be estimated and smaller differences in nitrite concentration may be detected.

It was also noted that somewhat greater consistency was obtained with the proposed reagents than with the reagents now in use. Definite variations in the slopes of the calibration curves were obtained occasionally with the mixed sulfanilic and α-naphthylamine reagents.

CONCLUSIONS

By the proposed method full color is developed much more rapidly than by the method now in use. This color is amply stable for convenient measurement of optical density, but it is not as stable as the color by the method now in use. The proposed method is much more sensitive than the accepted method. With the proposed reagents, the color intensity is proportional to nitrite concentration over the range of nitrite concentrations normally expected in sea water.

Literature Cited

Ilosvay, L.
1889. Determination of nitrite in saliva and exhaled air. Bull. Soc. chim. Fr., (3) *2:* 388–391.

Kershaw, N. F. and N. S. Chamberlin
1942. Determination of nitrites. Industr. Engng. Chem., Anal. Ed., *14:* 312–313.

Lyman, J. and R. H. Fleming
1940. Composition of sea water. J. Mar. Res., *3:* 134–146.

Rider, B. F. and M. G. Mellon
1946. Colorimetric determination of nitrites. Industr. Engng. Chem., Anal. Ed., *18:* 96–99.

Robinson, R. J. and T. G. Thompson
1948. The determination of nitrites in sea water. J. Mar. Res., *7:* 42–48.

Shinn, M. B.
1941. A colorimetric method for the determination of nitrite. Industr. Engng. Chem., Anal. Ed., *13:* 33–35.

NOTE TO AUTHORS

The pages of this Journal are open to all contributors, and manuscripts may be submitted to any member of the Board of Editors or to the Managing Editor. Publication will be made only in the English language, but copy may be submitted for consideration in other languages. Aid in translation of accepted manuscripts will be given when possible.

All manuscripts should be typewritten with double space, carefully corrected, with footnotes continuously numbered and set off in the body of the text. If an article is to appear as a contribution from another institution, it should be approved by that institution before submission; contribution numbers of such institutions are submitted with the return of galley proofs.

The author (or authors) of each article will receive a total of 50 free reprints (with covers). Additional reprints with or without covers may be ordered by authors or institutions at the cost of printing. Orders for reprints are given when galley proofs are returned.

Both galley and page proofs are submitted to the senior author of each article.

Tables should be prepared for clarity and as near as practicable to Journal pattern, without ruled lines if possible. Table footnotes should appear at the base of each Table.

Figures are required for consideration simultaneously with the manuscript. Original figures of inconvenient size for forwarding may be represented by photographs on first submission of a manuscript; originals are required for line cuts. Illustrations requiring half-tone reproduction should be avoided as far as possible, but they will be accepted when necessary. *It is very important that the proper size of characters and symbols should be used for the lettering of illustrations.* A diagram for determining suitable heights of letters for original drawings that will be reduced, together with an explanatory note, has been published in this Journal, Vol. III, No. 1: 89–91; reprints will be submitted to authors on request. Mechanical lettering is recommended. If facilities for lettering are not available to the author, it is preferable to receive illustrations with lettering indicated in pencil only, to be finished in ink in the editorial office. All illustrations will be subject to at least a minimum reduction at the rate of 1 : 1.2. Drawings which have been heavily patched and pasted must *not be rolled* for mailing. The legends for the figures, identified by corresponding figure numbers on the illustrations also, should be typed in sequence at the end of the manuscript.

A complete and *accurate list of references* in alphabetical order at the end of each article is essential. References may be indicated in the text by author's name (or names) and *year of publication*, or by italicized numbers which correspond to the numbers given in sequence in the list of references. Each reference should include the last name followed by at least two initials or first name; co-authors should be listed with the initials or first name preceding the last name. The date should be indented on the line below, followed by a complete title *verbatim* in lower case except for the first word. Publisher, city and pagination should be indicated for books; for periodicals (abbreviations from "World List of Scientific Periodicals," Oxford, as far as possible), the volume (italicized), number and pagination should be given.

Additional information regarding the preparation of manuscripts will be furnished by the Managing Editor.

TABLE OF CONTENTS

Page

1. **J. B. Hersey, H. R. Johnson and L. C. Davis:** Recent findings about the deep scattering layer 1

2. **C. H. Oppenheimer and C. E. ZoBell:** The growth and viability of sixty-three species of marine bacteria as influenced by hydrostatic pressure 10

3. **J. L. Kulp, H. L. Volchok, H. D. Holland and D. B. Ericson:** Thick source alpha activity of some North Atlantic cores 19

4. **D. L. Fox, J. D. Isaacs and E. F. Corcoran:** Marine leptopel, its recovery, measurement and distribution 29

5. **J. Wyman, Jr., P. F. Scholander, G. A. Edwards and L. Irving:** On the stability of gas bubbles in sea water 47

6. **J. D. Isaacs and A. E. Maxwell:** The ball-breaker, a deep water bottom signalling device 63

7. **E. C. LaFond and D. W. Pritchard:** Physical oceanographic investigations in the eastern Bering and Chukchi seas during the summer of 1947 69

8. **K. Bendschneider and R. J. Robinson:** A new spectrophotometric method for the determination of nitrite in sea water 87